Faculdade de Engenharia da Universidade do Porto
Leiden University Medical Center

Hypertrophy modeling using hESC-derived cardiomyocytes

António Pedro Araújo Gouveia

Integrated Master of Bioengineering branch of Biomedical Engineering

Supervisors: Dr. Robert Passier[1], Dr. Perpétua Pinto-do-Ó[2]

Co-supervisors: Dr Cristina C. Barrias[3], Marcelo C. Ribeiro[1]

[1]Department of Anatomy and Embryology, Leiden University Medical Center (LUMC), Leiden, Netherlands

[2]Microenvironments for Newtherapies Group, INEB - Instituto de Engenharia Biomédica, Universidade do Porto, Porto, Portugal

[3]Biocarrier Biomaterials for Multistage Drug and Cell Delivery Group, INEB - Instituto de Engenharia Biomédica, Universidade do Porto, Porto, Portugal

SEPTEMBER, 2014

Abstract

Cardiovascular diseases (CVDs) are more prevalent in comparison with other diseases and are one of the leading causes of death worldwide and although current treatments involving meticulous, complicated and expensive procedures had some success, in general, the improvement in survival and quality of life is not sufficient.

Cardiac hypertrophy, described as an increase in the mass and volume of individual cardiomyocytes (CMs), is an important determinant for cardiac disease. Although cardiac hypertrophy is an adaptive mechanism in specific situations to compensate for an increase in workload (for example in patients with hypertension or myocardial infarction), eventually the heart becomes incapable of meeting the increased workload imposed upon it, thus resulting in heart failure. Since the current animal models for studying heart disease have a low predictability, it is imperative to develop new human *in vitro* model-systems in which the disease phenotype can be thoroughly dissected. By combining the robustness of the *in vitro* human embryonic stem cells (hESC) model-system for differentiating towards CM-like cells with cutting edge bioengineering, it is proposed to develop a platform and a protocol/procedure that assembly efficiency, accuracy and automation, e.g. high-throughput, for analysis of the phenotypic characteristics of CM hypertrophy. It implies the attachment of a custom-made protein patterned coverslip to the bottom of a 96-well plate, enabling the control of CM shape and orientation, upon their culture. Cardiomyocytes were analysed and specific algorithms were created and optimized for measuring several CM features, which are altered during hypertrophy, such as area and sarcomere intensity, among others. Compounds that are known to be in the genesis of this disease are used in this work to experimentally induce hypertrophy in CMs. Compounds that are known to be in the genesis of this disease were used in this work to experimentally induce hypertrophy in CMs.

Results suggested an increase in CM area and sarcomere intensity, when cultured together with fetal calf serum (FCS) hypertrophic treatment in a fibronectin substrate, but were inconsistent for the remaining treatments. Evidences of a CM maladaptation to this type of substrate were observed, preventing accurate results, which lead to the pursuit of an optimal protein combination for CM culture, regarding this work.

Furthermore, regarding the limited proliferative capacity of CMs and their inability to repopulate/regenerate the adult heart after injury, it is critical to chase alternatives to successfully circumvent such hurdles. Thus, under the primary aim of improving the knowledge on cardiac diseases, it is anticipated that our strategy may be easily adapted to meet several other applications. The proposed high-throughput mode, in particular, is expected to improve the number and the time in which a set of compounds with potential to rescue the disease may be identified. Moreover, it is envisioned that this new device will be an add-on in the current available systems for testing cardiac toxicity and for pre-clinical settings.

Resumo

As doenças cardiovasculares (CVDs) são mais prevalentes em comparação com outras doenças e são uma das principais causas de morte em todo o mundo e embora os tratamentos atuais envolvendo procedimentos meticulosos, complicados e caros tiveram algum sucesso, em geral, a melhoria em sobrevivência e qualidade de vida não é suficiente.

A hipertrofia cardíaca, descrita como um aumento da massa e volume de cardiomiócitos (CMs) individuais, tem uma grande importância para as doenças cardíacas. Embora a hipertrofia cardíaca é um mecanismo adaptativo em situações específicas para compensar o aumento da carga de trabalho (por exemplo em pacientes com hipertensão ou com enfarte do miocárdio) eventualmente o coração torna-se incapaz de atender ao excesso da carga de trabalho que lhe é imposta, resultando em insuficiência cardíaca. Uma vez que os atuais modelos de animais que permitem o estudo das doenças cardíacas têm uma baixa previsibilidade é imperativo desenvolver novos sistemas-modelo humanos *in vitro* em que o fenótipo da doença pode ser cuidadosamente dissecado. Ao combinar a robustez do sistema-modelo de células estaminais embrionárias humanas (hESC), *in vitro,* para diferenciação em células semelhantes a cardiomiócitos com a inovação em bioengenharia, é proposto o desenvolvimento de uma plataforma que combine eficiência, precisão e automatização, ou seja, de alto rendimento, para análise das características fenotípicas dos CMs em hipertrofia. Isto implica o acoplamento de uma lamela feita por medida com padrões de proteínas impressos na sua superfície ao fundo de uma placa de 96 poços, permitindo o controlo da forma e orientação dos CMs, após sua cultura. Os cardiomiócitos foram analisados e algoritmos específicos foram criados e otimizados para a medição de várias características dos CMs, normalmente alterados durante hipertrofia, como área e intensidade dos sarcómeros, entre outros. Compostos que são conhecidos por estar na génese da doença são usados para induzir experimentalmente os cardiomiócitos em hipertrofia.

Os resultados sugeriram um aumento da área e da intensidade dos sarcómeros dos CMs, quando cultivados juntamente com o tratamento hipertrófico, com soro de fetal bovino (FCS), num substrato constituído por fibronectina, mas foram inconsistentes para os tratamentos restantes. Foram observadas evidências de uma má adaptação dos CMs a este tipo de substrato, impedindo a precisão dos resultados, que levou à procura da combinação de proteínas ideal para a cultura de CMs, para este trabalho.

Além disso, em relação ao limitado CMs natureza proliferativa e sua incapacidade para repovoar/regenerar o coração adulto após a lesão, é fundamental perseguir alternativas para contornar esses obstáculos com sucesso. Assim, sob o objetivo principal de melhorar o conhecimento sobre as doenças cardíacas, prevê-se que a estratégia possa ser facilmente adaptada para atender a diversas outras aplicações. O modo de alto rendimento proposto, em particular, espera-se aumentar o número e o tempo em que um conjunto de compostos com potencial para salvar a doença possam ser identificados. Além disso, prevê-se que este novo dispositivo seja uma melhoria nos atuais sistemas disponíveis para testar a toxicidade cardíaca e em configurações pré-clínicos.

Acknowledgements

As a bioengineering master student I wanted to perform my thesis work about an interesting theme with extreme future potential in the Medicine and/or Engineering world. I ended up by choosing the promising area of the pluripotent stem cells and working as an intern in the Leiden University Medical Center (LUMC), in the Netherlands, in the Anatomy & Embriology department, from February until August in 2014. For that I want to thank to my supervisor, at Porto's University, Dr. Perpétua Pinto-do-Ó which oriented and advised me in this choice of mine and established the necessary contacts with the institution, for not to say that helped me throughout the entire internship. I also want to thank to my co-supervisor, at Porto, Dr. Cristina Barrias that also gave me support during the time I was working in institute. They both pushed me to always do and be better since they became my supervisors and I want to thank for the motivation to aim for perfection.

Dr. Christine Mummery that accepted me right away for an internship in the LUMC and assigned me to work under the orientation of Dr. Robert Passier, in his group, and I would like thank them both for giving me this opportunity. I would like to thank to Dr. Robert Passier and to the entire group for providing me orientation and focus towards a final goal established for this project. I was daily supervised in the LUMC by the PhD student Marcelo Ribeiro which I want to specially thank for teaching and training me for all the tasks I needed to perform for this project, for advising me on daily basis during the time I was in the Netherlands and make me aspire for the gold. Another special thank to bioinformatic Dr. Lu Cao that was responsible for all of the image analysis presented in this work. Whenever I needed help relating cell culture, immunocytochemistry or other techniques I was kindly assisted by technicians BSc. Jantine Monshouwer-Kloots and BSc. Dorien Ward-van Oostwaard and I would like to thank them both and to the entire department, in general, which helped and provided me everything I needed at some point.

For last, I would like to thank to my family, in particular to my parents, that always supported me at all levels and always did, and do, the possible and impossible for me to prosper academically and professionally.

Table of contents

List of Figures

List of Tables

List of Abbreviations

CVD	cardiovascular disease
DALY	disability-adjusted life years
CM	cardiomyocyte
PKC	protein kinase C
MAPK	mitogen-activated protein kinase
JAK/STAT	Janus kinase/signal transducers and activators of transcription
ERK	extracellular signal-regulated kinases
ISO	isoprotenerol
Ca2+	calcium
PE	phenylephrine
ANG	angiotensin II
ET-1	endothelin-1
FCS	fetal calf serum
BSA	bovine serum albumin
DNA	deoxyribonucleic acid
MHC	myosin heavy chain
CPC	cardiac progenitor cells
ESC	embryonic stem cell
iPSC	induced pluripotent stem cell
EC	embryonal carcinoma
hESC	human embryonic stem cell
Oct4	Octamer-4
Sox2	Sex determining region Y-box 2
SSEA-4	stage specific embryonic antigen 4
TRA	tumor-related antigen
ECM	extracellular matrix
µCP	microcontact printing
PDMS	polydimethylsiloxane
AFM	atomic force microscope
HTS	high-Throughput Screening
HCI	high Content Imaging
LUMC	Leiden University Medical Center
FFN	fluorescence fibronectin
FN	fibronectin
PBS	phosphate buffered saline
eGFP	enhanced green fluorescence protein
MEF	mouse embryonic fibroblasts
EB	embryoid body
SCNT	somatic cell nuclear transfer
BPEL	polyvinyl alcohol and essential lipids
RT	room temperature
GFR	Growth Factor Reduced
NGS	Normal Goat Serum
DAPI	4',6-diamidino-2-phenylindole
LMN	laminin
COL	collagen

Chapter 1 Introduction

1.1 Cardiovascular diseases

Cardiovascular diseases (CVDs) are defined as a class of diseases that involves the heart and the associated blood vessels, or both. The causes for cardiovascular diseases are diverse; however the most common underlying conditions are arthrosclerosis and/or hypertension. Both may lead to a wide range of disorders such as coronary artery disease, cardiomyopathy, hypertensive heart disease, heart failure, *cor pulmonale*, cardiac dysrhythmias, inflammatory heart disease (endocarditis and myocarditis), valvular heart disease, cerebrovascular disease (stroke), peripheral arterial disease, congenital heart disease and rheumatic heart disease.

CVDs are more prevalent all over the world as compared to other diseases, being one of the leading causes of fatalities worldwide, accounting for 17.3 million deaths in 2008, from a total of 57 million deaths (Alderman, 2007). In the same year, a study was conducted by the World Health Organization, regarding the impact of noncommunicable diseases, which mainly include CVDs, cancer, respiratory diseases, digestive diseases and diabetes. It was estimated that, from a total of 36 million deaths worldwide caused by noncommunicable diseases, CVDS were responsible for the largest proportion of deaths under the age of 70 (39%), as represented in Figure 1 (Alderman, 2007; World Health Organization, 2011).

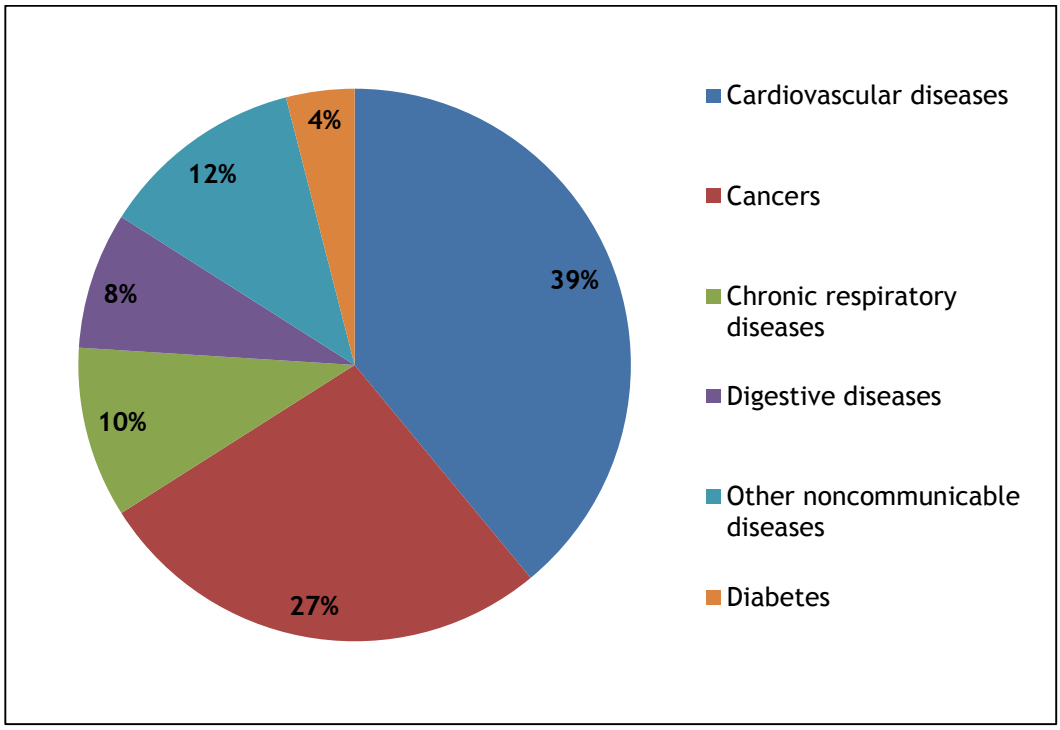

Figure 1 - Percentage of global non -communicable disease deaths under the age of 70, by cause of death in 2008. (Adapted from World Health Organization, 2011)

There is no expectation for these numbers to decrease and actually it has been estimated that by 2030, the number of deaths will increase and reach a total of 23.3 million people (Mathers and Loncar, 2006; World Health Organization, 2011). It is also projected that CVDs will remain the single leading cause of death (Mathers and Loncar, 2006).

CVD is not only one of the most relevant causes of death but is also one of the greatest contributors to the total burden of disease. Disability-adjusted life years (DALYs), which quantify the number of years lost due to disease, are a measure of the total impact of a disease including its fatal (premature death) and non-fatal (disability) outcomes (Kelly, Narula and Fuster, 2012). One DALY represents the loss of the equivalent of one year of full health. This concept is applied to the number of years lost due to premature death or by living in disability or in poor health, due to disease, being the measurement of gap between current health status and ideal health situation designated burden of disease (World Health Organization, 2004). Almost one half of the disease burden in low- and middle-income countries is caused by non-communicable diseases, where cardiovascular diseases account for more than one quarter of the total disease burden (World Health Organization, 2004). Ischaemic heart disease and stroke are the largest sources of this burden, as shown in Table I from a study carried by the World Health Organization in 2011 (World Health Organization, 2011).

Table I – 10 leading global causes of DALY.(Adpated from World Health Organization, 2011)

Rank	Cause	DALYs (thousands)	% DALYs
1	Ischaemic heart disease	165.717	6,0
2	Lower respiratory infections	146.864	5,4
3	Stroke	141.348	5,2
4	Preterm birth complications	107.210	3,9
5	Diarrhoeal diseases	99.728	3,6
6	Chronic obstructive pulmonary disease	92.377	3,4
7	HIV/AIDS	91.907	3,4
8	Road injury	78.724	2,9
9	Unipolar depressive disorders	76.500	2,8
10	Birth asphyxia and birth trauma	74.600	2,7

Overall, CVD represents one of the most dangerous diseases in the world and a very high index of disease burden. In spite of that, it also entails elevated costs related to the health system expenditure for the treatment of the disease (including ambulance, diagnostic tests, hospital charges, possible surgery, drugs, testing, cardiologist appointment, rehabilitation), representing one of the most expensive diseases throughout the world (Kelly, Narula and Fuster, 2012). Just in the USA it was estimated that direct and indirect cost was approximately of 400 billion American dollars, in 2006 (Graham *et al.*, 2006). In a recent study regarding the most expensive diseases, Stroke was listed in fourth place, Heart Attack in sixth and Coronary Artery Disease in seventh (Whelan, 2012). The former three are all cardiovascular diseases, or a cause of it, such as heart attack which is a progressive state that

follows from arthrosclerosis condition. Hereupon, this disease is a great concern that affects not only the people's health but also the economic status of the family and even the economic vitality of the countries, which have to be taken in count (Alderman, 2007). It is an increasing problem with no effective prevention or treatment that can restore the person's health.

Current remedy involve heart transplant, which implies the risk of immune rejection and shortage of organ donors. (Chiu *et al.*, 2012) Although this adverse response can be prevented by administration of immunosuppressive drugs for the rest of the life, this can lead to several unwanted side effects, such as infections. (Bryers, Giachelli and Ratner, 2012) Also, mechanical ventricular assistance devices can be used as a treatment, but the implantation of foreign materials into the organism can lead to immune rejection, being chronic inflammation and device failure a great concern in this matter (Ratner *et al.*, 2012). These problems need to be circumvented with appropriate strategies that enhance the heart function recovery. As such, the rapid development of stem cell technology has raised hopes for new and even revolutionary treatments for cardiac, promoting heart regeneration.

1.2 Cardiomyocyte hypertrophy

1.2.1 Morphological alterations

Cardiac hypertrophy is characterized by an increase in the mass and volume of individual CMs, enhanced protein synthesis and heightened organization of the sarcomeres, resulting in an increase of heart weight without affecting the number of CMs (Wang, Huang and Sah, 1998; Bray, Sheehy and Parker, 2008; Rohini *et al.*, 2010). Although it can have physiological origins and a healthy connotation, it is preoccupant when it is caused by pathological stimuli, developed when increased external stimuli such as, hemodynamic overload and neurohumoral factors are continuously imposed on cardiac myocytes. Classically, two different pathological hypertrophic phenotypes can be distinguished: concentric and eccentric hypertrophy (Bray, Sheehy and Parker, 2008). The first develops due to pressure overload, which is characterized by parallel addition of sarcomeres, resulting in an increase in individual CMs width, often related to hypertension and/or aortic stenosis (Grossman, Jones and McLaurin, 1975; Frey *et al.*, 2004; Bray, Sheehy and Parker, 2008; Buja and Vela, 2008). The second progresses owing to volume overload or prior infarction, and is characterized by addition of sarcomeres in series, producing a greater increase of CM length as compared to the width (Grossman, Jones and McLaurin, 1975; Frey *et al.*, 2004; Bray, Sheehy and Parker, 2008; Buja and Vela, 2008). The normal, healthy, value for the length-to-width CM ratio is approximately seven (Bray, Sheehy and Parker, 2008). Consequently, during concentric or eccentric hypertrophy this ratio decreases and increases, respectively, from the normal value (Bray, Sheehy and Parker, 2008). The heart alterations concerning the two different hypertrophic phenotypes are represented in Figure 2.

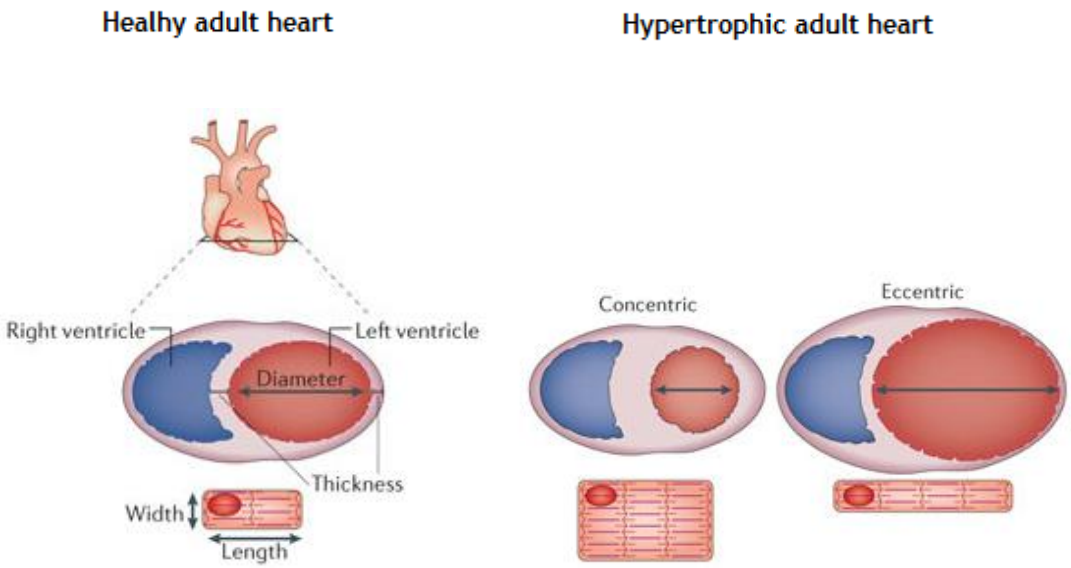

Figure 2 - Heart alterations during cardiac hypertrophy both in concentric and eccentric phenotypes. (Adapted from Maillet, van Berlo and Molkentin, 2013)

1.2.2 Genetic alterations

During the hypertrophic response, CMs are reprogrammed by activation of a distinct pattern of gene expression that eventually results in qualitative and quantitative alterations on contractile protein content and the induction of an embryonic gene program (Wang, Huang and Sah, 1998; Carèw *et al.*, 2007). Nevertheless, the genetic programs responsible for cardiac hypertrophy are diverse and complex and its pathways or proteins which are coupled to it and to the structural reorganization of the cell are still unknown. Usually, the fetal gene expression programs are derived from a trigger that stimulates key intercellular signalling pathways, converging on transcription factors and transduced into the nucleus (Lu and Yang, 2009; Putinski *et al.*, 2013). The CM hypertrophy process is represented in a simplified form in Figure 3. Several intracellular signalling molecules, such as protein kinase C (PKC), tyrosine kinases, mitogen-activated protein kinase (MAPK) family, the Janus kinase/signal transducers and activators of transcription (JAK/STAT) family, have been reported to play important roles in the development of CM hypertrophy (Zou, *et al.* 2001). Other studies underlie, also, the importance of extracellular signal regulated kinase signalling in CM hypertrophy, such as extracellular signal-regulated kinases (ERKs) (Carèw *et al.*, 2007). They have been found to play an essential role in hypertrophic responses on CMs both *in vitro* and *in vitro*, although, its activation does not always lead to that outcome (Taigen *et al.*, 2000).

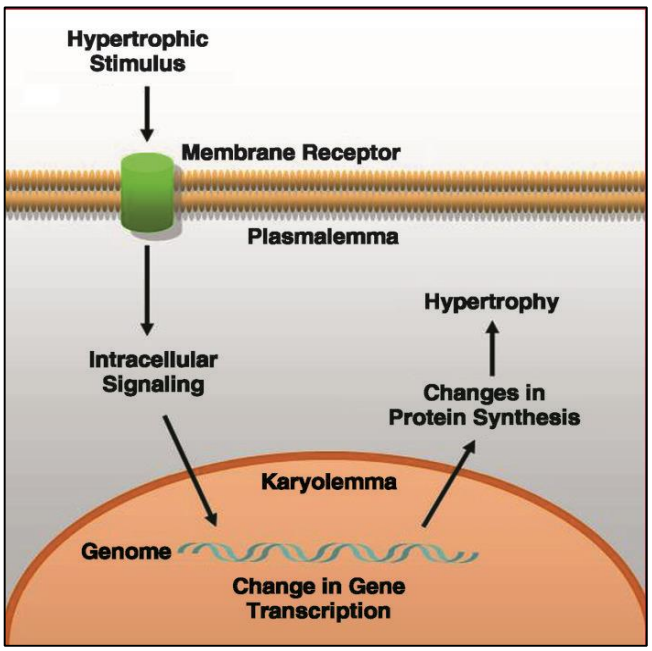

Figure 3 - Simplified representation of the hypertrophy process in cardiomyocytes. (Carreño *et al.*, 2006)

1.2.3 Hypertrophic compounds

It is a fact that the hypertrophic agonist isoprotenerol (ISO), a cathecolamine and a $ß_1$- and $ß_2$-adrenoreceptor agonist, induces expression of proto-oncogenes and cardiac growth. It was reported that ISO activates ERKs through both G_s and G_1-dependent pathways and also by Ca^{2+}, inducing cardiac hypertrophy (Zou *et al.*, 2001). Also, the cathecolamine and a α_1-adrenergic receptor agonist, phenylephrine (PE), induces the activation of the mitogen-activated protein kinases, ERK2 (MAPK1), which plays central roles in MAPK cascades and leads to a re-expression of fetal type proteins, a hallmark of CM hypertrophy (Taigen *et al.*, 2000; Schäfer *et al.*, 2002). MAPK cascades mediate diverse biological functions such as cell growth. Angiontensin II (ANG) is a peptide hormone and the predominant effector of the Renin-angiotensin system. It stimulates several signalling molecules, which subsequently activate their target genes in the nucleus, leading to CM hypertrophy (Sadoshima *et al.*, 1995; Takeishi *et al.*, 2001; Lu and Yang 2009). Endothelin-1 (ET-1) is a potent vasoconstriction agent and function as a stimulator of the renin-angiotensin system. Its hypertrophic effects have been widely studied and it acts on the G-protein coupled receptors, activating then phospholipase C which hydrolyses specific compounds. This leads to the activation of hypertrophic signals such as Raf-1 and MAPK (Yamazaki *et al.*, 1996). Fetal calf serum (FCS) is composed by several proteins, such as bovine serum albumin (BSA) and by several growth factors such as angiotensin II and ET-1 and, therefore, induces a hypertrophic response by a non-selective adrenoreceptor stimulation, because of its varied composition (Dubey *et al.*, 1997; Schäfer *et al.*, 2002).

It is generally assumed that cardiac muscle hypertrophy is a useful physiologic adaptation, which develops when an increased workload is chronically imposed on the

myocardium. Although the hypertrophied myocardium may allow maintenance of adequate cardiac compensation for many years, eventually it becomes incapable of meeting the increased workload imposed upon it, and heart failure ensues. For this reason, it has been suggested that myocardial hypertrophy may be considered the interface between the normal and failing heart (Grossman, Jones and McLaurin, 1975). In the next section, the mentioned transition between adaptive and maladaptive hypertrophy is explained in better detail.

1.2.4 Stages and consequences

In the 60s, Meerson and colleagues believed that hypertrophic transformation of the heart was divided into 3 stages. The first stage (or transient breakdown) involves the development of hypertrophy, in which load exceeds output. It is characterized by symptoms of left ventricular insufficiency leading to pulmonary congestion, hydrothorax, ascites and it can lead to death in some cases. In this stage cardiac dilation, inversion of the T wave with displacement of the S-T segment, swelling of heart muscle fibres, loosening of the myofibrils, and development of fatty dystrophy of the myocardium, among others, are observed. During the first four to five days, the weight of the heart increases at the rate of 10 to 12 per cent in each day; and the rate of protein synthesis in the myocardium increases about two-fold, as revealed by a metabolic label of cells (S-35 methionine). In this stage, a contractile insufficiency caused by acute cardiac strain and a deficiency in the activity of certain enzymes are also observed. Overall, this set of phenomena lead to the increase in CM weight, protein synthesis and loss of contractile force associated with cardiac hypertrophy (Meerson, 1962; Frey *et al.*, 2004).

The second stage is defined as the compensatory hypertrophy, in which the workload/mass ratio is normalized and resting cardiac output is maintained. At this time, almost all of the previous alterations on the physiology and functionality of the heart are restored, with exception of the heart weight (Meerson, 1962; Frey *et al.*, 2004). It is characterized by the absence of cardiac insufficiency and of pulmonary congestion, hydrothorax and ascites; by arrest of enlargement of the heart; by disappearance of pathological modifications of the T wave and the S-T segments as well as by absence of signs of fatty dystrophy of the myocardium. Hypertrophy of muscle fibres and compact organization of myofibrils are apparent (Meerson, 1962; Frey *et al.*, 2004). The weight of the heart is about twice that of the normal heart and remains stable and the rate of protein synthesis in the myocardium was shown to be normal, by the metabolic label (S-35 methionine). In summary, this stage is associated to hypertrophy of the myocardium in a large proportion, which gives rise to an adequate oxidation and oxidative phosphorylation, an inhibition of anaerobic resynthesis of ATP and a re-establishment to normal of creatine phosphate and glycogen content in the myocardium (Meerson, 1962; Frey *et al.*, 2004). Furthermore, hypertrophy leads to a decrease of the number of capillaries and consequently to myocardial hypoxia, with accumulation of acid lactic. These changes are typical of the condition of the

heart during clinical compensation to cardiac failure and hypertension (Meerson, 1962; Frey *et al.*, 2004).

The third stage is defined by the manifestation of heart failure, with ventricular dilation and progressive declines in cardiac output despite continuous activation of the hypertrophic program. It is characterized by the development of cardiac insufficiency, marked and continuously progressing myocardial fibrosis, the appearance of focal fatty degeneration, the deficit in DNA concentration in the myocardium that falls to 30 to 40 per cent of normal. It is also observed a decrease of 50 to 60 per cent in the rate of protein synthesis in the myocardium, through incorporation of S-35 methionine, and a decrease of the ATP level in the myocardium by 10 to 20 per cent. The others factors remain as stated in the second stage of this process. This period involves moderated hypoxia, which in turn leads to depression of the normal profile of protein resynthesis of the myocardial protein structure, to marked fibrotic response, and to decrease of contractile performance of the heart (Meerson, 1962; Frey *et al.*, 2004). The principal characteristics of each stage are summarized in Table II.

Table II - Characteristics of the 3 stages of the cardiomyocyte hypertrophy.

	1st stage	2nd stage	3rd stage
Cardiac function	Left ventricular insufficiency (pulmonary congestion, hydrothorax and ascites)	Normal (absence of pulmonary congestion, hydrothorax and ascites)	Insufficiency
	Fatty degeneration of myocardium	Fatty degeneration of myocardium	Myocardial fibrosis
	Twofold increase of protein synthesis in the myocardium	Normal rate of protein synthesis in the myocardium	50 to 60% decreased protein synthesis in the myocardium
	Myocardium contractile insufficiency	-	Decrease of contractile capacity of the myocardium
	Deficient heart's electric activity	Normal heart's electric activity	*
Cardiac morphology	Cardiac dilatation	Arrest of cardiac dilatation	*
	Heart weight increase	Twofold heart weight increase	*

*Remains the same as in the second stage

The chain of events previously described lead to an ultimate phase (cardiac remodelling), which leads to failure, associated to functional perturbations of cellular Ca^{2+} homeostasis and ionic currents (Frey *et al.*, 2004; Baba and Wohlschlaeger, 2008). This contributes to an adverse prognosis by predisposing to ventricular dysfunction and malignant arrhythmia (Frey *et al.*, 2004; Baba and Wohlschlaeger, 2008). Although, at the beginning, the response of individual CMs to an increase workload is an adaptive hypertrophic growth (size, volume, mass) in order to reduce wall tension, if a continuous load is imposed, hypertrophy becomes a maladaptive process, leading to chronic heart failure and eventually to death (Frey *et al.*, 2004; Baba and Wohlschlaeger, 2008). Dilation is followed by increased ventricular wall stress resulting in decreased coronary blood flow, impaired pump function and diminished cardiac output. Moreover, interstitial fibrosis is observed, further hindering systolic and diastolic cardiac function. Although the dichotomy between adaptive and maladaptive hypertrophy events are a long studied phenomena, mechanisms that determine the transition from the first to the second, and therefore, the transition to overt heart failure, are still poorly understood (Frey *et al.*, 2004; Baba and Wohlschlaeger, 2008). Figure 4 shows the main stages and characteristics of cardiac hypertrophy:

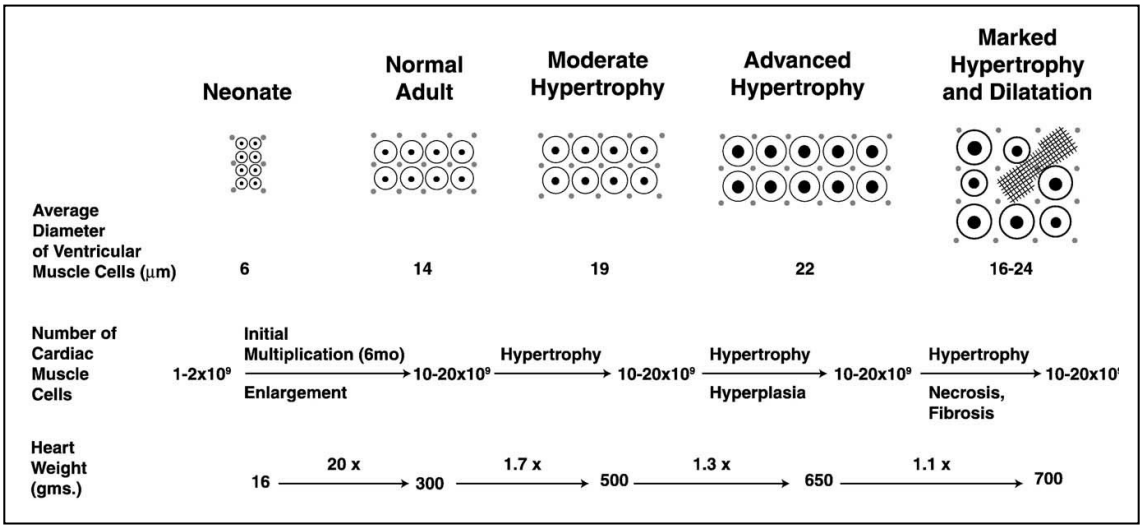

Figure 4 - Cellular basis for growth, hypertrophy, and failure of the human heart. This figure depicts various stages in the growth of the myocardium and the myocardial response to chronic stress (Buja and Vela 2008).

1.3 Cardiomyocyte development

The heart is hollow muscular organ composed by cardiac muscle (epicardium, myocardium, and endocardium) and connective tissue. Cardiomyocytes or myocardiocytes/cardiac myocytes (CMs) are binucleated or multinucleated cells that compose the myocardium being located at the walls. Cardiac muscle is one of the three major types of muscle along with skeletal and smooth muscle (Lee, 2010). Each CM contains myofibrils, which are long chains of sarcomeres, the contractile units of muscle cells. The CMs composing the myocardium, are responsible for the heart contraction and, therefore, for the heart's blood pumping throughout the cardiovascular system.

For more than 150 years, the heart regeneration was deeply studied and extremely controversial. Contradictive theories lead the discussion about the proliferation and self-renewal of mammalian adult CMs (Laflamme and Murry, 2011).

1.3.1 Embryogenesis

During the mammalian embryogenesis there is extensive CM proliferation, which is essential for the heart construction and organization (Mollova *et al.*, 2013). Shortly after birth, CMs undergo one last round of DNA synthesis without cytokinesis, resulting in the formation of mostly binucleated CMs. After this moment, cell cycle re-entry is blocked to the CMs, indicating a permanent cell-cycle withdrawal; cell division ceases and postnatal heart growth is achieved through hypertrophy of CMs (Lee, 2010; Ptaszek *et al.*, 2012; Mollova *et al.*, 2013). This switch in the growth potential of CMs, from a proliferative cell phenotype to an exclusively hypertrophic phenotype, occurs at different stages of development in different species. In the mouse it occurs at or shortly after birth, in the rat it occurs between 3 and 4 days post-natally, whereas in humans, CMs do not divide after 7 months of age (Bicknell, Coxon and Brooks, 2007). This process of nuclear division without cellular division is a specific form of endoreduplication, called acytokinesis mitosis. This phenomenon is shared by the most part of the mammals, as a consequence of DNA replication without cell division, leading to binucleated CMs, although the degree of binucleation varies from specie to specie, and represented at Figure 5 (Lee, 2010).

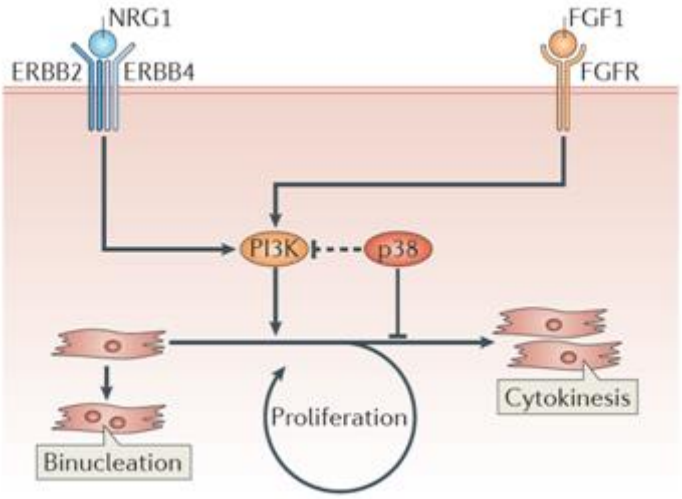

Figure 5 - Cardiomyocyte re-entry into the cell cycle by activating PI3K, leading to DNA synthesis and cytokinesis. However, most cardiomyocytes in mice become consequence of DNA replication without cell division (Xin, Olson and Bassel-Duby 2013).

1.3.2 Adult transition

Contradictive theories lead the discussion about the proliferation and self-renewal of adult cardiomyocytes, wherein it is hypothesized that they cannot perform such events because they are terminally differentiated, which involve two closely linked phenomena:

permanent withdrawal from the cell cycle and cell type-specific differentiation characterized by the upregulation of a panel of tissue-specific genes. For instance, fetal or neonatal rodent cardiac myocytes primarily express ß-myosin heavy chain (ß-MHC) and skeletal actin, but as cardiac myocytes undergo the process of terminal differentiation, these are downregulated and both α-MHC and cardiac actin upregulated (Laflamme and Murry, 2011). Consequently, although often used interchangeably in differentiated cell types, cell cycle exit and terminal differentiation are not synonymous. Usually, terminally differentiation is defined as the situation in which the majority of cells do not reenter the cell cycle in response to mitogens or normal physiological stress (Laflamme and Murry, 2011). Although cell cycle reentry occurs in CMs in response to stress or injury stimulus, there is cumulating evidence that it also occurs to a limited extent in the adult normal heart (Bergmann *et al.*, 2009; Laflamme and Murry, 2011). Studies have suggested that entrance of human CMs into the cell cycle after myocardial infarction is transient and limited and that, as opposed to cytokinesis and proliferation, it leads to endoreduplication (increased DNA per nuclei or increased nuclei per myocyte) (Ahuja, Sdek and Maclellan, 2007). Endoreduplication may account for the discordance between the observed regenerative capacity of the heart after injury and that proposed based on pathological examination of cycling myocytes (Ahuja, Sdek and Maclellan, 2007; Ptaszek *et al.*, 2012).

Others believe that the existence of cardiac stem cells or cardiac progenitor cells (CPCs) are responsible for CM proliferation associated with active mitotic processes accompanied by cytokinesis, resulting in a significant turnover and self-renewal of these cells after heart injury (Ahuja, Sdek and Maclellan, 2007). Most recently, the debate regarding the biological basis for CM renewal has undergone a major shift based on the recognition of the importance of stem cells in the biology of all organs of the body. These stem cells are recognized by the properties of continuous self-renewal and the potential for the production of a wide range of cellular progeny (self-renewing, clonogenic, and multipotent cells) (Buja and Vela, 2008). There is now evidence that stem cells from the bone marrow gain access to the circulation and migrate to other sites of the body during fetal development and likely contribute to the primitive cell population of multiple organs. These stem cells are localized to specialized regional environments referred to as niches (Pagliari *et al.*, 2011). These various populations of stem cells are now considered to be an important source of cells and could be involved in limited CM turnover and renewal (Pagliari *et al.*, 2011). Thus, in a paradigm shift, there is increasing recognition that the heart is a self-renewing organ. However, once committed to the myocyte lineage, the progeny of the stem cell can only undergo three to four rounds of cell division before permanently withdrawing from the cell cycle (Ahuja, Sdek and Maclellan, 2007; Pagliari *et al.*, 2011). Thus adult hearts, regardless of species, are likely composed of predominantly terminally differentiated myocytes that do not reenter the cell cycle, with a minority of myocytes or resident stem cells that are capable of some limited cell cycle reentry (Ahuja, Sdek and Maclellan, 2007; Pagliari *et al.*, 2011).

1.4 Pluripotent and multipotent stem cells for disease modeling

The stem cell field can be conceptually organized into work involving endogenous and exogenous cells. The many exogenous cell types can be further divided into pluripotent cells (such as embryonic stem cells, ESCs, and induced pluripotent stem cells, iPSCs) and multipotent cells of more limited potential (such as CPCs) (Laflamme and Murry, 2011).

For a cell to be considered pluripotent it needs to meet some requirements such as the ability: (1) to produce benign tumors (teratomas) in immunodefficient mice, which should consist of tissues arising from all three embryonic germ layers, such as cartilage, muscle, primitive neural cells and gastrointestinal tract tissue; (2) to generate chimeras, which demonstrates that cells can convey their genetic information to the next generation, assuring germline transmission (3) to express a set of specific markers associated with cell pluripotency (Freund *et al.*, 2010; Bianco *et al.*, 2013). Multipotency covers the above mentioned parameters, except for the first, since these cells are restricted to a limited range of cell types that they can give rise to (Freund *et al.*, 2010; Bianco *et al.*, 2013).

Since adult CMs are terminally differentiated and primary CMs cannot be maintained in cultured for long periods of time, stem cells offer a promising alternative for *in vitro* studies and generation of cardiac disease models, by allowing efficient and unlimited generation of CMs (although their differentiation appears to arrest at a fetal-like stage) (Beqqali *et al.*, 2009). Although animal models can better simulate the *in vivo* events associated to the heart hypertrophy, they lack of predictability when translating its mechanisms to human models (Musunuru, Domian and Chien, 2010).

1.4.1 Human embryonic stem cells

The term “embryonic stem cell” was introduced in 1981 to distinguish embryo-derived pluripotent cells from teratocarcinoma-derived pluripotent embryonal carcinoma (EC) cells (Martin, 1981). First ES cells were derived from mouse inner cell mass (ICM) in the same year, (Evans and Kaufman, 1981) and in 1994, Bongso and co-workers reported the successful isolation of human ICM cells and their continued culture for at least two passages *in vitro* (Bongso *et al.*, 1994). The first permanent human embryonic stem cell (hESC) lines were derived more than a decade ago by Thomson and co-workers (Thomson *et al.*, 1998) and these lines are still widely used.

HESCs are capable of proliferating extensively at undifferentiated state *in vitro* and have the ability to differentiate towards all three germ layers and furthermore can, in principle, give rise to all cell types of the body. This proliferative capacity makes these cells a powerful resource but it is also their disadvantage. Teratomas (benign tumors) are probably the most substantial risk associated to ESC-based therapies, and have been reported following transplantation (Wakitani *et al.*, 2003). Moreover, ESC-based therapies are allogeneic and require immunosuppression drugs. HESCs are usually derived from the ICM of the preimplantation-stage blastocysts that can later be differentiated into the different cell types

present in the human organism (Boheler *et al.*, 2002), as represented in Figure 6. Different embryonic cell lines can also be derived from the morula (Strelchenko *et al.*, 2004) or even from late stage (7-8 days) preimplantation embryos (Stojkovic *et al.*, 2004). This contributes to the ethical controversy surrounding their use. HESC express transcription factors and surface markers associated with an undifferentiating stage, such as Octamer-4, POU domain, class 5, transcription factor 1 (Oct4), Nanog, Sex determining region Y-box 2 (Sox2), stage specific embryonic antigen 4 (SSEA-4), tumor-related antigen 1-60 (TRA-1-60) and TRA-1-81(Hoffman and Carpenter, 2005). Telomerase and alkaline phosphatase activity of hESCs is high and the karyotype should be normal and remain unaltered during extended culture periods (Hoffman and Carpenter, 2005).

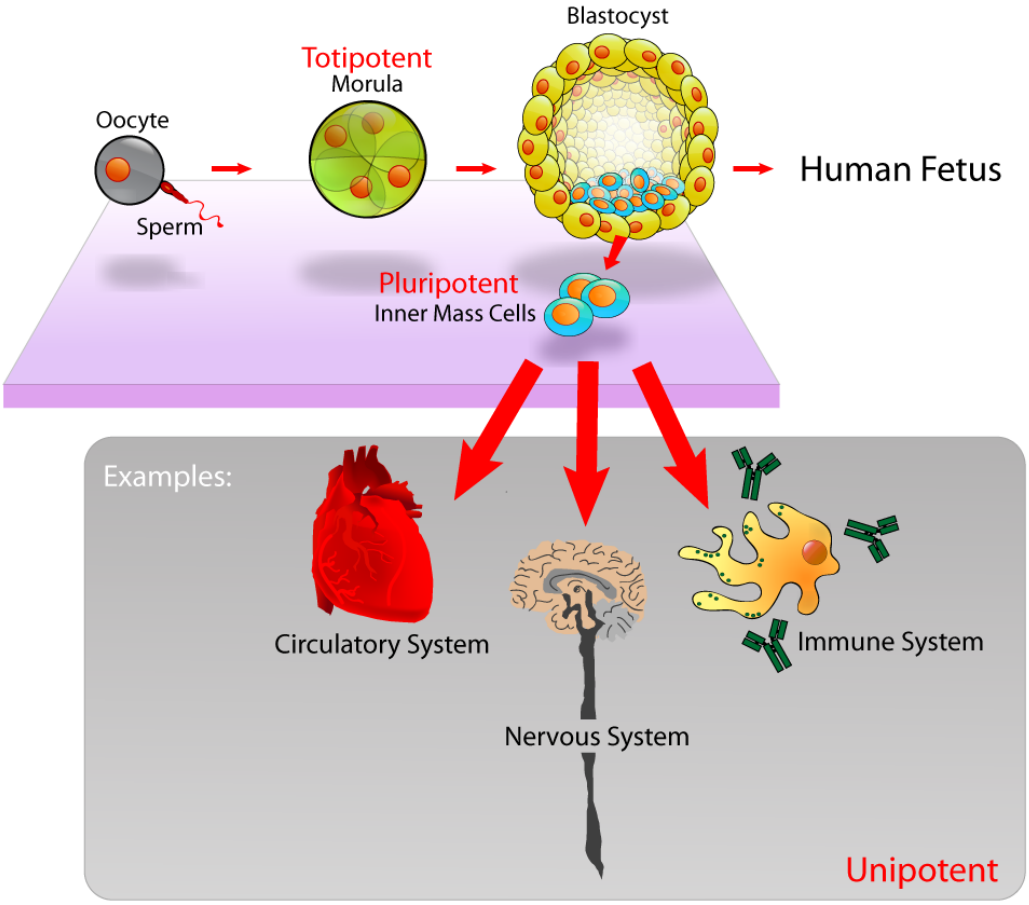

Figure 6 - Pluripotent, embryonic stem cells originate as inner mass cells within a blastocyst. The stem cells can become any tissue in the body, excluding a placenta. Only the morula's cells are totipotent, able to become all tissues and a placenta. (Jones, 2006)

In vitro differentiation of ES cells normally require an initial aggregation step that result in the formation of embryoid bodies (EBs) that spontaneously differentiate into the 3 primary germ layers (endoderm, ectoderm and mesoderm) (Wobus, Wallukat and Hescheler, 1991; Kehat *et al.*, 2001) and can be further stimulated towards the cardiac lineage by combinatorial addition of several factors from the Wnt, BMP, TGFß and FGF families (Beqqali *et al.*, 2009). Cardiomyocytes are readily identifiable, because within 1 to 4 days after

plating, they spontaneously contract. With continued differentiation, the number of spontaneously beating foci increase, and all the EBs may contain domains of beating cells. The rate of contraction within each beating area rapidly increases with differentiation, followed by a decrease in average beating rate with maturation. During early stages of differentiation, CMs within EBs are typically small and round (Wobus, Wallukat and Hescheler, 1991; Boheler *et al.*, 2002). The nascent myofibrils are sparse and irregularly organized or lacking, whereas others contain parallel bundles of myofibrils that show evidence of A and I bands. Adjacent CMs often show different degrees of myofibrillar organization. With maturation, ES cell–derived CMS become elongated with well-developed myofibrils and sarcomeres. Beating cells are primarily mononucleated and rod-shaped (Boheler *et al.*, 2002). They contain cell-cell junctions consistent with those observed in CMs developing in the heart. During terminal differentiation stages, densely packed well organized bundles of myofibrils can be observed, and the sarcomeres have clearly defined A bands, I bands, and Z disks. (Boheler *et al.*, 2002) Overall, the length, diameter, area, structure and architecture of ESC-derived CMs resemble that reported for fetal-to-neonatal rodent myocytes, although they can never reach the level of development of adult CMs (Boheler *et al.*, 2002).

1.4.2 Induced pluripotent stem cells

The cloning of the first mammal, "Dolly" the sheep, demonstrated that nuclei from a differentiated cell can be reprogrammed into undifferentiated state (Wilmut *et al.*, 1997). The cloning of Dolly was achieved by a technique called somatic cell nuclear transfer (SCNT), where the oocyte nucleus is replaced by a nucleus derived from a somatic cell. In principle, embryonic stem cells can also be derived from embryos produced by SCNT enabling the production of patient specific hESC lines. However, this technique has major ethical reservations, since human embryos would be produced only for ES cell production and a large number of human oocytes would be needed. In addition, many countries have prohibited human cloning by law (Yamanaka, 2008).

The technology to reprogram somatic cells to pluripotent stem cells (induced pluripotent stem or iPS cells), for the first time described in 2006 by the Japanese group headed by Yamanaka, had a major impact on the field of stem cell biology. Similar to hESC, human iPS cells have the potential to differentiate to any cell type of the human body, including cardiomyocytes. The advantage is that generation of iPS cells do not include embryo manipulation and destruction, and they could be used in autologous therapies without immune rejection since they can be derived from the patient's own somatic cells (Laflamme and Murry, 2011). Since iPS cells can be derived from specific groups of patients, it may be important for human disease modeling, since they carry the patient's genetic material (Beqqali *et al.*, 2009). The disease modeling process regarding these cells are schematized in Figure 7.

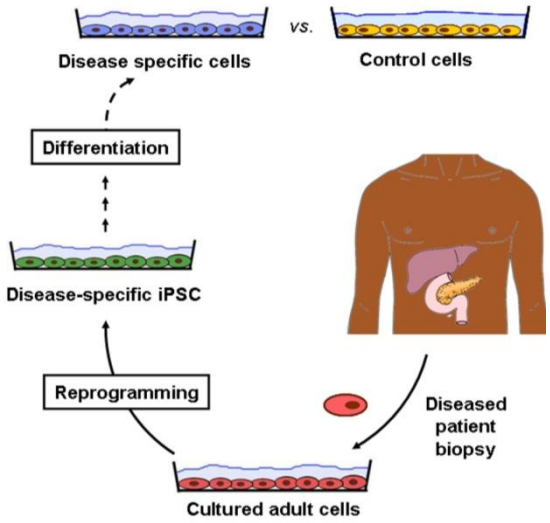

Figure 7 - Human disease modeling by extraction of patient's own cells, reprogrammation and differentiation into specific cells. (Adapted from Cincinnati Children's Hospital Medical Center, 2011)

HESC contain factors that can induce reprogramming of somatic cell nucleus (Cowan *et al.*, 2005, Allegrucci *et al.*, 2007). Therefore somatic cell fusion with ES cell regenerates pluripotent cells. However, pluripotent cells obtained by fusion contain both chromosomes from the ES cell and from the somatic cell resulting in rejection if implanted (Yamanaka, 2008). Nevertheless, the above-mentioned findings led researchers to search for factors that induce reprogramming. Finally, in 2006, Takahashi and Yamanaka discovered that by introducing four "pluripotency genes" (genes identified previously as being prominently expressed in ESCs: e Oct4, Sox2, Klf44 and c-myc) mouse embryonic as well as adult fibroblasts could be reprogrammed into pluripotent stem cells and able to form all cells in the body of an adult mouse (Takahashi and Yamanaka, 2006; Freund *et al.*, 2010; Laflamme and Murry, 2011). The following year the same factors were used to make induced pluripotent cells (iPS cells) from human fibroblasts (Takahashi *et al.*, 2007). Human iPS cells were also obtained, contemporaneously, by Thomson and co-workers, in 2007, by using Oct4 and Sox2 in combination with Nanog and Lin-28 homolog (Lin28) instead of c-myc and Klf4 (Yu *et al.*, 2007). Ever since, the development in this field has been very intensive and this technique has been designated as a major breakthrough in stem cell research. Recent developments in the field were registered in Netherland, by the Christine Mummery group, where human iPS cell lines were derived from skin fibroblasts and reprogrammed by retroviral overexpression of the four transcription factors Oct3/4, Sox-2, Klf4 and c-myc (Freund *et al.*, 2010). After retroviral infection, colonies displaying the typical morphology of human embryonic stem cells emerged and proved self-renewal and differentiation in a wide spectrum of cell phenotypes when appropriately stimulated in culture, including CMs (Freund *et al.*, 2010). Ever since, the development in this field has been very intensive and this technique has been designated as a major breakthrough in stem cell research.

1.4.3 Cardiac progenitor cells

Over the past decade, extensive studies have provided the evidence of a reservoir of cardiac stem/the cardiac progenitor cells (CPCs) (Messina, Giacomello and Marbán, 2007; Beqqali *et al.*, 2009), within the adult heart, either derived in the heart or recruited from the bone marrow through the bloodstream (Di Nardo *et al.*, 2010). Studies revealed that these endogenous cells express markers normally related to stem cells (c-kit, MDR-1 and Sca-1) and harbor telomerase activity, characteristics only related to "stemness". (Barile *et al.*, 2007; Guan and Hasenfuss, 2012) The *in vivo* evidence for the replicative feature of these CPCs was emphasized for the fact their number registered more than a 13-fold increase in the hypertrophic myocardium of heart disease patients, able to differentiate in CMs. (Barile *et al.*, 2007) Contrariwise to what was previously considered, these evidences point for the fact that the heart is not completely terminally differentiated and instead is capable of limited proliferation. Although lineage tracing and isolation of these cells could already establish their identity and multipotency, protocols to reliably purify, expand and differentiate the CPCs are necessary for their practical use as disease models (Beqqali *et al.*, 2009; Musunuru, Domian and Chien, 2010).

1.5 Advances in cardiac disease characterization

1.5.1 Extracellular matrix in cardiomyocyte differentiation

Cells are extremely influenced by the signalling cues originated from the extracellular matrix (ECM), which provides them with structural and biochemical support, and contributes not only to individual cellular but also to collaborative organ-level functions. In cardiac physiology, the ECM induces mechanical, electrical and chemical signals during development, homeostasis and injury. These signalling mechanisms modulate in cellular interactions and activities interactions, such as proliferation, migration, adhesion and changes in gene expression (Bowers, Banerjee and Baudino, 2010). The components of the ECM can either play an agonistic or antagonistic role, contributing to the progression towards either heart recovery or heart failure, during cardiac disease period (Miner and Miller, 2006). The understanding of the paradoxal relationship between cellular and acellular signals that are involved in cell-ECM interactions is vital for proper cell-cell communication and cell behaviour in the development of the heart (Miner and Miller, 2006; Bowers, Banerjee and Baudino, 2010). The ECM also plays a fundamental role, particularly, during the embryonic development, by guiding stem cell differentiation into the different lineages, and, specifically in the heart, it is imperative the presence of these components so organ differentiation can occur. Different ECM components can selectively affect many types of signal transduction pathways that result in different cell response and behaviour (Streuli, 1999).

It has been shown that cells can be maintained in *in vitro* culture much more efficiently if they are supported on substrate components that closely resemble the ECM in

which they occurred in vivo (Baharvand *et al.*, 2005). The establishment of adequate *in vitro* conditions, that mimic the in vivo differentiation process, still represents a challenge concerning the derivation of pluripotent cells into CMs. The ECM of CMs is primarily composed by: type I, II and III collagen; laminin, type IV collagen mainly (basement membrane); fibronectin, entactin and several proteoglycans, such as heparan sulphate, (pericellular membrane); and also proteinases (Farhadian *et al.*, 1996; Pelouch *et al.*, 1994). Combinations of these molecules would beneficiate the differentiation of stem cells into a state resembling native cardiomyocyte's phenotype and genotype.

With the establishment of ESCs cultures it became possible to study the differentiation of these pluripotent cells *in vitro* and the success in CM adhesion and development to the experimental surface and, as previously related, ECM components have a special role in this subject. In fact, it is expected that a balanced composition of specific ECM proteins and/or molecules ensure adequate adhesion and promote CM differentiation. Table II presents the most important ECM compounds and their function, which demonstrated positive results in the differentiation of ESCs into cardiomyocyte-like cells.

Table III - Revision of the ECM components used for ESC differentiation and development into cardiomyocyte-like cells

ECM component	Function	References
Vimentin	Cardiomyocyte flexibility	Boheler *et al.*, 2002
Desmin	Cardiac muscle formation	Boheler *et al.*, 2002
β_1-integrin	Cardiac differentiation, expression of α-MHC and β-MHC, arrange of sarcomeric architecture	Boheler *et al.*, 2002
Collagen I	Mechanical stability, cell attachment, differentiation and angiogenesis	Boheler *et al.*, 2002; Horton *et al.*, 2009
Collagen IV	cell-ECM adhesion, transmission of force during diastole and systole, binds to laminin	Pelouch *et al.*, 1994; Wu *et al.*, 2010
Laminin	Cardiomyocyte adhesion, growth, proliferation, differentiation, cardiomyogenesis, binds to collagen IV	Bruggink *et al.*, 2007
Fibronectin	Cardiomyocyte adhesion, proliferation, migration, differentiation, angiogenesis, binds to collagens and heparin	Horton *et al.*, 2009; Wu *et al.*, 2010
Heparan sulfate	Developmental processes, angiogenesis, inhibition of AngII-induced hypertrophy	Akimoto *et al.*, 1996; Strunz *et al.*, 2011
Entactin/Nidogen-1 (NID-1).	Cardiomyocyte structural support and growth regulatory functions, crosslinking of collagens and laminins	Grimm *et al.*, 1998; Yurchenko and Patton, 2009

1.5.2 Protein patterning

Protein pattern is a valuable tool to evaluate CM hypertrophy phenotype *in vitro*. Despite of guiding CM differentiation of ESCs, the patterns also allow size and shape control of the cells. It was recently shown that the imposed geometrical boundaries of the ECM proteins promote sarcomere alignment by altering the myocyte shape and directing the orientation of the myofibrillar network (Bray, Sheehy and Parker, 2008). Cells react to the patterns by architecturally reconfigure, reassemble and reorganize their contractile cytoskeleton in response to the geometrical cues in the ECM proteins (Bray, Sheehy and Parker, 2008). Since it is denoted morphology alterations in cardiac myocytes during hypertrophy and being these cells morphological inconstant, when in culture, it is necessary a procedure to control cell size and shape, in order to standardize those parameters. When size and shape conditions are imposed to these cells, a hypertrophic stimuli can be applied and morphological changes can be quantified, allowing a better understanding of the hypertrophy condition, associated to several heart diseases. Several techniques that have been developed to pattern proteins on planar substrates can be used to achieve such cell control and will be revised next.

Photolithography

For many years, the semiconductor industry has developed and optimized the photolithographic methods to create high resolution features in semiconductors and metals. In photolithography, a substrate is coated with a photoactive polymer. When specific regions of this polymer are selectively exposed to UV light, the solubility of the exposed regions is altered, such that they can be dissolved while leaving the unexposed regions unaffected (or vice versa, depending on chosen photoactive polymer) (Britland *et al.*, 1992; Lom, Healy and Hockberger, 1993). Further, this development step leaves portions of the underlying substrate exposed to modification, such as etching, doping, or metal coating.

More recently, these methods have been applied to generate protein patterns. In general, the substrate regions that have been exposed after the development step are functionalized in order to bind, or promote binding, of target proteins. For example, an exposed silicon dioxide surface may be covalently modified with an aminosilane, leaving a reactive amine group which can preferentially bind proteins (Britland *et al.*, 1992; Lom, Healy and Hockberger, 1993).

Photolithography is a mature technology, optimized over many years by the semiconductor industry, and this extensive development makes it an attractive technique for microscale protein patterning. The resolution of these techniques is fundamentally limited, though, by the diffraction limit of the light used during exposure. Additionally, the harsh chemicals typically used limit the compatibility of the process with biological media, though progress has been made in the development of biocompatible photoresists (Douvas *et al.*, 2002).

Microcontact printing

Microcontact printing (μCP) is a form of soft lithography and is able to perform fast and efficient adhesive micropatterns of proteins that can be used to control individual cell shape and adhesion patterns. It is a stamping based method technique where a polymeric mold (stamp) is fabricated from a template (master) (Bernard *et al.*, 1998; Xia and Whitesides, 1998; Kane *et al.*, 1999; Quist *et al.*, 2005; Ruiz and Chen, 2007). The process can be subdivided into three parts: fabrication of the master, micropatterned stamp fabrication and content deposition, as schematized on Figure 8 (Théry and Piel, 2009). To create the stamp, containing the microfeatures of interest for subsequent microcontact printing, the first step is to fabricate a master. The master is created from a silicon wafer and from the application of a photoresist mask on its surface. The wafer is spin coated so the photoresist coated the entire wafer. Then, it is exposed to UV light in the desired regions of photoresistance which are etched. The topography of the wafer is altered, according to regions that are exposed to the radiation, the final step of creating the master. From this template it is possible to obtain replicates (stamp), containing the microfeatures on the surface, by casting a PDMS solution onto the master, followed by baking it in the oven. Afterwards, the stamp can be removed from the master and is ready to be used. This process is schematized in Figure 8A. Subsequently, a drop of protein solution "ink" is deposited on the stamp, it is dried after a incubation period and it is brought into gentle contact with the substrate to be modified, as represented in Figure 8B (Bernard *et al.*, 1998; Xia and Whitesides, 1998; Kane *et al.*, 1999; Quist *et al.*, 2005; Ruiz and Chen, 2007). The protein solution is transferred from the protrusions in the stamp to the substrate (Bernard *et al.*, 1998; Xia and Whitesides, 1998; Kane *et al.*, 1999; Quist *et al.*, 2005). In some cases the substrate requires to be spin-coated previously to the microcontact printing, depending on the type of substance that composes the material (e.g. substrates composed by silica such as glass). This arises from the fact that the wettability degree of the material needs to be enhanced for a proper ink bonding, which can be achieved by chemical activation of the substrate (Blinka *et al.*, 2010). However, in the case of silica based materials it is required a complex chemical activation for a long-term stability, where another type of surface modification, such as Polydimethylsiloxane (PDMS) coating, by spin coating, can offer a better solution for being suitable for usual chemical activation (Griffin, 1954; Kaufmann and Ravoo, 2010; Blinka *et al.*, 2010). In brief, spin coating is a technique used for the application of thin films into a substrate surface, by depositing a small puddle of a fluid resin or a solution onto the center of a substrate and then spinning the substrate at high speed to thin the fluid and spread all over the surface (Théry and Piel, 2009).

The use of a broadly biologically friendly polymer, PDMS, for the stamp material makes this technique highly biocompatible (Bernard *et al.*, 1998; Xia and Whitesides, 1998; Kane *et al.*, 1999). Depending primarily on the technique used to fabricate the initial template from which the stamp is generated, this technique is capable of features from hundreds of microns down to tens of nanometers (Csucs *et al.*, 2003). Some disadvantages of

this technique lie in the potential of the flexible polymeric stamp to generate deformed or distorted patterns, non-uniformity of coverage over the patterned area, and potential for surface contamination of the same (Torres *et al.*, 2008).

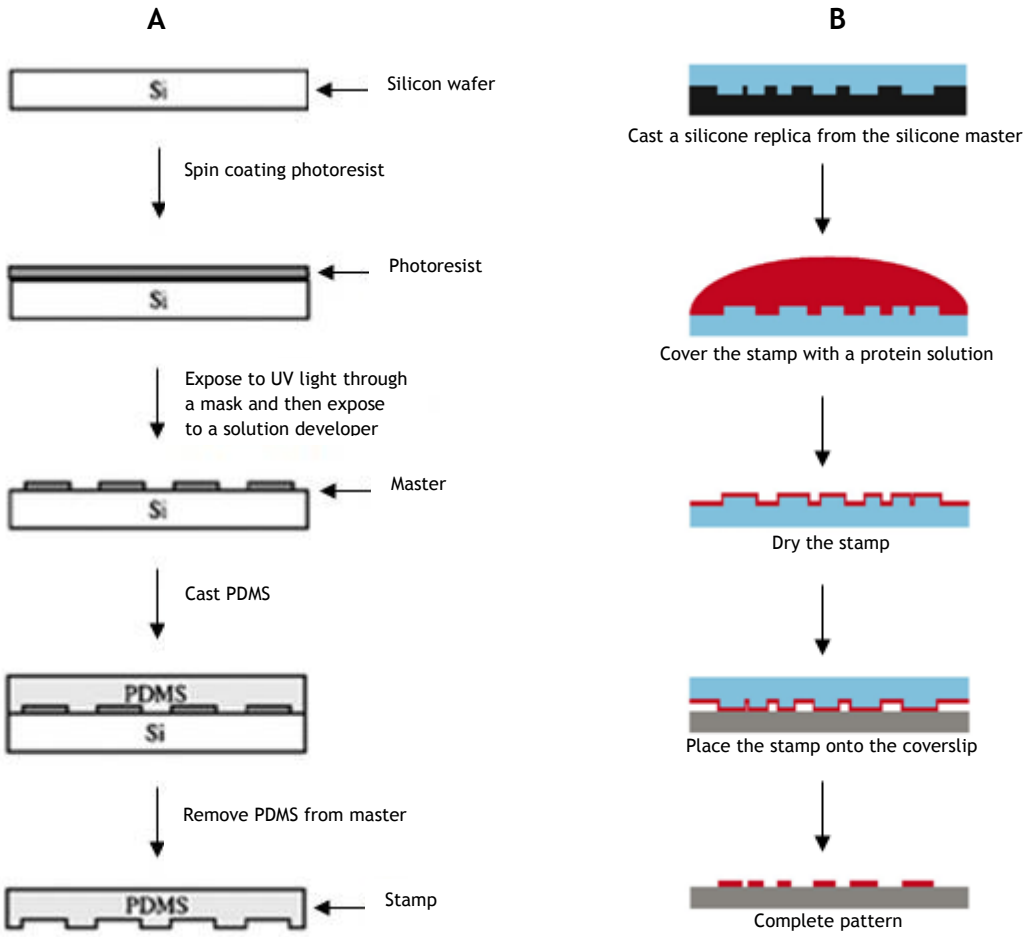

Figure 8 - Resumed microcontact printing process. (A) The steps involved in producing molds by photolithography and subsequent stamp (adapted from Gonzalez-Macia *et al.*, 2010); in (B) is schematized the stamping process of the molecules of interest onto the substrate (coverslip) (adapted from Von Philipsborn *et al.*, 2006).

Dip-pen nanolithography

Patterning via dip-pen nanolithography is similar conceptually to writing using a quill and ink. An atomic force microscope (AFM) tip is dipped in an "ink" solution containing protein or a cross-linking molecule, which will bind protein in subsequent steps. The coated tip is then dragged across the substrate, leaving a trail of target molecule in the vicinity of its path, patterning directly on a variety range of substances. This technique is capable of very small feature sizes, down to tens of nanometers, and can conceivably place an arbitrary number of different protein types by using different ink solutions (Piner *et al.*, 1999). Thus, it is one of the few existing methods that are capable of generating arrays with hundreds of features (Lee *et al.*, 2006). However, due to its serial nature and the limited amount of "ink" that can be loaded on each loaded tip, this technique is slow and cannot easily generate large patterns.

Ink-jet printing

The ink-jet printing of proteins makes use of a mechanism very similar to what one would find in a desktop ink-jet printer. It is a versatile technique widely used for the direct-writing of two-dimensional features, and increasingly, for three-dimensional structures (Delaney, Smith and Schubert, 2009). It can be divided into two categories: drop-on-demand and impulse inkjet, whereby droplets are generated when required and patterned onto the substrate. Ink-jet printing can also be subdivided according to the mechanism mode in which the droplets are created, such as piezoelectric, thermal and electrostatic (Delaney, Smith and Schubert, 2009). In general, a protein-containing solution is loaded into a channel and pressure is applied on the fluid in the same channel, for example by expansion of a piezoelectric wall or rapid localized heating, causing a droplet of solution to be expelled onto a substrate (Pardo, Wilson and Boland, 2003; Roda *et al.*, 2000; Barron *et al.*, 2005).

This technique is relatively inexpensive, simple, and based on existing commercial technology. By placing the protein solution only in designated regions, the technique avoids problems associated with non-specific binding of target proteins outside of the desired region. Waste and contamination are reduced with this technique. Its primary disadvantage is that the feature size is generally limited to tens of microns (Barron *et al.*, 2005).

Self-assembled patterns

A variety number of techniques have demonstrated that under certain conditions, molecules may self-assemble into distinct geometries. These shapes can be functionalized, generating protein patterns which follow the self-assembled geometries, or act as a mask for functionalization of the underlying substrate. For example, some groups have used micro- or nano-scale spheres which self-assemble into a close-packed pattern on a surface to create a colloidal mask. Biomolecules can be adsorbed in the interstices between the spheres, leaving a hexagonal pattern of the target biomolecule on the surface after the spheres are removed. Protein feature sizes down to tens of nanometers have been demonstrated with this technique (Cai and Ocko, 2005; Valsesia *et al.*, 2006).

Other groups have used lattices of DNA tiles to create protein arrays. The sticky ends of the DNA tiles are engineered to self-assemble into a regular array. Periodic patterns of the protein streptavidin were demonstrated by Yan *et al.* by incorporating a biotin group in the center of each tile, giving a regular spacing between individual streptavidin molecules of approximately 19nm (Yan *et al.*, 2003). By engineering multiple tiles which self-assemble into more complicated geometries, and incorporating biotin into only a portion of them, the spacing between streptavidin molecules can be modified (Park *et al.*, 2005).

Bacterial membrane support proteins, S-layers, self-assemble into periodic lattices of various geometries, and have also been functionalized to serve as a scaffold to generate regular periodic patterns of biomolecules such as streptavidin, with individual proteins arrayed with approximately 10nm spacing (Sleytr *et al.*, 2007).

Broadly, these self-assembly techniques are capable of generating periodic patterns with extremely small feature sizes over wide areas. However, it is a quite rudimentary technique that limits the variation and control of the resultant geometries. The feature size and spacing over the entire patterned region are predetermined by the choice of templating molecules or particles (Sleytr *et al.*, 2007).

1.5.3 High-throughput bioimaging systems

Recently, the combination of the High-Throughput Screening (HTS) technology with High Content Imaging (HCI) has been arousing interest in the research community (Unterreiner and Gabriel, 2011). This evolution was possible mainly due to the hardware improvements of the automated microscopes, as the auto-focusing, as well as the enhancement of the image analysis software enabling fast data acquisition saving both time and costs in the screening process (Zanella, Lorens and Link, 2010; Unterreiner and Gabriel, 2011; BD Biosciences, 2007) HCI can be characterized by the use of fluorescent label techniques to track phenotypic alterations in cells (Zanella, Lorens and Link, 2010). It enables simultaneous assays of multiple cellular targets allowing the extraction of numerous features within a single experiment (Zanella, Lorens and Link, 2010; BD Biosciences, 2009) It provides cellular or sub cellular resolution and generates data in a fast fashion. These assays can give different insights of the compound's action as well as their unspecific effects (e.g. toxicity) (Unterreiner and Gabriel, 2011; BD Biosciences, 2007; BD Biosciences, 2009) The disadvantage of this technique relies on the limited throughput that can be offered, due to the complexity of the HCI assays (Unterreiner and Gabriel, 2011). For the other hand, automated HTS assays are able of performing fast screenings and of fast data acquisition of multiple compounds simultaneously but with limited resolution, relevant for biological and chemical fields (Unterreiner and Gabriel, 2011; Major, 1998; Macarron *et al.*, 2011; Martis, Radhakrishnan and Badve, 2011). High-Throughput HCI assays are the resulting combination of both worlds enabling fully automated primary screenings of large amount of samples with high resolution acquisition in multiplexed mode (Unterreiner and Gabriel, 2011). In Table IV it is revised some of the commercially existing bioimaging systems and some characteristics:

Table IV- Available high-throughput bioimaging systems. (Adapted from Comley, 2005; Zanella, Lorens and Link, 2010).

Company	Brand name	Light source	Optics*
Amnis	ImageStream	Laser/Arc lamp	WF
BD Biosciences	BD Pathway 855	Arc lamp	WF/CF
BD Biosciences	BD Pathway 435	Arc lamp	WF/CF
GE Healthcare	IN Cell Analyzer 2000	Arc lamp	WF
Intelligent Imaging Innovations	3i Marianas	Arc lamp	WF
Leica Microsystems	TCS SP5	Laser	CF
Molecular Devices	ImageXpressULTRA	Laser	CF
Molecular Devices	ImageXpressMICRO	Arc lamp	WF
Olympus	Scan^R	Arc lamp	WF
Perkin Elmer	Opera	Laser	CF
Perkin Elmer	Operetta	Arc lamp	WF/CF
Thermo Scientific	Cellomics ArrayScan VTI	Arc lamp	WF/CF
Thermo Scientific	CellWoRx	Arc lamp	WF
TTP Labtech	Acumen eX3	Laser	WF

*Abbreviations: CF, confocal microscope; WF, wide field.

1.5.4 Cellular phenotypic characterization

For decades, the visualization of cells on the microscopy was the primary method for cell identification, characterization and function (Carpenter *et al.*, 2006). While nothing can fully replace the expertise of an experienced biologist, observing a vast set of samples by eye is a time-consuming, subjective and non-quantitative (Lamprecht, Sabatini and Carpenter, 2007) and nowadays that method substituted. By fluorescently label specific proteins or antigens of cells, by immunocytochemistry techniques, they can be localized with the detection of the different wavelengths associated to the dyes coupled to the secondary antibody used in this cell staining technique (Rojo, Bueno and Slodkowska, 2009). The different cell stainings can be detected by HCI systems, mentioned in the previous subsection, and stored as an image format (Unterreiner and Gabriel, 2011). Software for image analysis are available using specific algorithms that can automatically analyze specific features of images, providing several advantages, such as, speed, quantitative and reproducible results and simultaneous measurement of a huge variety of cell features (Lamprecht, Sabatini and Carpenter, 2007; Kamentsky *et al.*, 2011). Currently, innumerous image analysis software are commercially and freely available.

The open-source ImageJ, Image-Pro Plus and the Metamorph® are image processing programs able to read several image formats, perform several enhancing operations to them,

to perform some quantity analysis, such as cell counting, and still remain very flexible (Lamprecht, Sabatini and Carpenter, 2007; Schneider, Rasband, Eliceiri, 2012). Custom-made programs can be added to this software and be used to measure different cell features (e.g. area and pixel intensity) (Lamprecht, Sabatini and Carpenter, 2007). CellProfiler is an open-source platform for automated image analysis with several integrated cell measurements available, such as size, intensity and texture of fluorescent stains. (Lamprecht, Sabatini and Carpenter, 2007) Overall, these programs assemble characteristics, which are useful for phenotype characterization of determined cell types.

As referred previously, the cardiomyocyte hypertrophic phenotype is characterized by an increase of cell size and sarcomeres. Cell area measurements are the golden-standard method for the assessment of hypertrophy phenotype, *in vitro,* since it is the easiest type of feature that can be monitored (Dorn II, Robbins and Sugden, 2003). Sarcomere expression can also be monitored by evaluating the average pixel intensity within each cardiomyocyte.

1.6 Thesis overview

The herein dissertation reports the experimental design and the results obtained while attempting to create more suitable assays for the understanding of cardiomyocyte hypertrophy, a critical precursor to the progress into heart failure. This work was performed during an internship in the Leiden University Medical Center (LUMC), Leiden, Netherlands, under the supervision of Dr Robert Passier and Marcelo Ribeiro (PhD-student).

As stated before cardiomyocyte hypertrophy is a major determinant for cardiac disease and therefore it is important to understand the underlying mechanisms for cardiac hypertrophy and to identify druggable targets that may lead to new therapeutic approaches. Overall, we set out to replicate *in vitro* cardiomyocyte hypertrophy and thus to establish a system for modelling and further dissecting the disease mechanisms. Concomitantly, we went further to generate tools for specifically easing the phenotypic characterization of hypertrophied cardiomyocyte-like cells. A platform was designed and constructed by the use of a bottomless 96-well plate and the attachment of a protein patterned custom-made coverslip, acquired to specifically fit the bottom of the plate. The coverslips were patterned with a protein solution (initially a fibronectin solution) through the microcontact printing technique, before being attached to the plate. Following the platform attachment, ESC-derived cardiomyocytes were cultured on it and permitted to adhere to the fibronectin pattern, assuming their shape and orientation. Later on, other ECM proteins were tested alone and in combination to obtain the best CM adherence and development. Meanwhile, specific stimuli known to produce a hypertrophic effect on CMs were added to their environment. With the hypertrophic treatments the CMs suffer a morphological alteration, such as an increase in area, which is standardized by their adherence to the protein patterns. Cardiomyocytes grow in an irregular form and the protein patterns have the function to guide and lock the orientation and geometrical parameters of the cell growth. This intended to allow a more precise area measurement of the CMs and also to improve the readout for other

measurements, e.g. sarcomere intensity and elongation. These measurements were performed through the analysis of the images taken by the high throughput imaging system BD Pathway 855.

Considering that the existent techniques to evaluate the CM hypertrophy are still very ineffective and time consuming, this platform emerged from a need to optimize the process.

Chapter 2 Materials and Methods

2.1 Construction of the hypertrophy platform

2.1.1 Coverslip characteristics

Two types of coverslips were used: one made of a polycarbonate optical grade plastic, Lexan, (RD477624 – Hybrislip, Grace Bio-Labs) and the other made of glass material (NEXTERION® Coverslip custom, #4; Glass: D263; Edge finishing: cut; Cleaning level: uncleansed). Both of them were custom-made to possess specific dimensions, 110mm x 75mm, although with different thicknesses, 0.25mm and 0.50mm, for the glass and plastic coverslips, correspondingly. The two different coverslips required different methodologies and handling. While glass coverslips entail the need to be spin coated with a PDMS solution (as described in the next subsections) for subsequent microcontact printing, the plastic coverslips do not necessitate spin coating, and instead, microcontact printing can be performed directly.

2.1.2 Spin coating

A polydimethylsiloxane (PDMS) solution was prepared by mixing a polymer base and a curing agent (two-component, Dow Corning Sylgard 184) at a 10:1 mass ratio. The PDMS solution was centrifuged at 3000 rcf for 3 min in the Rotina 48R (Hettich) apparatus to remove air bubbles (Kroetch, 2004; Dow Corning Corporation, 2005). When the liquid was properly degassed it was ready to be poured.

The custom-made glass coverslips were spin-coated with the Laurell WS-650MZ-23NPP spin coater, after a cleaning process of the substrates with sonication in ethanol and dried by shortly submitting the substrate through a Bunsen burner. Different spin coating programs were designed and tested to efficiently coat such substrates with PDMS. The coverslip was placed on top of the chuck and the vacuum was turned on to fix the coverslip into it and then the PDMS solution was gently deposited on top of it, with a Pasteur pipette. Once this step is accomplished the program is started and the PDMS solution is spread all over the coverslip, which becomes covered with a soft layer of this hydrophobic polymer at the end of the procedure.

2.1.3 Stamp fabrication

A stamp was produced from a pre-existent master by casting a PDMS solution onto the master, which then was baked on the oven at 40 ºC for 1 hour. The PDMS solution was produced by mixing PDMS 527 (Dow Corning) part A with part B in a 1:1 mass ratio. After solidification, the PDMS was removed from the master, originating a negative copy of the micropatterns (lines) inscribed on the master. A stamp with approximately 60x40mm and lines inscribed with 20µm of width was produced.

2.1.4 Microcontact printing

Fluorescence fibronectin (FFN) was produced through mixing 200µl of 8M Guanidine Hydrocholoride (G3272 - 100G), 200µl of 1mg/ml fibronectin (FN; BD Biosciences fibronectin from human plasma) and 10µl of Alexa Fluor 546 Maleimide dye (Invitrogen). The resulting solution was incubated for 1h, and then loaded into a syringe and injected into a dyalisys membrane (Slide-A-Lyzer Dialysis cassette Prod#66333; Thermo Scientific). The membrane was placed between a floating pouch (Slide-A-Lyzer Bouys; Thermo Scientific) in phosphate buffered saline (PBS) solution overnight. Afterwards, the solution was taken from the membrane and divided into aliquots for further use.

A FN/FFN solution was prepared from a mixture of 1mg/ml FN and 0,5mg/ml FFN in a 1:1 ratio, which were diluted in distilled water in order to obtain a final concentration of 50 µg/ml and stored away from the light. Drops of FN/FFN solution were deposited onto the stamp, assuring that the entire surface would be totally covered. The stamp was left in incubation for 30 minutes (or 1 hour if it was the first usage of the stamp) so the fibronectin could adsorb to the surface.

Meanwhile, the substrate (coverslip) was chemically activated by being exposed to plasma radiation in a remote plasma reactor, to avoid direct bombardment of the surface, between 20 and 30 mA for 30 seconds (Lopera and Mansano, 2012). Plasma treatment was performed to raise the surface energy of the material, and in turn increasing also its wettability, improving its bonding characteristics regarding a posterior inking. Afterwards, the coverslip was immediately stored in a covered Petri dish to avoid contamination.

Then, the fluorescence-labeled FN solution was aspirated from the stamp, which was immediately dried with nitrogen gas. Finally, the micropatterned face of the stamp was placed in contact with the substrate (coverslip) and gentle pressure was applied in it. After 1 minute, the stamp was removed and the FN micropattern was printed on the coverslip.

2.1.5 Attachment process

Spin coating and microcontact printing techniques, above described, were combined in order to obtain protein micropatterns in the glass coverslips. As stated before, the protein micropatterns can be obtained directly by microcontact printing, regarding the plastic coverslips. This construct will be used for cell culture, enabling control of cell's shape and orientation.

Since coverslips had the same dimensions of the bottom of the bottomless 96-well plates, they could fit and be attached to these well plates. For this procedure, High-Vacuum Grease (Dow Corning) was used, which was carefully spread with a syringe onto the bottom of the plates. This silicone lubricant was chosen as glue because of its biocompatibility and effective sealing capacity. After assuring that the entire spaces between the wells were filled with this glue, the patterned side of the coverslip was placed in contact with the bottom of the plate, and a uniform pressure was applied with a cylinder roll. In an attempt to optimize this time-consuming process, a double sided tape (0,13mm thick adhesive film, 3M) was used in alternative, so that one of it sides could be attached to bottom of the well plate and the other attached to the coverslip.. However, it was necessary to cut circular holes in the tape with the same diameter and position of the wells, so the coverslip could be overlapped and fill those wells.

2.2 Cell culture

2.2.1 Origin of cell lines and ethical approval

To enable purification and characterization of the hESC-derived cardiomyocytes, sequences encoding enhanced GFP (eGFP) were introduced into the NKX2-5 locus by homologous recombination, giving origin to the NKX2-5$^{eGFP/w}$ hESC line (Elliott *et al*, 2011). These cells can be either differentiated as embryiod bodies or by culture with END2, developing GFP+ contractile areas by day 8-9. (Elliott *et al*, 2011) The hESC line used with the targeted NKX2-5$^{eGFP/w}$ was the HES-3 and it was first derived in the ES Cell International Pte Ltd. - hES Cell Provision (Singapore). This cell line was generated by isolation of the inner cell mass, developing teratomas upon inoculation beneath the testis capsule of SCID mice. (Reubinoff *et al*, 2000) It was derived with the donor's informed consent and approved by the Institutional review board.

2.2.2 HESC-derived cardiomyocytes handling

HESC-derived cardiomyocytes already in a differentiated state, through spin EB method, were acquired directly from Pluriomics (Pluricyte-Cardiomyocyte, NKX2-5$^{eGFP/w}$ line). They are frozen at day 14 of differentiation and it is advised to thaw them in 37 degrees waterbath for 4 minutes. They were gently transferred to a 50ml falcon tube and it was added 1ml of Cardiomyocyte medium (Pluriomics) at RT drop by drop every 4-6 seconds while gently swirling the cells after each addition. Another 1ml of Cardiomyocyte medium was added to the cardiomyocytes in the same drop-wise fashion while swirling the cells. Then, 3.7ml of Cardiomyocyte medium was added drop by drop every 2-4 this time, while swirling the cells. They were spun for 3 minutes at 1100rpm and resuspended in appropriate amount of Cardiomyocyte medium, depending on plating conditions. A sample of the cell suspension was taken and diluted in a 1:1 ratio of Trypan Blue (Sigma-Aldrich). The sample was then transferred to a Neubauer Chamber for cell counting purposes. Cells were finally plated at the desired density.

2.3 Cardiomyocyte hypertrophy experiment

2.3.1 Matrigel and fibronectin preparation

BD Matrigel™ Matrix Growth Factor Reduced (GFR) (BD Biosciences) was thawed by submerging the vial in ice at 4ºC. Once it was thawed, the vial was swirled to ensure that the material was evenly dispersed. Tips, tubes and medium were pre-cooled before in contact with BD Matrigel™ Matrix GFR. It was diluted in 1/10 using serum-free cell culture medium DMEM-F12 (Gibco®). A volume of 50µl of the diluted BD Matrigel™ Matrix GFR was added to each well. The plate was then incubated at RT for one hour before use.

Fibronectin 1mg/ml stock was thawed in ice and diluted in distilled water to a concentration of 20µg/ml. Wells from 96-well plates were coated with 50µl of the diluted fibronectin solution. The plate was incubated at room temperature for one hour before use.

2.3.2 Hypertrophy induction in Matrigel and fibronectin

After purification steps, through centrifugation of the collected EBs, they were dissociated with TrypLE to obtain single cells. MEF was added to the solution containing the EBs in a fourfold proportion, regarding the volume added of TrypLE. The solution was centrifuged again and resuspended in BPEL. Cardiomyocyte medium was later used instead of BPEL. Posteriorly, these above mentioned steps were instead performed by Pluriomics because of the direct acquisition of the Pluricyte Cardiomyocytes. Cardiomyocytes were plated in Matrigel- and 20ug/ml fibronectin-coated 96 well-plates, at 5, 10 and 20 cell/well densities, together with Cardiomyocyte medium and changed to Maturation medium after 1 day.

After three days of incubation period the hypertrophic stimulus 1µM ISO, 10µM PE and 5% FCS, were added to the plated CMs. The treatments were refreshed ounce, after 2 days from the initial treatment and the total duration of the experiments were of 7 days.

2.3.3 Hypertrohpy induction in fibronectin patterns

After observation of the cardiomyocyte's behavior on the different substrates it was used the constructed platform, with the fibronectin patterns printed on the bottom of the wells of the 96-well plates. hESC-cardiomyocytes (already differentiated from Pluriomics) were seeded on these plates by the same methodology described in the previous subsection, although a pre-step procedure was added to the protocol in the attempt to improve cardiomyocyte adaptation to the fibronectin. Cardiomyocytes were firstly seeded onto a 20 µg/ml fibronectin coated 6-well plates with Cardiomyocyte medium and changed to Maturation medium 1 day after. The cells were refreshed at day 3 with Maturation medium and at day 7 the medium was aspirated and 1ml/well of TrypLE added. They were incubated for 10min and detached from the wells by pipetting up and down. It was added 4ml MEF for each ml of Tryple, transferred to a tube and spun down at 1100rpm for 3min. The supernatant was aspirated and the cells were resuspended in Maturation medium. After counting, the cardiomyocytes were seeded at 10 and 15 cells/well densities onto the plates with fibronectin

patterns, together with Maturation medium. Hypertrophic treatments, 1μM ISO, 10μM PE and 5% FCS, diluted in Maturation medium, were added to the cardiomyocytes at day 10. The treatments were refreshed at day 12 and cardiomyocytes were fixed at day 14.

2.4 ECM protein combination

2.4.1 Monolayer coating

A combination of proteins, similar to the composition of Matrigel, was prepared which contained fibronectin, laminin (from Engelbreth-Holm-Swarm murine sarcoma basement membrane, aqueous solution, Sigma-Aldrich) and collagen IV (from human placenta Bornstein and Traub type IV, lyophilized powder, Sigma Aldrich) at different concentrations. To obtain the optimal concentration for each component an experiment was designed, in which every possible combinations of the protein at concentrations of 10, 20 and 50 μg/ml each were tested, resulting in a total of twenty seven different combinations.

To obtain solutions at the pre-defined concentrations, fibronectin and laminin were diluted in distilled water, while collagen IV was incubated overnight in a 0.25% acid acetic solution to reconstitute the lyophilized powder and then diluted in distilled water. The combinations and also the individual proteins at the different concentrations (controls) were used to coat wells from a 96-well plate and incubated at RT for two hours. HESC-derived cardiomyocytes were seeded onto these wells at the density of 5000 cells/well with Cardiomyocyte medium, and changed to Maturation medium after 1 day. The experiment had the duration of 7 days and the medium was refreshed twice.

2.4.2 Protein patterns

It was prepared two mixes of the combined solution composed by fluorescence fibronectin, fibronectin, laminin and collagen IV. One with a final concentration of 20 μg/ml (each protein solution at 20 μg/ml) and the other of 50 μg/ml (each protein solution at 50 μg/ml), being the last concentration based on Rodrigez and colleagues (2014) studies, although the three proteins were not used in combination in this article. The microcontact printing technique was performed as described before, and a platform was constructed with patterns of combined proteins printed on the bottom of the wells. HESC-derived cardiomyocytes were seeded onto these wells at the density of 10000 cells/well with Cardiomyocyte medium. In this experiment two controls were used to evaluate the cardiomyocyte response to the different medium. It was used Cardiomyocyte medium and a mix of this medium with Maturation medium, by changing to the last after one day. The above-mentioned hypertrophic treatments were started at day 3 and refreshed at day 5 with a total duration of the experiment of 7 days.

2.5 Immunocytochemistry

Cells were fixed with 4% Paraformaldehyde in PBS solution for 30 minutes and permeabilized with 0.1% Triton X-100 for 8 minutes, both at RT. Afterwards, they were

washed 3x5 min with PBS and blocked in 4% Normal Goat Serum (NGS) for 1 hour. After these steps, the cells were labeled with a mouse anti-rabbit α-actinin (sarcomeric) (Sigma, 1:800) and diluted in PBS containing 4% NGS. The primary antibody solution was removed after 1h and the cells were washed 3x10min with PBS and 0.05% Tween20. They were then labeled with donkey anti-mouse Alexa 488 (Invitrogen, 1:250) conjugated secondary antibody, after 3x10 min washings with PBS and 0.05% Tween20. Secondary antibody was diluted in PBS containing 4% NGS and incubated for 1h at RT. Afterwards, the cells were washed 3x10min in PBS and 0.05% Tween20 and cell nuclei were visualized through DNA staining with DAPI (Sigma; 1:1000) diluted in PBS. Images were acquired with the BD Pathway 855 (BD Biosciences) and posterior image analysis was conducted.

2.6 Image analysis

In this work, the BD Pathway 855 Bioimaging system was used, which is a high-content cell analyser that combines superior image quality, flexible image capture, and live-cell analysis to address a wide range of applications. It provides fluorescence intensity measurements, kinetic imaging, and morphological analysis, including subcellular imaging. A binocular eyepiece allows for direct viewing of cells in both fluorescence and transmitted light modes. This system has the ability to analyze multiple well-plate samples in an automated fashion, increasing the efficiency of the process by providing results in a fast manner.

Immunocytochemistry markers were combined in order to characterize further the phenotypic properties of hESC-CM culture in the hypertrophy state. Images from the 96-well plates with fixed and stained cells in it were taken with the BD Pathway 855 bioimaging system. The images were taken through the system's automated and highly sensitive fluorescence imaging microscope with the 20x objective magnification. At this magnification level, the cardiomyocyte's sarcomere structure and size could be easily detected and measured. Each well was automatically focused by the bioimaging system with its integrated laser autofocus. The laser autofocus was specifically calibrated and optimized for the acquisition settings that this work required. The different cell stainings were identified by specific channels that are able to detect the wavelength emitted from the different dyes coupled to the cells, previously mentioned.

Images taken to the CMs were acquired, processed with ImageJ software, and area, sarcomere intensity, cardiomyocyte ratio and elongation measurements were specifically designed and implemented on CellProfiller software, for this work. They were programmed and optimized by the bioinformatic Dr. Lu Cao, from the Embryology & Anatomy department in the Leiden University Medical Center (LUMC).

Chapter 3 Results

3.1 Hypertrophy model construction

3.1.1 Spin coating

A PDMS coating was necessary for the custom-made glass coverslips in order to perform microcontact printing, but not for the plastic ones, as stated previously.

It is a very standard procedure to spin coat round and small coverslips and there are defined spin coating recipes for a complete, uniform and perfect coating of these substrates. However, the same cannot be stated for square, specially, for the high-dimension coverslips used in this work. These square coverslips were spin coated using the same recipe as advised for the round coverslips, but the results were not the satisfactory, yielding a defective coating, especially on the borders, as depicted in Figure 9A and 9B. For that reason, there was the need to optimize the spin coating procedure for this kind of coverslips, which implied the acquisition of a new chuck for the spin coater, specifically designed for spin coating of square and bigger substrates. Also, slight changes of the spin coating recipe were implemented in an attempt to perfectly coat the coverslips. Nevertheless, a series of unsuccessful attempts led us to decide using only the plastic coverslips throughout this project, which do not require the spin coating procedure.

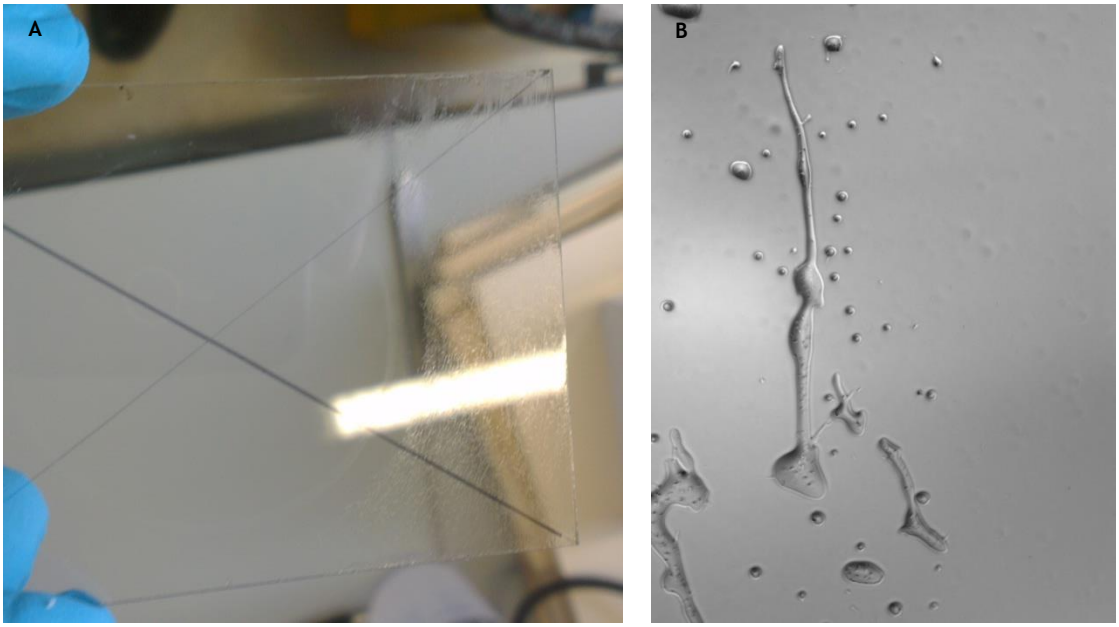

Figure 9 - Defective PDMS coating in the custom-made glass coverslip, (A) seen with the naked eye and (B) amplified with a 4x magnification.

3.1.2 Microcontact printing

Microcontact printing is a technique that requires a high methodology precision to achieve it perfectly. Several variables can influence the results of this technique and the process needs to be carefully and thoroughly executed to achieve perfect patterns, fully

filled with protein. In Figure 10A it is represented the stamp which was produced from a master, with the micropatterns (lines) inscribed on the top surface. The surface needed to be filled with the protein solution. In Figure 10B it is shown the stamp with the fibronectin solution on its surface and after dried with nitrogen gas. The micropatterned surface of the stamp was then turned and placed against the custom-made coverslip, as represented in Figure 10C, while manual pressure applied. Due to the lack of a stamp big enough that could cover the entire coverslip with the specified dimensions, it was necessary to perform this technique 3 times in order to pattern the entire coverslip. The fibronectin protein patterns were printed on the coverslip and images were taken by the BD Pathway 855, in the Cy3 (red) channel and are represented in Figure 10D.

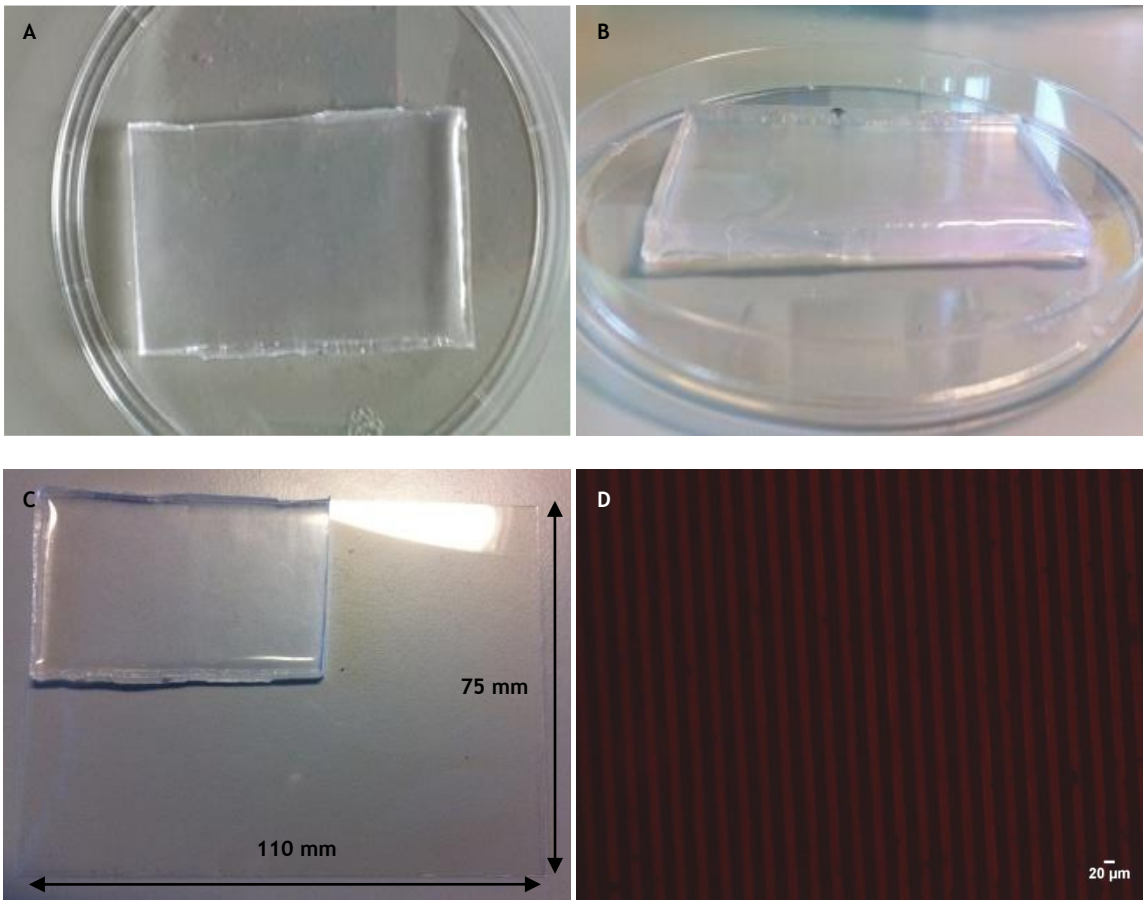

Figure 10 - Protein patterns production on the custom-made coverslip. (A) Micropatterns created on the stamp by master replication; (B) fibronectin solution on the stamp's surface; (C) Custom-made plastic coverslip used as substrate for uCP; (D) result of the uCP on the custom-made plastic coverslip, with a 4x magnification.

3.1.3 Platform attachment

Once the microcontact printing was performed on the coverslip, it was ready to be attached to the bottomless 96-well plate. All the regions of the bottom were carefully filled with glue and the development of the gluing process can be observed on Figure 11A and 11B. After the plate was entirely filled with glue, the coverslip side with printed protein patterns was carefully overlapped to the plate and released when it perfectly fitted the bottom of the plate. Some pressure was first applied on the edges of the coverslip, so that it could be fixed

to the plate without sliding. An uniform pressure was applied with the cylinder roll to glue the rest of the coverslip to the plate, making sure that there were no air bubbles trapped between them, as exemplified in Figure 11C, otherwise there would be a “leakage effect” when performing cell culture in the plate, and the liquid within each well would be exchanged between the neighboring wells. The final result of the gluing procedure of the coverslip to the plate is shown in Figure 11D.

Figure 11 - Attachment steps of the customized coverslip to the bottomless 96-well plate, resulting in the obtainment of a functional platform. (A) and (B) Development of the gluing process of the bottom of the bottomless 96-well plate. (C) Attachment of the protein patterned coverslip to the 96-well plate by applying uniform pressure with the cylinder roll. (D) Final result of the constructed platform.

3.2 Hypertrophy experiment

3.2.1 Matrigel and fibronectin

Two different types of substrate were used to induce hypertrophy in an experimental setting. Although the intention was to control cardiomyocyte shape and orientation using the protein patterns, initially, cardiomyocytes were cultured in Matrigel- and fibronectin-coated 96-well plates, at 5000 cells/well to monitor their behavior on these different substrates. After a 7 days culture, cells were fixed and stained for α-actinin and DNA counterstained by DAPI. The results for the control (Cardiomyocyte medium + Maturation medium) and for the two main hypertrophic stimuli used, i.e. ISO and FCS are shown in Figure 12.

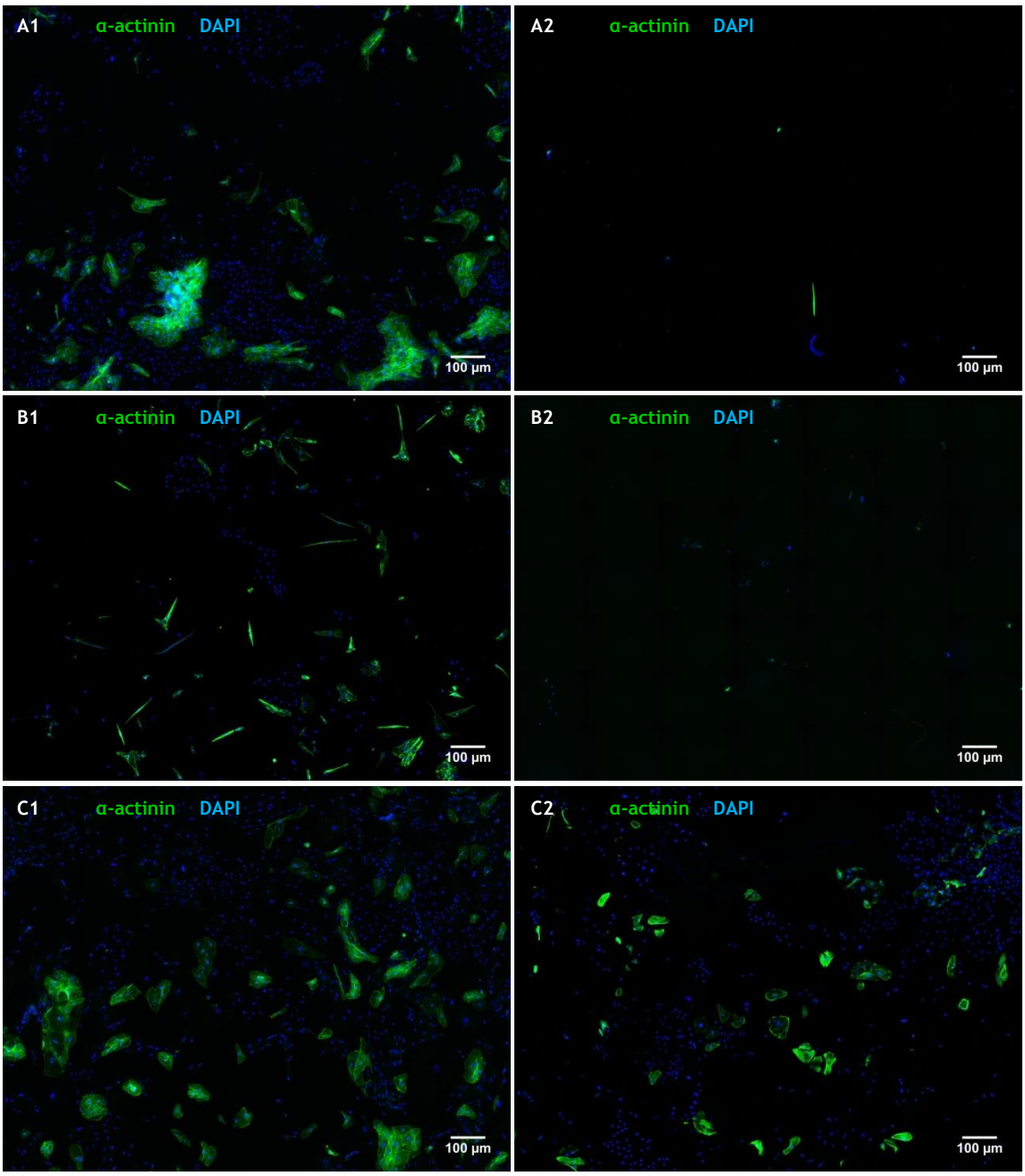

Figure 12 - Cardiomyocytes cultured on Matrigel monolayer (A1, B1 and C1) and in fibronectin monolayer (A2, B2 and C2) in (A) control, (B) ISO and (C) FCS treatments, at 5000 cells/well, and immunostained for α-actinin (green) and DAPI (blue) (magnification: 20x).

Figure 11 observation makes it clear that cardiomyocytes failed to develop on the fibronectin substrate, especially when compared to Matrigel, with the exception of the FCS treated cells. Only in the latter treatment cardiomyocytes seemed to have adhered and further developed on the fibronectin. The same outcome was seen for higher cell densities, where cardiomyocytes failed to develop on fibronectin in (control and ISO conditions), being the FCS treatment the exception. Given that almost no cardiomyocytes could be detected in fibronectin, image analysis could not be performed for the fibronectin experimental-set; thus

only the pictures of higher densities, 10000 and 20000 cells/well, in Matrigel are shown in Figures 13 and 14, (also for the PE treatment).

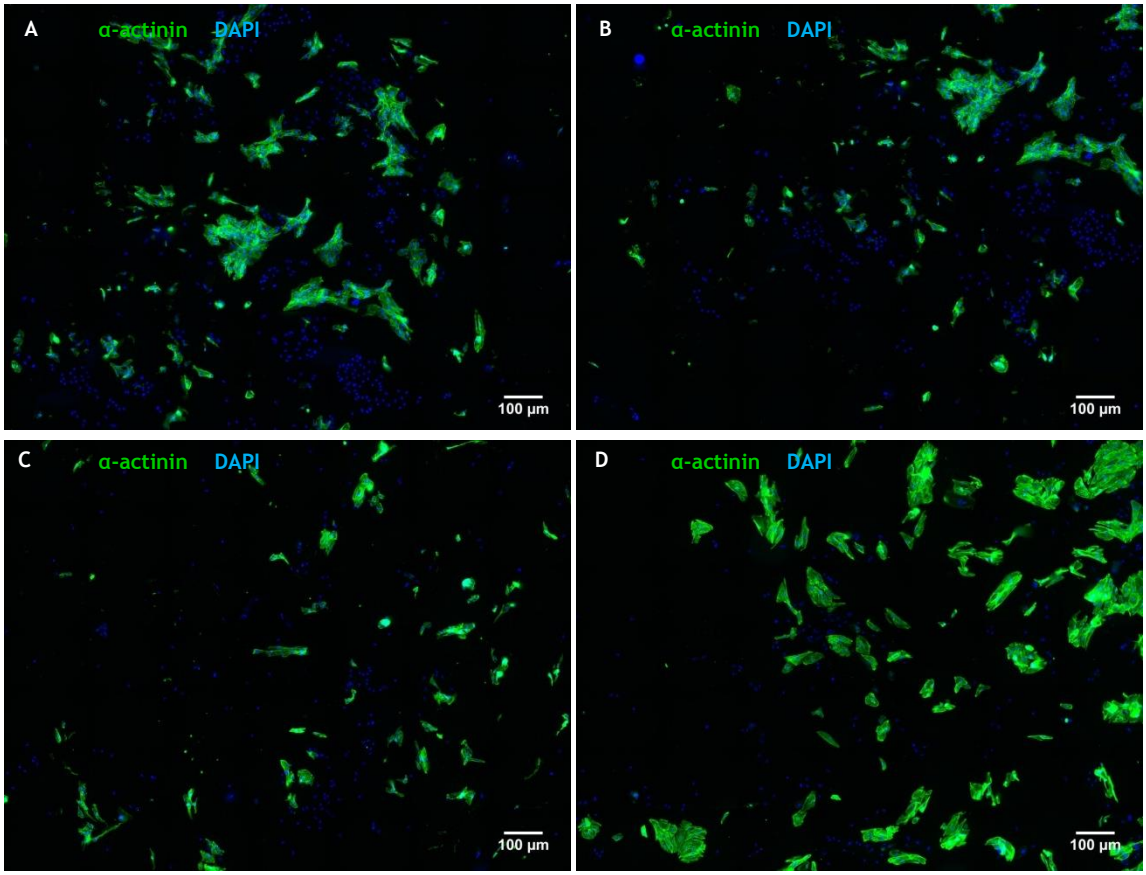

Figure 13 - Cardiomyocytes cultured on Matrigel monolayer in (A) control, (B) ISO, (C) PE and (D) FCS, at 10000 cells/well, and immunostained for α-actinin (green) and DAPI (blue) (magnification: 20x).

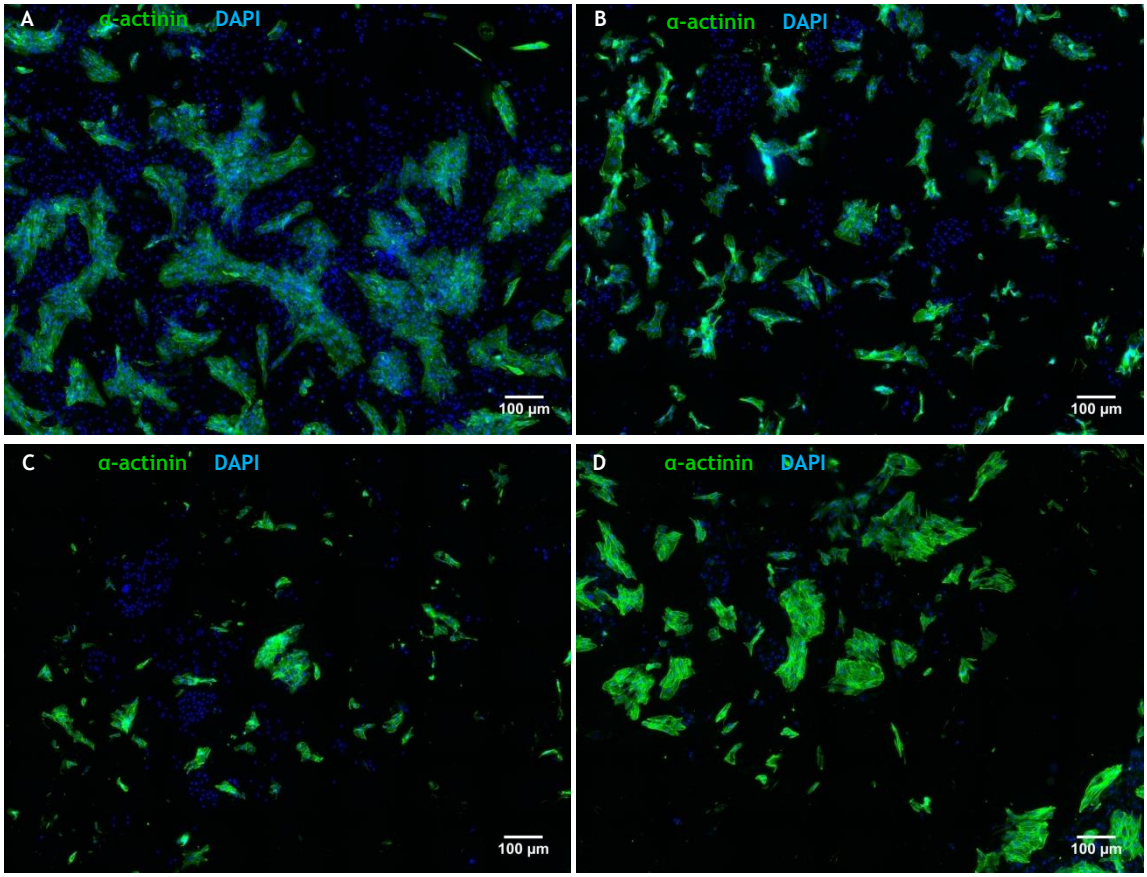

Figure 14 - Cardiomyocytes cultured on Matrigel monolayer in (A) control, (B) ISO, (C) PE and (D) FCS, at 20000 cells/well, and immunostained for α-actinin (green) and DAPI (blue) (magnification: 20x).

It was noticeable CMs adapted well in the Matrigel substrate, as seen previously for lower cell density. It is also observable an increase of the CMs and cell-agglomeration in control conditions, when compared to the hypertrophic treatments (Figure 14) which may lead to misleading and contradictory conclusions, regarding the treatments. Cell agglomeration may lead into the conclusion that "control" leads to increase of the CMs area, although we have had solid proof that the single CMs within the clusters were increased. This issue will be addressed and below in the "Measurements" subsection.

3.2.2 Fibronectin patterns

When the attachment of patterned coverslip to the bottomless 96-well plate was complete, cell culture was performed on it. The cardiomyocytes adhere only to the protein patterns and their shape and orientation was controlled. After result observation of the cultured cardiomyocytes on fibronectin monolayer it was added a pre-step on this experiment, so the cells could adapt better to this type of substrate in this assay. The images were processed and amplified from the originals, using ImageJ, to better observe the CMs. Processed results are shown in the Figures 15 and 16 and the original images are shown in the Supplementary data.

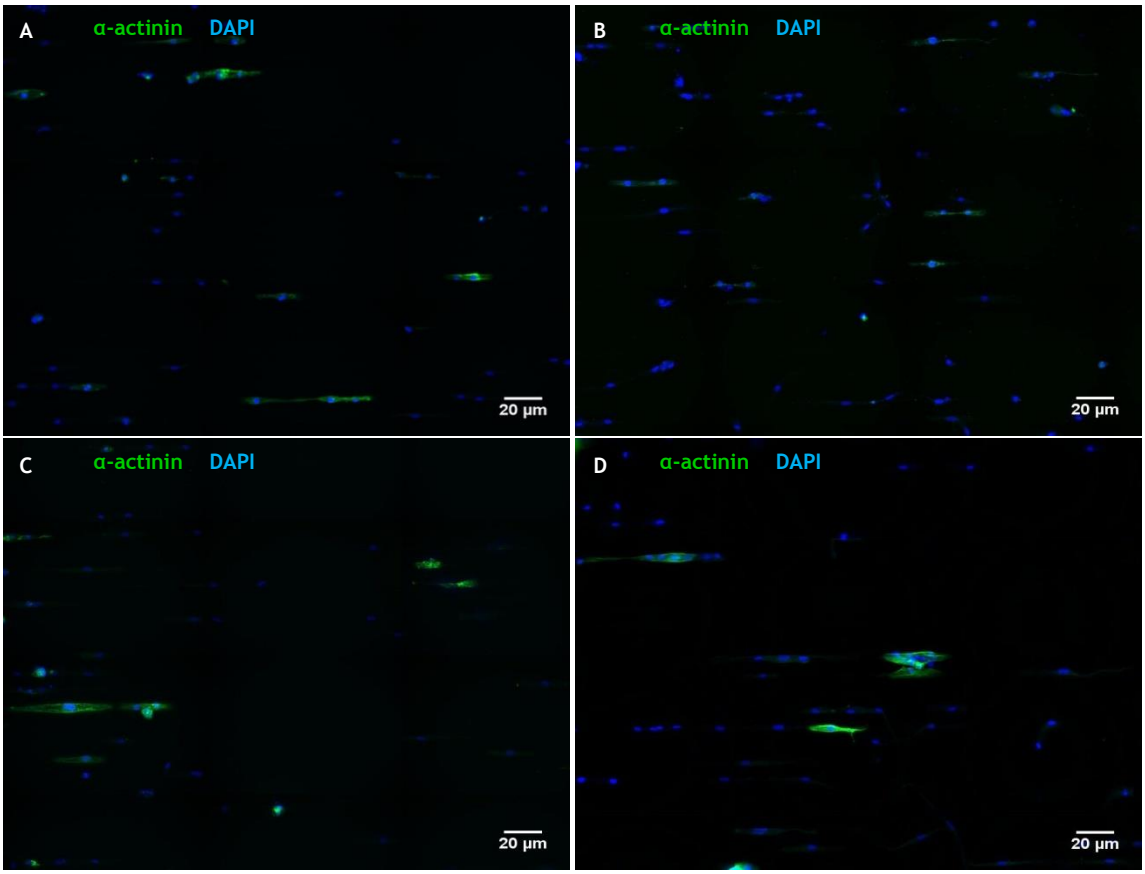

Figure 15 - Cardiomyocytes cultured on fibronectin patterns (horizontal lines) in (A) control, (B) ISO, (C) PE and (D) FCS, at 10000 cells/well, and immunostained for α-actinin (green) and DAPI (blue) (magnification: 20x).

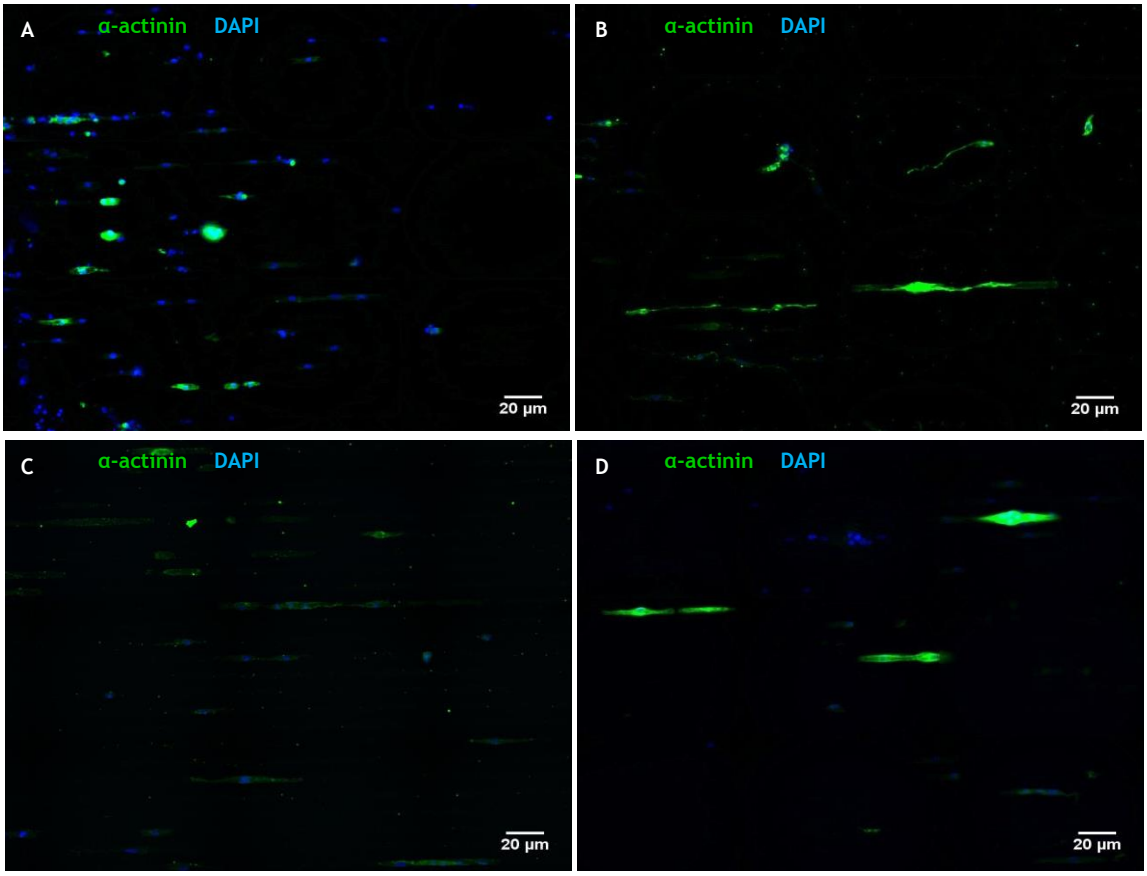

Figure 16 - Cardiomyocytes cultured on fibronectin patterns (horizontal lines) in (A) control, (B) ISO, (C) PE and (D) FCS, at 15000 cells/well, and immunostained for α-actinin (green) and DAPI (blue) (magnification: 20x)

Contrarily to the expected, i.e. more adhered and developed cardiomyocytes, so that analysis could be correctly performed and yield statistically significant differences, very few cardiomyocytes could be detected when cultured on the fibronectin patterned lines, for all the treatments and cell densities tested (Figures 15 and 16).

3.3 Segmentation

To perform single cardiomyocyte analysis it was firstly necessary to segment each cell within each picture. This segmentation process was based on the cardiomyocyte's nuclei, given by the DAPI staining and tracked by the BD Pathway 855, using a nuclei propagation method for that purpose. DAPI has the ability to stain the nucleus of every cell (cardiomyocytes and non-cardiomyocytes) of each setting. With the nuclei propagation method, the nucleus of each cell is identified and expanded until meeting the boundaries imposed by the α-actinin staining. α-actinin expression identifies only the structures and limits of the cardiomyocytes present in each setting. Therefore, the segmentation was only performed to the existent cardiomyocytes of the acquired pictures, through these two different channels. It is taken into account that each cardiomyocyte can be mono or binucleated and the distance between each of the nuclei was measured to assess whether they belong to the same cell or not. When the segmentation mask can fully define the

contours of each cell, the measurements can be made to single cardiomyocytes. An example of the segmentation mask used in this work is shown in Figure 17.

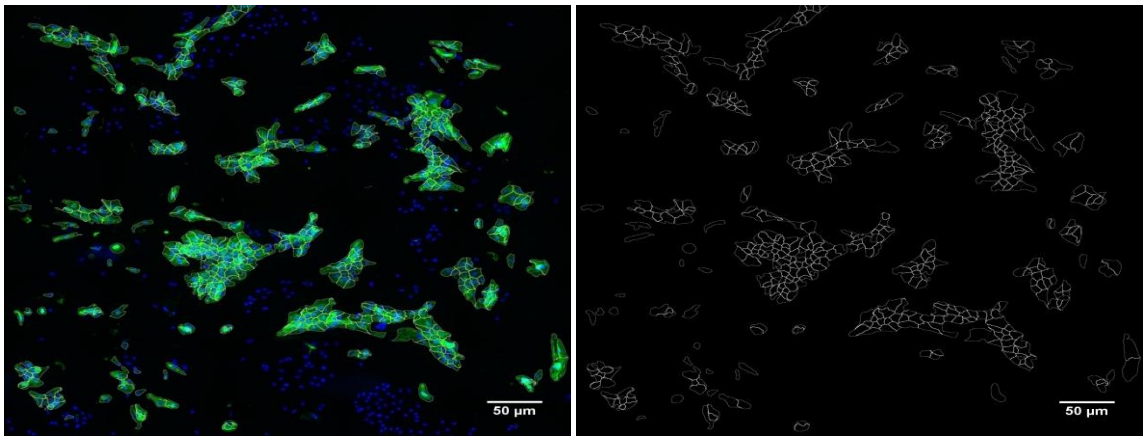

Figure 17 - Single cardiomyocyte's limits detected and given by the segmentation mask (magnification: 20x). (A) Cardiomyocytes detected by the α-actinin (green) channel and cardiomyocyte segmentation represented with white lines. (B) Segmentation mask defining the cardiomyocyte's contours represented with white lines.

3.4 Measurements

3.4.1 Cardiomyocyte area

The segmentation mask was used to determine the limits of each cardiomyocyte and their area was estimated from it. The area units are provided in pixels, allowing only relative comparisons between the different treatments at different cell densities, both in Matrigel monolayer and on fibronectin microcontact printing (µCP) patterns, as shown in Figure 18.

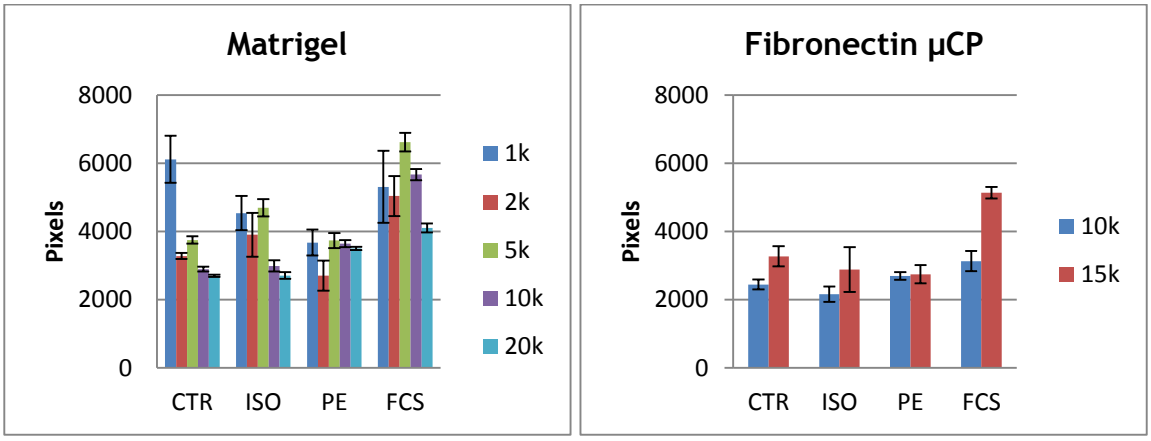

Figure 18 - Cardiomyocyte's area (in pixels) of the different treatments on Matrigel (on the left) and in fibronectin µCP patterns (on the right), for different cell densities.

Regarding the Matrigel substrate (Figure 18) it is shown that the FCS treatment was increasing the cardiomyocyte's area reaching almost a two-fold increase for some of the cell densities used, when compared to the control. This area increase pattern could be observed for the 2000, 5000 and 10000 cells/well densities. Contrariwise, in the 1000 cells/well density a bigger area increase in control rather than in FCS treated was registered, although in the 20000 cells/well density, there was not a significant area increase in FCS. The other hypertrophic treatments, ISO and PE, did not result in significant area increase and even

revealed to be smaller for 1000 cell/well density, as happened to the FCS treatment for the same density. Also, the cardiomyocyte's area showed to be smaller for PE in the 2000 cell/well density. A similar outcome could be observed for the fibronectin μCP patterns, in which a significant increase could only be observed for the FCS treatment and only at the 15000 cells/well density.

3.4.2 Sarcomere intensity

With each cell perfectly delimited the cardiomyocyte's sarcomeres can be evaluated. This is performed by using an integrational procedure that measure and sums the color intensity of each pixel within each cardiomyocyte. In the end, it is made an average from the entire set of cardiomyocytes for each image and cell density. The result is displayed in Figure 19.

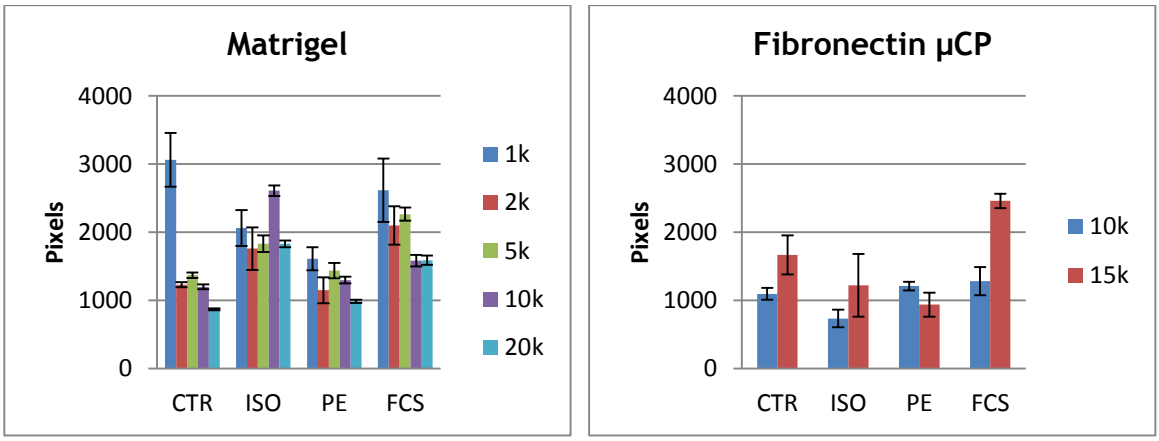

Figure 19 - Cardiomyocyte's sarcomere intensity (in pixels) of the different treatments on Matrigel monolayer (on the left) and in fibronectin μCP patterns (on the right), for different cell densities.

It was shown that in Matrigel the sarcomere intensity was increasing in ISO, reaching more than a two-fold increase on the 10000 cell/well density, and in FCS, except for the 1000 cells/well density. Thus, in the FCS treatment it is observed an overall sarcomere intensity increase, also with the exception for the 1000 cells/well density set. Regarding the fibronectin patterns, only FCS treatment, in the 15000 cells/well density, led to a relevant intensity increase.

3.4.3 Cardiomyocyte ratio

This measure is performed through the calculation of the total nuclei number present and the number of nuclei that belong indeed to cardiomyocytes. For each image, it is used the DAPI channel acquisition to evaluate the total number of nuclei and the α-actinin channel acquisition to verify which nuclei are also an integrant part of cardiomyocytes. With the resulting values from this operation it is constructed a ratio between the cardiomyocyte's nuclei and the total number of nuclei, and represented as a percentage (Figure 20).

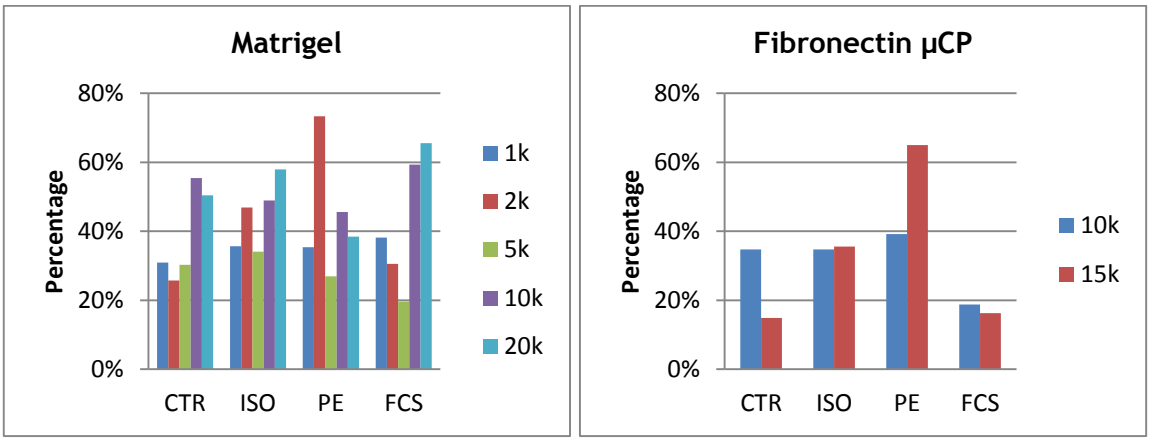

Figure 20 - Cardiomyocyte's ratio (in percentage) of the different treatments on Matrigel monolayer (on the left) and in fibronectin µCP patterns (on the right), for different cell densities.

The results displayed in Figure 20 indicate that in Matrigel, PE treatment enhanced the cardiomyocyte proliferation to close to 40%, when compared to control for the 2000 cells/well density. The same cannot be affirmed for the other cell-densities analyzed where instead it was even registered a decrease in CM ratio. A consistent trend that would enable drawing conclusions about the CM ratio was not obtained for any of the hypertrophic treatments. In the fibronectin pattern experiment it was also registered an increase on cardiomyocyte's ratio of 50% in PE, when compared to control, but only for the 15000 cells/well density. Although not significant, the 10000 cells/well density showed also an increase in PE as compared to the control. These results point for a certain effect of PE treatment in CM ratio, however, further experiments will be necessary for full confirmation.

3.4.4 Elongation

Elongation is a measure of the degree of stretching acquired by cardiomyocytes, after being cultured in the presence of different hypertrophic treatments, where the null value means that the cardiomyocyte is completely circular and the highest percentage (100%) means that it is fully elongated. The obtained results are represented in Figure 21.

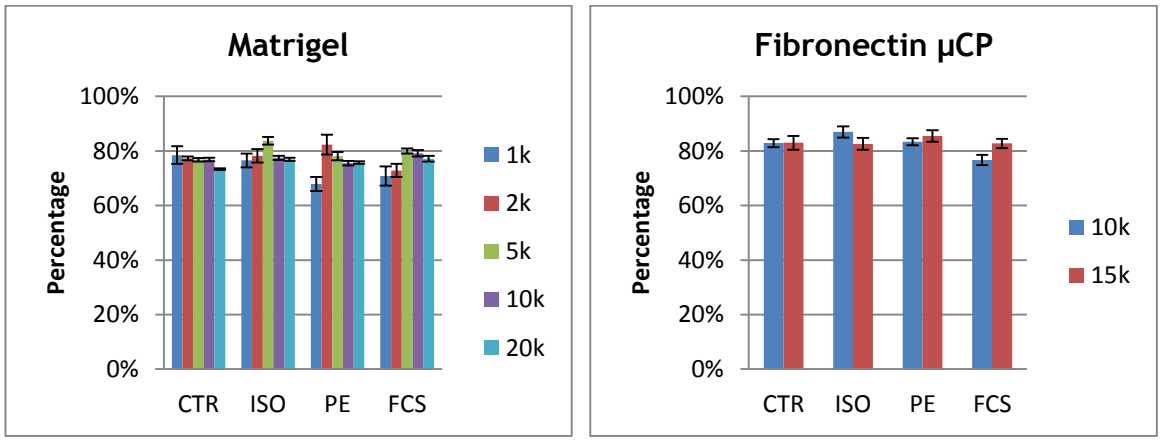

Figure 21 - Cardiomyocyte's elongation (in percentage) of the different treatments on Matrigel monolayer (on the left) and in fibronectin µCP patterns (on the right), for different cell densities.

Both Matrigel and fibronectin substrates produced a similar effect on CM elongation, although the latter registered a slight increase when results are compared. It was not determined any significant changes in elongation when results are compared between the treatments and control in both substrates, indicating that neither the substrates nor the hypertrophic treatments used are relevant in CM elongation

3.5 ECM protein combination

3.5.1 Optimal concentration

A total of twenty seven protein combinations, using fibronectin, laminin and collagen IV and varying their individual concentration from 10, 20 to 50 µg/ml, were performed. The solutions were used to coat 96-well plates and each one was tagged, as schematized below on Table V.

Table V - Identification of the different protein concentrations for fibronectin (FN), laminin (LMN) and collagen IV (COL), used for each tagged combination.

	µg/ml				µg/ml				µg/ml		
Combination	**FN**	**LMN**	**COL**	**Combination**	**FN**	**LMN**	**COL**	**Combination**	**FN**	**LMN**	**COL**
1	20	10	10	**11**	50	10	20	**21**	10	10	50
2	20	10	20	**12**	50	10	50	**22**	10	20	10
3	20	10	50	**13**	50	20	10	**23**	10	20	20
4	20	20	10	**14**	50	20	20	**24**	10	20	50
5	20	20	20	**15**	50	20	50	**25**	10	50	10
6	20	20	50	**16**	50	50	10	**26**	10	50	20
7	20	50	10	**17**	50	50	20	**27**	10	50	50
8	20	50	20	**18**	50	50	50				
9	20	50	50	**19**	10	10	10				
10	50	10	10	**20**	10	10	20				

It is important to stress that this experiment did not imply the use of the hypertrophic stimuli, since the primary goal was to identify the optimal protein combination that would provide the essential stimuli for enhanced cardiomyocyte adaptation and development. Pictures were acquired by using the BD Pathway 855, after cell staining, and image analysis was executed. Area, sarcomere color intensity and cardiomyocyte ratio measurements were applied to evaluate the optimal ECM protein combination and are represented in Figures 22, 23 and 24, respectively.

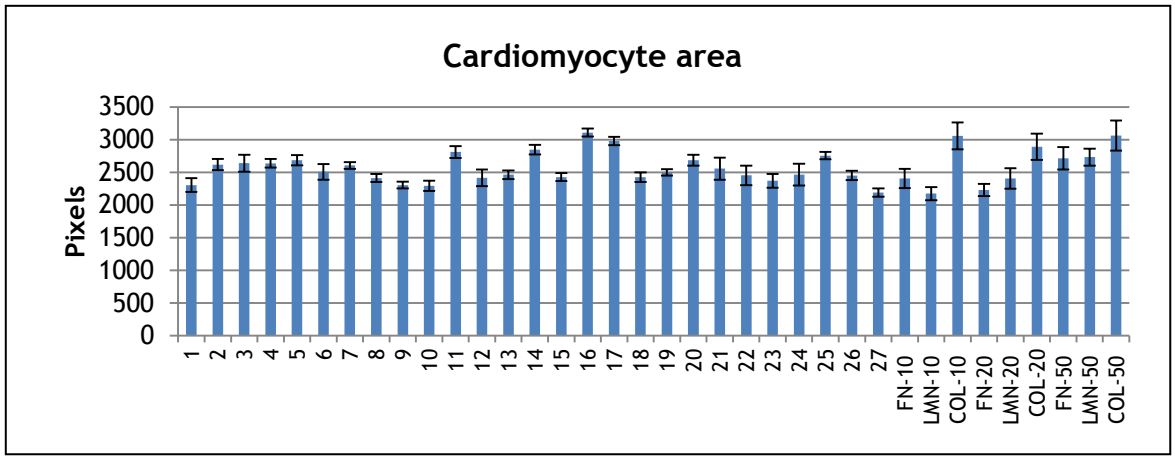

Figure 22 - Cardiomyocyte's area (in pixels) on the different ECM protein combinations (from 1 to 27) and in controls: FN-10, FN-20 and FN-50 (fibronectin at 10, 20 and 50 µg/ml, correspondingly); LMN-10, LMN-20 and LMN-50 (laminin at 10, 20 and 50 µg/ml, correspondingly); COL-10, COL-20 and COL-50 (collagen IV at 10, 20 and 50 µg/ml, correspondingly).

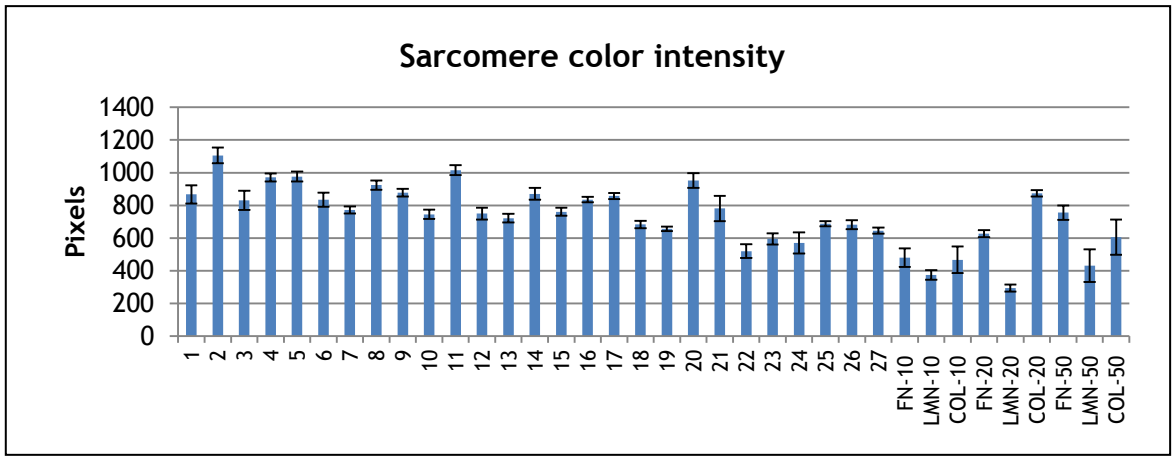

Figure 23 - Cardiomyocyte's sarcomere color intensity (in pixels) on the different ECM protein combinations (from 1 to 27) and in controls: FN-10, FN-20 and FN-50 (fibronectin at 10, 20 and 50 µg/ml, correspondingly); LMN-10, LMN-20 and LMN-50 (laminin at 10, 20 and 50 µg/ml, correspondingly); COL-10, COL-20 and COL-50 (collagen IV at 10, 20 and 50 µg/ml, correspondingly).

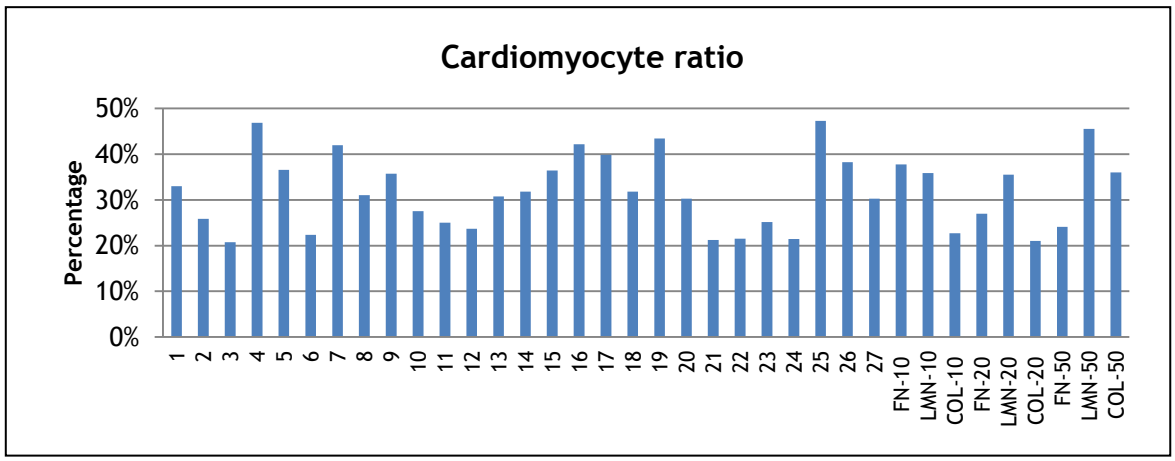

Figure 24 - Percentage of cardiomyocytes present on the different ECM protein combinations (from 1 to 27) and in controls: FN-10, FN-20 and FN-50 (fibronectin at 10, 20 and 50 µg/ml, correspondingly); LMN-10, LMN-20 and LMN-50 (laminin at 10, 20 and 50 µg/ml, correspondingly); COL-10, COL-20 and COL-50 (collagen IV at 10, 20 and 50 µg/ml, correspondingly).

Image analysis enabled us to identify the optimal protein combination to be used in microcontact printing within our experimental setting. The cardiomyocyte adaptation and development were extracted by the interception of the area, sarcomere color intensity and cardiomyocyte ratio measurements (Figure 22, 23 and 24, respectively). A bigger area, higher sarcomere color intensity and higher cardiomyocyte ratio is assumed to confer a better phenotype status to the cardiomyocytes and, regarding these parameters, it was concluded that the combination 4 (area: 2638 pixels; intensity: 971 pixels; ratio: 47%) produced overall the best result.

3.5.2 Protein patterns

In parallel, microcontact printing was performed on the plastic coverslips with two of the twenty seven combinations, chosen before obtaining results from the previous subsection due to a lack of time available to accomplish this last experiment. It was selected the combination 5 (fibronectin 20 µg/ml, laminin 20 µg/ml and collagen IV 20 µg/ml) and combination 18 (fibronectin 50 µg/ml, laminin 50 µg/ml and collagen IV 50 µg/ml) for that purpose and cardiomyocytes were seeded at 10000 cells/well and cultured for 7 days with the hypertrophic inducing treatments, ISO, PE and FCS with the two controls (Cardiomyocyte medium and Maturation medium). At day 7, cardiomyocytes were stained for α-actinin and DAPI. The results are shown below in Figure 25.

Combination 5 - 20µg/ml **Combination 18 - 50µg/ml**

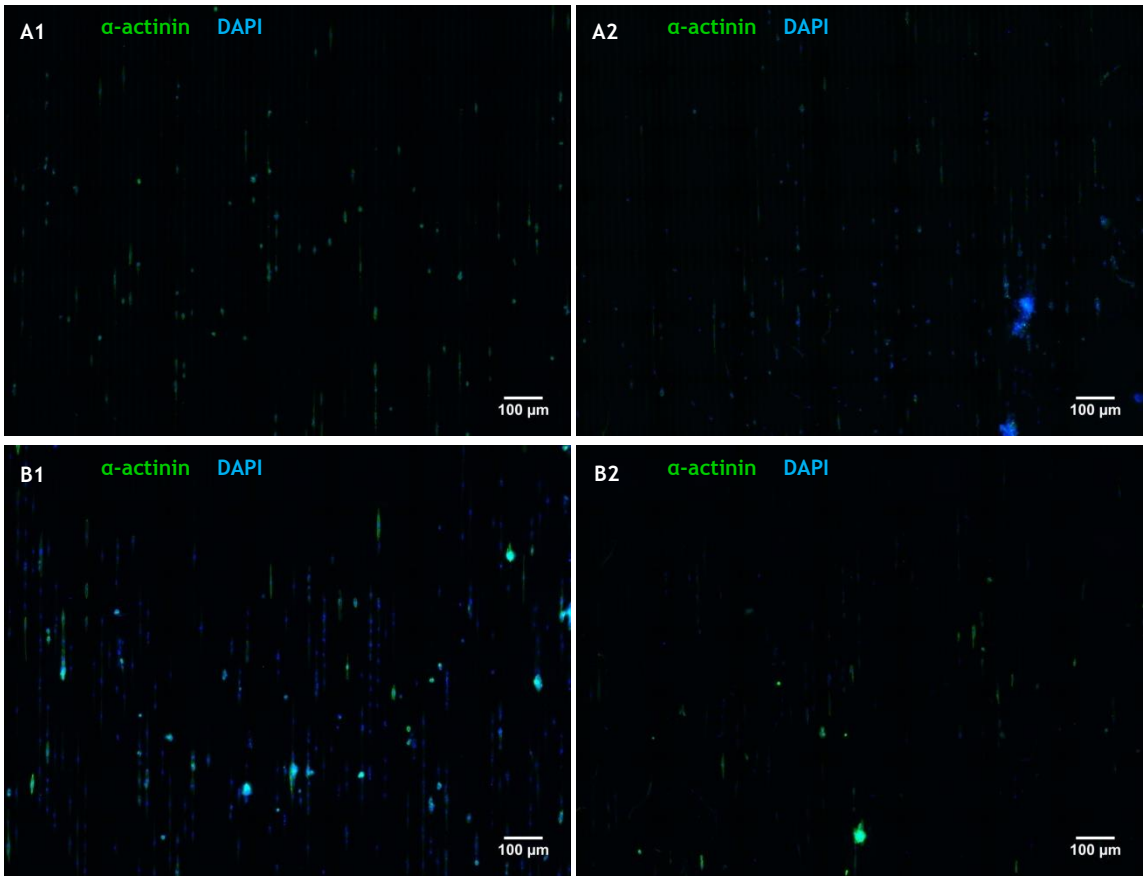

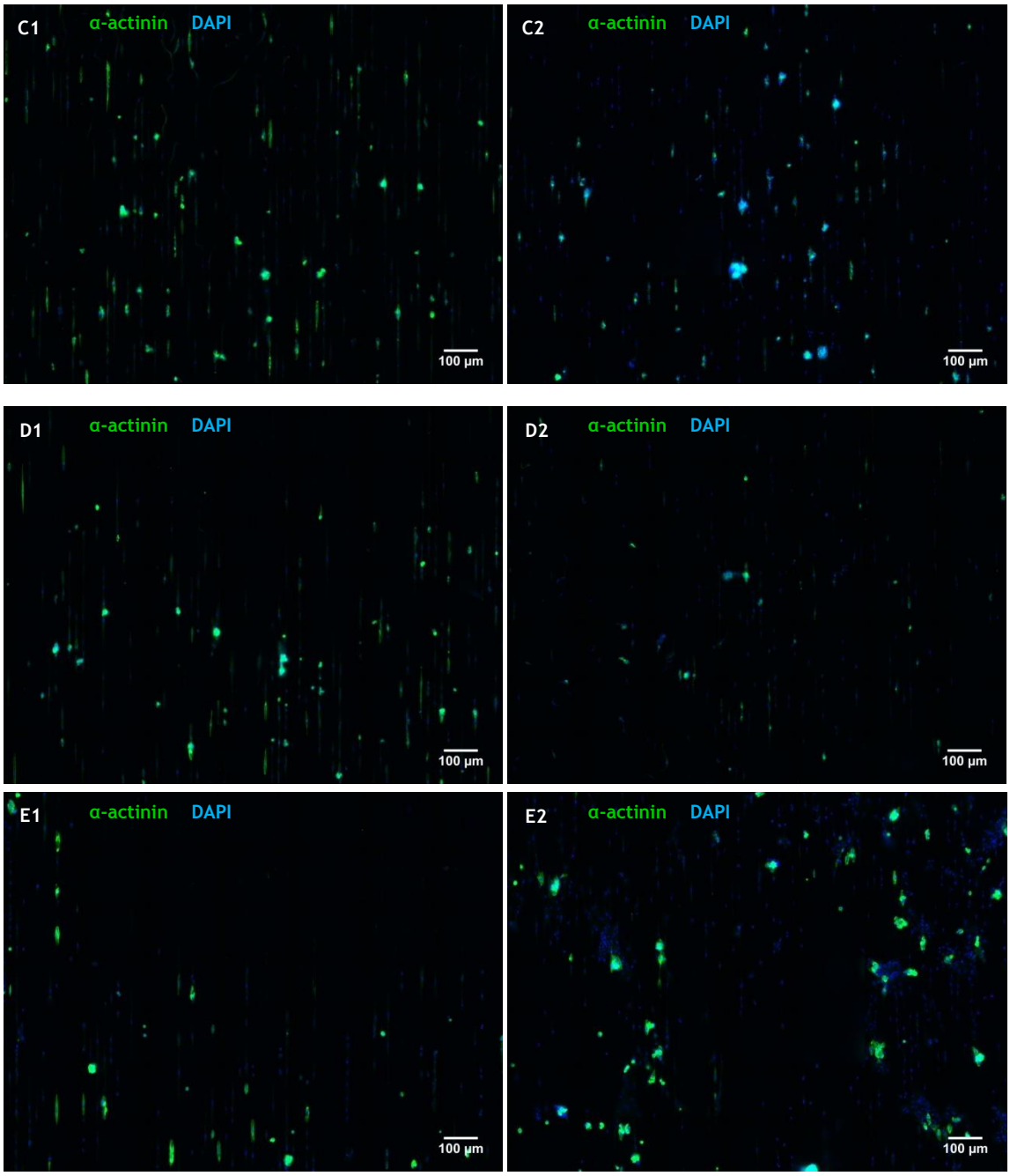

Figure 25 - Cardiomyocytes cultured on protein combination patterns (vertical lines) at 20 µg/ml (A1, B1, C1, D1 and E1) and at 50 µg/ml (A2, B2, C2, D2 and E2) in (A) Cardiomyocyte medium, (B) Maturation medium, (C) ISO, (D) PE and (E) FCS, with a density of 10000 cells/well, and immunostained for α-actinin (green) and DAPI (blue) (magnification: 20x).

Overall, the microphotographs on the two different combinations appear to indicate that there is a higher percentage and a better development of cardiomyocytes on combination 5 (left panel in Figure 25). Image analysis was performed to better determine which of these two combinations promote more adherence and higher development of cardiomyocytes, represented in Figure 26.

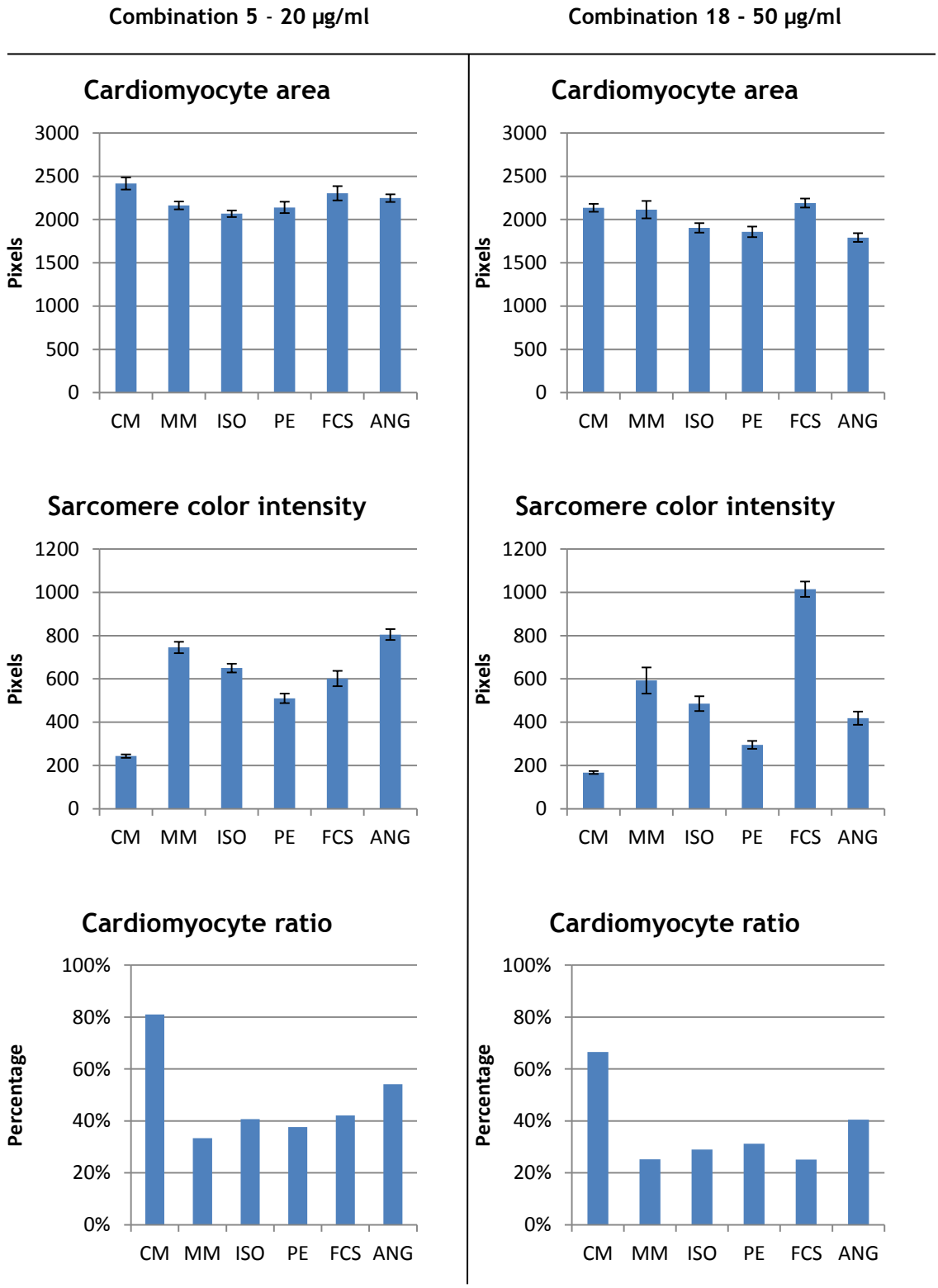

Figure 26 - Area, sarcomere color intensity and cardiomyocyte ratio measurements of the cardiomyocytes on ECM protein patterns using combinations 5 (on the left) and 18 (on the right).

No relevant differences could be spotted regarding cardiomyocyte's area, when comparing between the different treatments for both combinations. Sarcomere color intensity presented the lowest values in CM control for both combinations and the highest for FCS treatment in combination 18. Cardiomyocyte ratio evidenced the highest values in CM

control, in both combinations. In general, no significant alterations on cardiomyocyte's phenotype occurred when comparing the two different combinations, based on these measurements.

Chapter 4 Discussion

The two different acquired types of custom-made coverslips (glass and plastic) require the printing of protein patterns on their surface, through microcontact printing. As stated before, glass coverslips entail need to be spin coated with a PDMS solution for subsequent microcontact printing. This occurs due to the difficulty on enhancing the protein bonding by chemical activation of the glass material. On the other hand, plastic coverslips do not necessitate spin coating, and instead, microcontact printing can be performed directly, prior to the attaching to the bottom of a bottomless 96 well-plate. The final goal is to culture cardiomyocytes in these plates, induce CM hypertrophy and perform image analysis in order to obtain area and sarcomere intensity measurements. To this end, it was required that the coverslips met specific characteristics. First, they needed to be as flat as possible for an efficient spin coating and microcontact printing to be accomplished. Secondly, they needed to possess specific dimensions so they could perfectly fit into the bottom of the bottomless 96 well-plate. Also, it was very important to control the thickness of the coverslips to guarantee optimal imaging resolution. If the coverslip is too thick, imaging would not be precise and cardiomyocyte's structure would not be clearly displayed. Thirdly, it was crucial for them to be transparent to allow proper image acquisition.

While testing the acquired glass coverslips it was found that they were not suitable for the kind of work required in the herein thesis plan. As stated before, these coverslips need to be spin coated with PDMS first, due to the nature of their composition, before printing the protein patterns onto it (Griffin, 1954; Blinka *et al.*, 2010; Kaufmann and Ravoo, 2010). However, after several attempts it was observed the same "string effect" pattern on the borders. This could be consequence of several factors which could not be exactly determined. It could be the effect caused by non-suitable spin coating program implemented for a coverslip with such big dimensions (i.e.111mmx75mm). The PDMS solution deposited upon the coverslip dries within the first minutes of the spin coating program (Théry and Piel, 2009) and if the program is too fast or too slow the coating will not be perfect. An optimization of the recipe program could not be successfully determined to address this problem. It can also rely on the geometry of the substrate and there are three main issues regarding the spin coating of rectangular substrates: (1) the properties of fluid coating the substrate can produce edge beads which can also occur regardless of the substrate geometry (Carcano, Ceriani and Soglio, 1993; Atthi *et al.*, 2009); (2) the geometrical effect of the substrate can create irregular coating patterns. This happens because of the increasing friction with the air at the periphery, which causes an increase of the evaporation rate of the

coating fluid and the formation of a dry skin at the corners of the substrate, restricting fluid flow. The fluid at the center of the substrate, which is still being driven out by centrifugal forces, flows over the dry film and dries, building up at the corners (Carcano, Ceriani and Soglio, 1993; Hui, Blosiu and Wiberg, 1998; Atthi *et al.*, 2009); (3) the Bernoulli effects, which results of the leading edge of the substrate and because of the contact angle formed by the edge bead, creating an airfoil and causing the air streamline to separate while the substrate spins. Upon the formation of an edge bead on the top side, the air streamline is cut into unequal paths causing the air, which is flowing over the longest path (top side) to accelerate and the one which is flowing over the shortest path (bottom side) to decelerate. The acceleration on the top decreases pressure, enhancing the evaporation rate and causing a buildup in the corners (Carcano, Ceriani and Soglio, 1993; Atthi *et al.*, 2009). A feasible solution to perfectly spin coat the rectangular custom-made glass coverslips could rely on the optimization of the spin coater machine. The chuck incorporated in the spin coater is, generally, used for smaller and round coverslips and it is not adapted for the type of coverslips used in this project, mainly due to aerodynamics constrains. It was advised by the supplier to acquire a specialized chuck for the purpose of the work herein, i.e. Embedded Vacuum chuck (Laurell Technologies). However, due to the lead time and financial costs required for this acquisition, different solutions were considered.

For these reasons and due to the complications implied in the process a solution was found that involved a different approach. Thus, plastic coverslips were acquired with the same dimensions of the previous ordered glass coverslips, which do not require a spin coating process, and allowed for direct microcontact printing. Microcontact printing is a technique which requires a high methodology precision. First, the stamp needs to be completely dried in order for the technique to be succeeded, otherwise, the fibronectin, which is placed on the surface of the stamp will not spread over the entire surface (Théry and Piel, 2009). Secondly, the fibronectin solution needs to be in incubation on the stamp for long enough so it can infiltrate into the patterns designed on it (Théry and Piel, 2009). The first utilization of the day of the stamp requires more time than usual for the fibronectin penetrate into the patterns (1 hour). However, if the stamp is wet for long and for constant periods of time, it can be noticed that the fibronectin does not spread as easily on the next utilizations. It means that the incubation time cannot be for too short because the solution will not penetrate the entire stamp pattern, but it also cannot be for very long time or it will not be able to dry completely for the next utilizations. Thirdly, after the incubation period it is possible to print the protein pattern in the substrate and it will be transferred from the stamp to the substrate. For this to happen, the stamp needs to be placed in contact with the substrate and pressure needs to be applied on it. If enough pressure is not applied, the pattern that will be transferred to the substrate will be imperfect and defective because the protein will not be transferred in its totality. The regions where not enough pressure was applied will present lack of intensity or even a gap, which indicates no protein to almost none, was passed to the substrate. That can later influence cell's adhesion and phenotype to

the protein patterned on the substrate. On the other hand, if too much pressure is applied unwanted protein lines will be observed on the substrate. It happens when the stamp's sealing touches the substrate causing an extra unwanted line between the desired protein lines. This can, also, influence cell organization and can give rise to cardiomyocyte clusters because of the proximity of the lines. So it is always a compromise with the optimum amount of force to be applied to accomplish the best results. Once the protein patterns are printed on the coverslip, the process of its attachment to a bottomless 96-well plate can be initialized. Despite the optimizations regarding the platform construction it is still a low-throughput process, contrary to what was initially intended. The bottom of the plate needs to be entirely covered by glue to assure that the space between the coverslips and the plate is completely sealed. Since the attachment procedure is done manually, it accounts for a certain amount of time (aprox. 30 min) for each constructed plate, contradicting the principle of high-throughput system. However, the implementation of a faster process for that purpose seems not to be a concern, since there are commercial solutions available. The commercial existence of a bottomless 96-well plate with a double sided tape, with one of the sides already attached to the plate would be a solution for the problem, where it would just be needed to attach the patterned coverslip.

Initially, different substrates were used to test the hESC-derived cardiomyocyte behavior when cultured on them such as fibronectin and Matrigel. These experiments were conducted on fibronectin- and Matrigel-coated 96-well plates so the CM behavior could be compared between both substrates and for later estimation of CM adaptation and development on fibronectin patterned lines. It was undoubtedly shown that CM adaptation and development on fibronectin monolayer was very low, especially when compared to the CM status on the Matrigel formulation. This indicates that it would be more suitable to perform Matrigel protein patterns through microcontact printing, than the FN patterns, once it is evidenced that CM failed to develop on the FN substrate. However, the nature of the Matrigel formulation makes it very difficult to use for that purpose. Matrigel polymerizes very fast when at room temperature (RT) and microcontact printing requires a period of incubation of, at least, 30 min, at RT, hence decreasing the probabilities of successful printing. For this reason, Matrigel was not used to create protein patterns on the coverslips in this project, presenting, although, as a good alternative for other potential settings. Despite the inability to meet the expected results in the initial experiments, FN was tested for the creation of the protein patterns, in microcontact printing. However, the experimental setting suffered an alteration, aiming for a better adaption of the CMs. The time-course of the experiment was prolonged to a total of 14 days (7 days more than the usual duration of the previous experiments) in which CMs are cultured on FN coated-6-welll plates for the first 7 days. This prolongation was carried on the attempt for the CMs to adapt better to this substrate before culturing them into the confined FN lines. Nevertheless, after the 14 days, very few CMs could be observed after cell staining, possibly indicating that FN by itself was not being capable to properly regulate CM adherence and/or development. Several attempts

to culture CMs in fibronectin substrate (either on monolayer or patterns) failed, which lead us to this conclusion. Thus, different fibronectin batches were used always with the same outcome. Studies suggest an important contribution of fibronectin in CM adhesion and differentiation (Horton *et al.*, 2009; Wu *et al.*, 2010), contradicting such conclusions. Reasons for the maladaptation of CMs to this substrate were undetermined.

Regarding the image analysis performed for the Matrigel experiment some trends could be revealed, although more repetitions are needed to substantiate conclusions. In fact, results were not totally consistent, but it could be observed that FCS treatment triggered higher hypertrophic responses when compared to the remaining treatments used in this work (ISO and PE), considerably increasing area and sarcomere intensity on CMs. That is not visible, from the mentioned measurements, for all of the tested cell densities which is a source of uncertainty in regard to the collected experimental data, given that the added stimulus is well known as inducing a hypertrophic effect on CMs (Dubey *et al.*, 1997; Schäfer *et al.*, 2002). Plus, the same can be said about the other used hypertrophic stimuli, ISO and PE, (Taigen *et al.*, 2000; Zou *et al.*, 2001) which did not show in this work to have the effects reported on the CMs. Further experiments would be necessary to clarify these results and to obtain more consistent conclusions. A hypothesis for the lack and/or inconsistent hypertrophic response on the CMs could be the administration of low concentrations of the hypertrophic inducers used. Although, support is found in the literature for the used concentrations, the reports in the area seem contradictory. For example, Putinsky and colleagues (2013) use 100μM of PE, instead of the 10μM used in this project. On the other hand, Földes and colleagues (2011) used the same concentration of PE as in the present study (10μM) and registered an area increase, sarcomere rearrangement and others markers that pointed to CM hypertrophy. However, the hESC-derived CMs used in the later work were in a more mature state which may or may not influence hypertrophy. Also, the period of treatment administration was shorter. Treatment concentration and duration and/or CM maturation level can be influencing the results, although we have not got so far the evidence to support such assumption.

The area and sarcomere color intensity analysis performed on the CMs cultured on the FN μCP patterns appears to indicate that the FCS treatment produces higher hypertrophic effects, presenting a bigger area and higher sarcomere intensity when compared to the other stimuli. However, the results do not show consistency, since this is not observed for all the cell densities. This may also derive from the difficulty in the CMs adaptation and development on the confined patterns on the well. The CM ratio performed both to Matrigel and FN patterns did not provide additional useful information to better describe the hypertrophy state of the CMs, since the results were not conclusive. Nevertheless, the CM culture conditions at higher densities, 10 and 20 cells/well, seems to enhance CM proliferation, as shown by the general higher CM percentage at these cell-densities. There is also the possibility that the PE treatment enhances proliferation, just confirmed by the high percentages on the 2000 cells/well density in Matrigel and in 15000 cells/well density in the

FN patterns. Although it is important to stress that the CM ratio is relative to the total number of cells present, i.e. cardiomyocytes and non-cardiomyocytes, being not truly reliable when assessing the cardiomyocyte's adaptation, development and/or proliferation on the different substrates and treatments. Contrariwise, area, sarcomere intensity and elongation are absolute measurements, in which just the CMs are evaluated, and can better describe CM behavior in the different treatments. The elongation study proved that the treatments do not significantly alter the elongation profile of CMs.

The results obtained from the FN patterns are not very elucidative because very few CMs could be observed in the images, thereby indicating they did not adapt well to the μCP lines. A different approach was needed for the optimal adherence of the CMs to the protein patterns for accurate analysis to be conducted. Considering the high CM population seen on the Matrigel substrate, that option was explored to produce the protein patterns. The Matrigel's composition was investigated to determine which compound(s) where decisive in CM adaptation and development. It was found that it is mainly composed by laminin (60%), collagen IV (30%) and entactin (8%) (Kosovsky, 2009). Knowing the importance of these compounds and also of fibronectin in native CM development (Horton *et al*. 2009) it was rehearsed a combination of laminin, fibronectin and collagen IV. It was experimented every possible combination from using the three proteins together to varying their individual concentration between 10, 20 and 50 μg/ml, making a total of twenty seven different combinations (3 different concentrations that can be assigned for each of the 3 proteins), to determine which one would provide the best results. Microphotographs were obtained for each combination and for the controls (they were all seeded in duplicate) which were then further analyzed. Cardiomyocyte's area, sarcomere color intensity and ratio parameter were analyzed for aiding on determining the best protein combination to be used. High values for these three measurements would mean a greater CM adaptation and development to the substrate. The best protein combination was determined based on the overall best score of the interception of the three measurements. Owing to the lack of time available to identify the optimal individual protein concentration to be used in a combined solution, two of the twenty seven combinations were chosen before full data analysis. In parallel it was performed microcontact printing with these two combinations: 20 and 50 ug/ml for each and all of the three proteins, reaching a solution final concentration of 20 and 50 ug/ml (combination 5 and 18). These concentrations were chosen since they were used throughout the project for coating and patterning processes, respectively.

Later, it was concluded that the combination number 4 was the one that had the best relative higher results in the three measurements. This combination is composed by fibronectin at 20 μg/ml, laminin at 20 μg/ml and collagen IV at 10 μg/ml and by this analysis it would be the selected formulation to use for microcontact printing, since it would be the one capable of providing the stimuli for a better cardiomyocyte's growth, development and adaptation, under our culture conditions. These conditions are fundamental to obtain proper and reliable information about the hypertrophy phenotype. However and as stated before,

due to the delay on obtaining knowledge of the optimal concentration to use, combination 5 and 18 were used for microcontact printing instead. Both protein combination patterns showed to produce a better effect than the fibronectin patterns. It is visible the existence of more CMs that adhered and developed on these combinations, when compared to the fibronectin patterns with the same cell density, suggesting that future work should involve more testing with similar protein combination.

The evaluation of the measurements destined to establish the optimal concentration, performed by monolayer coating (subsection 3.5.1) indicated a better CM overall status in combination 5 rather than combination 18. However, the measurements performed to the CMs cultured in the patterned protein combinations 5 and 18 (section 3.5.2), showed no relevant differences to report. Thus, hypertrophic treatments seem, once again not be producing the expected effects on CMs, or at least, their effect seem not to be conclusive, which can mean that either the used CMs do not respond to these stimuli for the reasons previously addressed, the procedure is not correctly performed and/or image analysis and measurements need to be optimized.

Chapter 5 Conclusions

The aim of this study was to create in vitro a system to model cardiac disease, namely that relating to CM hypertrophy, in which multiple samples could be screened in high-throughput fashion. Such system would have to be robust and enable thorough evaluation the hypertrophy phenotype. Based on this study the following conclusions can be taken:

- The platform used to study the hypertrophy was successfully constructed and optimized for high-throughput studies, offering the ability to culture a high number of cells on a vast area filled with protein patterns.
- Fibronectin substrate on its own, does not seem to be suitable for this assay.
- Matrigel’s components support better CM adherence, development and proliferation when compared to fibronectin.
- Cardiomyocyte's area seems to be slightly increased with the FCS treatment, although further experimentation is needed to consistently affirm that.
- CM maturation level, concentration and duration of hypertrophic treatments, experimental errors and/or lack of optimization of image analysis for this work can be influencing the results.

Chapter 6 Future Perspectives

Nowadays, the study of the heart has been increasing through the improvement of the signalling cascade needed to provide, in order to successfully differentiate the pluripotent stem cells into cardiomyocytes (Beqqali *et al.*, 2009). However, many questions remain unanswered relating to the phenotype and genotype of the cardiomyocytes obtained by this process, which may not completely resemble the native ones. For a better understanding of the phenomena associated with cardiomyocyte hypertrophy, which can lead to heart failure, it is imperative to develop new tools that can be used to study this event in better detail. With the knowledge acquired from this study will come beneficial progresses that allow a more efficient methodology to address this problem. The created platform to study this disease was constructed with those purposes, although several optimizations are still required to increase the throughput of platform construction and sample screening, and also improve result precision.

The platform construction implies a long manufacture gluing procedure, affecting the analysis efficiency. The bottom of the 96-well plate needs to be fully glued, to avoid fluid leakage when the coverslip is attached and cell culture is performed on the platform. Even though a double-sided tape was implemented in an attempt to optimize this process, its efficiency did not increase. This time consuming procedure could be avoided by the acquisition of an existent commercial product. A 96-well plate with an integrated adhesive tape on its bottom (ProPlate MP™ microtiter plate superstructure GBL204969, Grace Bio-Labs) is presently available in the market and could be easily used to attach the patterned coverslip, increasing process' efficiency and the throughput level. A robotic arm incorporated to the BD Pathway 855 could also be used to automatically insert in the system and screen multiple cell culture plates, enhancing efficiency.

An inherent problem regarding the plastic coverslips derives from the flexible properties of it. Their ability to easily bend when force is applied can produce topographic irregularities when attaching it to the bottomless 96-well plate. This would create different undulations in each well and, therefore, origin different cell depth, which would alter camera focus for each well. Although many of the present bioimaging systems have an automatic focus feature, it was working deficiently for the system used in this project, the BD Pathway 855, compromising the image focus randomly. Both of the shortcomings, topography irregularity and deficient focus, would need to be corrected and optimized for a proper hypertrophy analysis of cardiomyocytes. The re-incorporation of the glass coverslips in the platform and the repair and optimization of the autofocus system would be fundamental for improving results precision.

After applying the mentioned functional optimizations, other hypothesis and theories would be tested in the attempt to obtain numerous and "healthy" cardiomyocytes to be analysed, such as the use of the proper protein combination for microcontact printing. Regarding the results on section 3.5.1 the optimal protein combination that would allow a

better cardiomyocyte development and adaptation would be combination 4 (fibronectin at 20 µg/ml, laminin at 20 µg/ml and collagen IV at 10 µg/ml) and this would be the one used in the future, since the lack of time available dictated that it would not be performed. Concerning the apparent lack of hypertrophic effect on the cardiomyocytes after hypertrophic treatments administration, it would be interesting to use a DNA microarray to measure the gene expression level of multiple regions of the genome, with special interest in the immediate early genes (c-jun, c-fos, c-myc) and the fetal genes (ANF, ß-MHC and SKA) (Friddle *et al.,* 2000; Du, 2007; Rohini *et al.*, 2010). This genes are known to be activated during the development of cardiomyocyte hypertrophy condition and it would be possible to determine if the hypertrophic treatments used in this project were triggering or not those effects, since the data analysis could not totally conclude about that. The proper decisions would be adopted regarding the DNA microarray results.

As soon as the platform is properly working and optimized it can be used as a human disease *in vitro* model for pre-clinical studies. The certification of a drug is known to be a very slow and expensive procedure and it may take the minimum duration of 15 years, being divided into 3 phases: drug discovery, drug development and clinical trials. The last stage, only, can cost up to 120 million American dollars (DiMasi, Hansen and Grabowski, 2003). For this fact, the created model can be used to test drugs and if they indirectly affect the heart, it would be shown by the morphological analysis. Since almost all therapeutic drugs used to cure certain organs, such as the liver and kidney, produce an adverse effect on the heart, it would be extremely useful and beneficial the use of such a platform in pre-clinical studies, to obtain an immediate response of the heart cells to such compound. This would also prevent drug owners to disburse the enormous quantity of money needed to proceed to clinical trials, if cardiomyocyte's response to the drug is not appropriate (e.g. induction of hypertrophy) (DiMasi, Hansen and Grabowski, 2003; Braam, Passier and Mummery, 2009).

Another application of the created tool relies in the possibility of testing cardiac toxicity when a specific compound is introduced on the hESC-cardiomyocyte environment. The measure of key parameters, such as the effect of the test substance on the viability of the ESCs, can be used to predict the response of native cardiomyocytes to specific drugs (Rolletschek, Blyszczuk and Wobus, 2004). Plus, the model can be applied to many other projects where cardiomyocyte's morphologic characteristics need to be followed and studied.

Finally, but not the least, this work can provide interesting information about the ECM proteins and optimal protein concentration for an enhanced cardiomyocyte development.

References

Ahuja, P., Sdek P and Maclellan, W.R. (2007) Cardiac Myocyte Cell Cycle Control in Development, Disease, and Regeneration. Physiological Rev, 87, 521-544.

Akimoto, H., Ito, H., Tanaka, M., Adachi, S., Hata, M., Lin, M., Fujisaki, H., Marumo, F. and Hiroe, M. (1996) Heparin and heparan sulfate block angiotensin II-induced hypertrophy

in cultured neonatal rat cardiomyocytes. A possible role of intrinsic heparin-like molecules in regulation of cardiomyocyte hypertrophy. Circulation, 93(4), 810-816.

Alderman, M.H. (2007) Worksite Treatment for Cardiovascular Disease Prevention. Current Hypertension Reports, 9, 342-343.

Allegrucci, C., Wu, Y. Z., Thurston, A., Denning, C. N., Priddle, H., Mummery, C. L., Ward-van Oostwaard, D., Andrews, P. W., Stojkovic, M., Smith, N., Parkin, T., Jones, M. E., Warren, G., Yu, L., Brena, R. M., Plass, C. and Young, L. E. (2007) Restriction landmark genome scanning identifies culture-induced DNA methylation instability in the human embryonic stem cell epigenome. Human molecular genetics, 16(10), 1253-1268.

Atthi, N., Nimittrakoolchai, O. U., Jeamsaksiri, W., Supothina, S., Hruanun, C., and Poyai, A. (2009) Study of optimization condition for spin coating of the photoresist film on rectangular substrate by Taguchi design of an experiment. Songklanakarin J. Sci. Technol., 31 (3), 331-335.

Baba, H.A., and Wohlschlaeger J. (2008) Morphological and Molecular Changes of the Myocardium After Left Ventricular Mechanical Support. Current Cardiology Reviews, 4, 157-169.

Baharvand, H., Azarnia, M., Parivar, K., and Ashtiani, S. K. (2005) The effect of extracellular matrix on embryonic stem cell-derived cardiomyocytes. J Mol Cell Cardiol, 38(3), 495-503.

Barile, L., Messina, E., Giacomello, A., and Marbán, E. (2007) Endogenous Cardiac Stem Cells. Progress in Cardiovascular Diseases, 50(1), 31-48.

Barron, J. A., Young, H. D., Dlott, D. D., Darfler, M. M., Krizman, D. B., and Ringeisen, B. R. (2005) Printing of protein microarrays via a capillary-free fluid jetting mechanism. Proteomics, 5, 4138-4144.

Bass, G. T., Ryall, K. A., Katikapalli, A., Taylor, B. E., Dang, S. T., Acton, S. T., and Saucerman, J. J. (2012) Automated image analysis identifies signaling pathways regulating distinct signatures of cardiac myocyte hypertrophy. Journal of Molecular and Cellular Cardiology, 52, 923-930.

BD Biosciences. (2007) Navigation the High-Content Imaging Process. [Online] Available from: http://www.bdbiosciences.com/documents/AppNote_High-Content_Imaging.pdf [Accessed 11th August 2014].

BD Biosciences. (2009) BD Pathway Bioimaging Systems Brochure. [Online] Available from: http://www.bdbiosciences.com/documents/Pathway_brochure.pdf [Accessed 21th January 2014].

Beqqali, A., Van Eldik, W., Mummery, C. L., and Passier, R. (2009) Human stem cells as a model for cardiac differentiation and disease. Cell. Mol. Life Sci., 66, 800-813.

Bergmann, O., Bhardwaj, R. D., Bernard, S., Zdunek, S., Barnabé-Heider, F., Walsh, S., Zupicich, J., Alkass, K., Buchholz, B. A., Druid, H., Jovinge, S., and Frisén, J. (2009) Evidence for Cardiomyocyte Renewal in Humans. Science, 324 (5923), 98-102.

Bernard, A., Delamarche, E., Schmid, H., Michel, B., Bosshard, H. R., and Biebuyck, H. (1998) Printing patterns of proteins. Langmuir, 14, 2225-2229.

Bianco, P., Cao, X., Frenette, P. S., Mao, J. J., Robey, P. G., Simmons, P. J., and Wang, C. Y. (2013) The meaning, the sense and the significance: translating the science of mesenchymal stem cell into medicine. Nature Medicine, 19, 35-42.

Bicknell, K.A., Coxon, C.H. and Brooks, G. (2007) Can the cardiomyocyte cell cycle be reprogrammed?. Journal of Molecular and Cellular Cardiology, 42, 706–721.

Blinka, E., Loeffler, K., Hu, Y., Gopal, A., Hoshino, K., Lin, K., Ferrari, M., and Zhang, J. X. (2010) Enhanced microcontact printing of proteins on nanoporous silica surface. Nanotechnology 21(41), 415302.

Boheler, K. R., Czyz, J., Tweedie, D., Yang, H. T., Anisimov, S. V., and Wobus, A. M. (2002) Differentiation of Pluripotent Embryonic Stem Cells Into Cardiomyocytes. Circulation Research, 91, 189-201.

Bolini, S., Smart, N. and Riley, P.R. (2011) Resident cardiac progenitor cells: At the heart of regeneration. Journal of Molecular and Cellular Cardiology, 50, 296-303.

Bongso, A., Fong, C. Y., Ng, S. C., and Ratnam, S. (1994) Fertilization and early embryology: Isolation and culture of inner cell mass cells from human blastocysts. Human Reproduction 9(11), 2110-2117.

Bowers, S.L.K., Banerjee, I. and Baudino, T.A. (2010) The extracellular matrix: At the center of it all. Journal of Molecular and Cellular Cardiology, 48, 474-482.

Braam, S.R., Passier, R. and Mummery, C.L. (2009) Cardiomyocytes from human pluripotent stem cells in regenerative medicine and drug discovery. Trends in pharmacological sciences, 30(10), 536-545.

Bray, M.A., Sheehy, S.P. and Parker, K.K. (2008) Sarcomere Alignment is Regulated by Myocyte Shape. Cell Motility and the Cytoskeleton, 65, 641–651.

Britland, S., Perez-Arnaud, E., Clark, P., McGinn, B., Connolly, P., & Moores, G. (1992) Micropatterning Proteins and Synthetic Peptides on Solid Supports – A Novel Application for Microelectronics Fabrication Technology. Biotechnology Progress, 8, 155-160.

Bruggink, A.H., van Oosterhout, M. F. M., de Jonge, N., Cleutjens, J. P. M., van Wichen, D. F., van Kuik, J., Tilanus, M. G. J., Gmelig-Meyling, F. H. J., van den Tweel, J. G., and de Weger, R. A. (2007) Type IV collagen degradation in the myocardial basement membrane after unloading of the failing heart by a left ventricular assist device. Laboratory Investigation 87(11), 1125-1137.

Bryers, J.D., Giachelli, C.M., and Ratner, B.D. (2012) Engineering Biomaterials to Integrate and Heal: The Biocompatibility Paradigm Shifts. Biotechnology and Bioengineering, 109, 1898-1911.

Buja, L.M., and Vela D. (2008) Cardiomyocyte death and renewal in the normal and diseased heart. Cardiovascular Pathology, 17, 349–374.

Cai, Y.G., and Ocko, B.M. (2005) Large-scale fabrication of protein nanoarrays based on nanosphere lithography. Langmuir, 21, 9274-9279.

Carcano, G., Ceriani, M., and Soglio, F. (1993) Spin Coating with High Viscosity Photoresist on Square Substrates - Applications in the Thin Film Hybrid Microwave Integrated Circuit Field. Microelectronics International, 10 (3), 12-20.

Carèw, A, Catalucci, D., Felicetti, F., Bonci, D., Addario, A., Gallo, P., Bang, M., Segnalini, P., Gu, Y., Dalton, N. D., Elia, L., Latronico, M. V. G., Høydal, M., Autore, C., Russo, M. A., Dorn II, G. W., Ellingsen, O., Ruiz-Lozano, P., Peterson, K. L., Croce, C. M., Peschle, C., and Condorelli, G. (2007) MicroRNA-133 controls cardiac hypertrophy. Nature Medicine, 13(5), 613-618.

Carpenter, A. E., Jones, T. R., Lamprecht, M. R., Clarke, C., Kang, I. H., Friman, O., Guertin, D. A., Chang, J. H., Lindquist, R. A., Moffat, J., Golland, P., and Sabatini, D. M. (2006) CellProfiler: image analysis software for identifying and quantifying cell phenotypes. Genome Biology 7(10), 1-11.

Carreño, J. E., Apablaza, F., Ocaranza, M. P., and Jalil, J. E. (2006) Cardiac hypertrophy: molecular and cellular events. Revista Española de Cardiología (English Edition), 59(5), 473-486.

Chiu, L. L., Iyer, R. K., Reis, L. A., Nunes, S. S., and Radisic, M. (2012) Cardiac tissue engineering: current state and perspectives. Frontiers in Bioscience 17, 1533–1550.

Cincinnati Children's Hospital Medical Center. (2011) Pluripotent Stem Cell Facility: Induced Pluripotent Stem Cells. [Online] Available from: https://research.cchmc.org/stemcell/iPSC [Accessed on 22nd October 2014]

Claybomb, W.C., Lanson, N. A., Stallworth, B. S., Egeland, D. B., Delcarpio, J. B., Bahinski, A., & Izzo, N. J. (1998) HL-1 cells: A cardiac muscle cell line that contracts and retains phenotypic characteristics of the adult cardiomyocyte. Cell Biology, 95, 979-2984

Comley, J. (2005) High content screening. Drug Discovery, 31.

Cowan, C.A., Atienza, J., Melton, D. A., and Eggan, K. (2005) Nuclear reprogramming of somatic cells after fusion with human embryonic stem cells. Science 309(5739), 1369-1373.

Csucs, G., Künzler, T., Feldman, K., Robin, F., & Spencer, N. D. (2003) Microcontact printing of macromolecules with submicrometer resolution by means of polyolefin stamps. Langmuir, 19, 6104-6109.

Delaney, J. T., Smith, P. J. and Schubert, U. S. (2009) Inkjet printing of proteins. Soft Matter, 5, 4866-4877.

Di Nardo, P., Forte, G., Ahluwalia, A., and Minieri, M. (2010) Cardiac progenitor cells: potency and control. Journal of cellular physiology, 224, 590–600.

DiMasi, J. A., Hansen, R.W. and Grabowski, H.G. (2003) The price of innovation: new estimates of drug development costs. Journal of Health Economics, 22, 151-185.

Dorn II, G. W., Robbins, J. and Sugden, P.H. (2003) Phenotyping Hypertrophy: Eschew Obfuscation. Circulation Research, 92, 1171-1175.

Douvas, A., Argitis, P., Misiakos, K., Dimotikali, D., Petrou, P. S., & Kakabakos, S. E. (2002) Biocompatible photolithographic process for the patterning of biomolecules. Biosensors and Bioelectronics, 17, 269-278.

Dow Corning Corporation. (2005) Information about Dow Corning brand Silicone Encapsulants. Form 10-898F-01.

Du, X. J. (2007) Divergence of hypertrophic growth and fetal gene profile: the influence of ß-blockers. British journal of pharmacology, 152(2), 169-171.

Dubey, R. K., Gillespie, D. G., Mi, Z., and Jackson, E. K. (1997) Exogenous and Endogenous Adenosine Inhibits Fetal Calf Serum–Induced Growth of Rat Cardiac Fibroblasts: Role of A2B Receptors. Circulation, 96, 2656-2666.

Elliott, A. D., Braam, S. R., Koutsis, K., Ng, E. S., Jenny, R., Lagerqvist, E. L., Biben, C., Hatzistavrou, T., Hirst, C. E., Yu, Q. C., Skelton, R. J. P., Ward-van Oostwaard, D., Lim, S. M., Khammy, O., Li, X., Hawes, S. M., Davis, R. D., Goulburn, A. L., Passier, R., Prall, O. W. J, Haynes, J. M., Pouton, C. W., Kaye, D. M., Mummery, C. L., Elefanty, A. G., and Stanley, E. G. (2011) NKX2-5$^{eGFP/w}$ hESCs for isolation of human cardiac progenitors and cardiomyocytes. Nature Methods, 8, 12.

Evans, M. J., and Kaufman, M. H. (1981) Establishment in culture of pluripotential cells from mouse embryos. Nature, 292(5819), 154-156.

Farhadian, F., Contard, F., Sabri, A., Samuel, J. L., and Rappaport, L. (1996) Fibronectin and basement membrane in cardiovascular organogenesis and disease pathogenesis. Cardiovascular Research, 32, 433-442.

Földes, G., Mioulane, M., Wright, J. S., Liu, A. Q., Novak, P., Merkely, B., Gorelik, J., Schneider, M. D., Ali, N. N., and Harding, S. E. (2010) Modulation of human embryonic stem cell-derived cardiomyocyte growth: A testbed for studying human cardiac hypertrophy? Journal of Molecular and Cellular Cardiology, 50, 367-376.

Freund, C., and Mummery, C.L. (2009). Prospects for pluripotent stem cell-derived cardiomyocytes in cardiac cell therapy and as disease models. Journal of cellular biochemistry, 107(4), 592-599.

Freund, C., Davis, R. P., Gkatzis, K., Ward-van Oostwaard, D., and Mummery, C. L. (2010) The first reported generation of human induced pluripotent stem cells (iPS cells) and iPS cell- derived cardiomyocytes in the Netherlands. Netherlands Heart Journal, 18, 51-54

Frey, N., and Olson, E. N. (2003) Cardiac Hypertrophy: The Good, the Bad, and the Ugly. Annu. Rev. Physiol., 65, 45-79.

Frey, N., Katus, H. A., Olson, E. N., and Hill, J. A. (2004) Hypertrophy of the Heart: A New Therapeutic Target?. Circulation, 109, 1580-1589.

Friddle, C. J, Koga, T., Rubin, E. M., and Bristow, J. (2000) Expression profiling reveals distinct sets of genes altered during induction and regression of cardiac hypertrophy. PNAS, 96(12), 6745-6750.

Gonzalez-Macia, L., Morrin, A., Smyth, M. R., and Killard, A. J. (2010) Advanced printing and deposition methodologies for the fabrication of biosensors and biodevices. Analyst, 135(5), 845-867.

Graham, G. N., Guendelman, M., Leong, B. S., Hogan, S., and Dennison, A. (2006) Impact of Heart Disease and Quality of Care on Minority Populations in the United States. Journal of the National Medical Association, 98 (10), 1579-1586.

Griffin, A. E. (1954) Preparation and Use of Activated Silica. Journal (American Water Works Association), 571-574.

Grimm, D., Cameron, D., Griese, D. P., Riegger, G. A., & Kromer, E. P. (1998) Differential effects of growth hormone on cardiomyocyte and extracellular matrix protein remodeling following experimental myocardial infarction. Cardiosvascular Research, 40, 297-306.

Grossman, W., Jones, D., and McLaurin, L. P. (1975) Wall Stress and Patterns of Hypertrophy in the Human Left Ventricle. The Journal of Clinical Investigation, 56, 56-64.

Guan, K., and Hasenfuss, G. (2013) Cardiac resident progenitor cells: evidence and functional significance. European Heart Journal, 34, 2784-2787.

Hoffman, L. M., and Carpenter, M. K. (2005) Characterization and culture of human embryonic stem cells. Nat Biotechnol, 23, 699-708.

Horton, R. E., Millman, J. R., Colton, C. K., & Auguste, D. T. (2009) Engineering microenvironments for embryonic stem cell differentiation to cardiomyocytes. Regenerative medicine 4(5), 721-732.

Hui, A., Blosiu, J. O., and Wiberg, D. V. (1998) Taguchi Method Applied in Optimization of Shipley SJR5740 Positive Resist Deposition. Proceedings of SPIE, 3333, 1304-1313.

Jones, M. (2006) Embryonic stem cells. Wikipedia [Online] Available from: http://commons.wikimedia.org/wiki/File:Stem_cells_diagram.png [Accessed on 20th October 2014]

Kamentsky, L., Jones, T. R., Fraser, A., Bray, M., Logan, D. J., Madden, K. L., Ljosa, V., Rueden, C., Eliceiri, K. W., and Carpenter, A. E. (2011) Improved structure, function and compatibility for CellProfiler: modular high-throughput image analysis software. Bioinformatics, 27(8), 1179-1180.

Kane, R. S., Takayama, S., Ostuni, E., Ingber, D. E., and Whitesides, G. M. (1999) Patterning proteins and cells using soft lithography. Biomaterials, 20, 2363-2376.

Kaufmann, T., and Ravoo, B. J. (2010) Stamps, inks and substrates: polymers in microcontact printing. Polymer Chemistry, 1(4), 371-387.

Kehat, I., Kenyagin-Karsenti, D., Snir, M., Segev, H., Amit, M., Gepstein, A., Livne, E., Binah, O., Itskovitz-Eldor, J. and Gepstein, L. (2001). Human embryonic stem cells can differentiate into myocytes with structural and functional properties of cardiomyocytes. The Journal of clinical investigation, 108(3), 407-414.

Kelly, B. B., Narula, J., and Fuster, V. (2012) Recognizing Global Burden of Cardiovascular Disease and Related Chronic Diseases. Mount Sinai Journal of Medicine, 79, 632-640.

Kosovsky, M. (2009) A synthetic Hydrogel for 3D Cell Culture: BD™ PuraMatrix™ Peptide Hydrogel. BD Biosciences.

Kroetch, A. (2004) NanoFab's PDMS Microfluid Device Fabrication Manual.

Laflamme, M. A., and Murry, C. E. (2011) Heart regeneration. Nature, 473, 326-335.

Lamprecht, M. R., Sabatini, D. M., and Carpenter, A. E. (2007) CellProfiler™: free, versatile software for automated biological image analysis. Biotechniques, 42(1), 71-75.

Lee, S. W., Oh, B. K., Sanedrin, R. G., Salaita, K., Fujigaya, T., and Mirkin, C. A. (2006) Biologically Active Protein Nanoarrays Generated Using Parallel Dip-Pen Nanolithography. Adv. Mater., 18, 1133-1136.

Lee, Y. (2010) To proliferate or not to proliferate. Cardiovascular Research, 86, 347-348.

Lom, B., Healy, K. E., and Hockberger, P. E. (1993) A Versatile Technique for Patterning Biomolecules Onto Glass Coverslips. Journal of Neuroscience Methods, 50, 385-397.

Lopera, S. and Mansano, R.D. (2012) Plasma-Based Surface Modification of Polydimethylsiloxane for PDMS-PDMS Molding. ISRN Polymer Science, 2012, 1-5.

Lu, Y., and Yang, S. (2009) Angiotensin II Induces Cardiomiocyte Hypertrophy Probably through Histone Deacetylases. Tohoku J. Exp. Med., 219, 17-23.

Macarron, R., Banks, M. N., Bojanic, D., Burns, D. J., Cirovic, D. A., Garyantes, T., Green, D. V. S., Hertzberg, R. P., Janzen, W. P., Paslay, J. W., Schopfer, U., and Sittampalam, G. S. (2011) Impact of high-throughput screening in biomedical research. Nature Reviews Drug Discovery, 10(3), 188-195.

Maillet, M., van Berlo, J. H., and Molkentin, J. D. (2013) Molecular basis of physiological heart growth: fundamental concepts and new players. Nature Reviews Molecular Cell Biology, 14, 38-48.

Major, J. (1998) Challenges and Opportunities in High-throughput Screening: Implications for New Technologies. Journal of Biomolecular Screening, 3(1), 13-17.

Martin, G. R. (1981) Isolation of a pluripotent cell line from early mouse embryos cultured in medium conditioned by teratocarcinoma stem cells. Proceedings of the National Academy of Sciences, 78(12), 7634-7638.

Martis, E. A., Radhakrishnan, R., and Badve, R. R. (2011) High-Throughput Screening: The Hits and Leads of Drug Discovery – An Overview. Journal of Applied Pharmaceutical Science, 01(01), 02-10.

Mathers, C. D., and Loncar, D. (2006) Projections of global mortality and burden of disease from 2002 to 2030. PLoS Med, 3(11), 442.

Meerson F. Z. (1962) Compensatory Hyperfunction of the Heart and Cardiac Insufficiency. Circulation Research, 10, 250-258.

Messina, E., Giacomello, A., and Marban, E. (2007) Chapter 7 - Endogenous Stem Cells. Stem Cells and Myocardial Regeneration, 83–115.

Miner, E. C., and Miller, W. L. (2006) Look Between the Cardiomyocytes: The Extracellular Matrix in Heart Failure. Mayo Clin Proc., 81(1), 71-76.

Mollova, M., Bersell, K., Walsh, S., Savla, J., Das, L. T., Park, S., Silberstein, L. E., dos Remedios, C. G., Graham, D., Colan, S., and Kühn, B. (2013) Cardiomyocyte proliferation contributes to heart growth in young humans. Proceedings of the National Academy of Sciences, 110, 1446-1451.

Musunuru, K., Domian, I. J., and Chien, K. R. (2010) Stem Cell Models of Cardiac Development and Disease. Annual review of cell and developmental biology, 26, 667.

Pagliari, S., Vilela-Silva, A. C., Forte, G., Mandoli, C., Vozzi, G., Pietronave, S., Prat, M., Licoccia, S., Ahluwalia, A., Traversa, E., Minieri, M., and Di Nardo, P. (2011) Cooperation of Biological and Mechanical Signals in Cardiac Progenitor Cell Differentiation. Adv. Mater., 23, 514-518.

Pardo, L., Wilson, W. C., and Boland, T. J. (2003) Characterization of patterned selfassembled monolayers and protein arrays generated by the ink-jet method, Langmuir, 19, 1462-1466.

Park, S. H., Yin, P., Liu, Y., Reif, J. H., LaBean, T. H., and Yan, H (2005) Programmable DNA self-assemblies for nanoscale organization of ligands and proteins. Nano Letters, 5, 729-733.

Pelouch, V., Dixon, I. M., Golfman, L., Beamish, R. E., & Dhalla, N. S. (1994) Role of extracellular matrix proteins in heart function. Molecular and Cellular Biochemistry. 129, 101-120.

Piner, R. D., Zhu, J., Xu, F., Hong, S., and Mirkin, C. A. (1999) "Dip-Pen" Nanolithography. Science, 283, 661-663.

Ptaszek, L. M., Mansour, M., Ruskin, J. N., and Chien, K. R. (2012) Towards regenerative therapy for cardiac disease. Lancet, 379, 933-942.

Putinski, C., Abdul-Ghani, M., Stiles, R., Brunette, S., Dick, S. A., Fernando, P., and Megeney, L. A. (2013) Intrinsic-mediated caspase activation is essential for cardiomyocyte hypertrophy. PNAS, 110 (43), 4079-4087.

Quist, A. P., Pavlovic, E., and Oscarsson, S. (2005) Recent advances in microcontact printing. Analytical and Bioanalytical Chemistry, 381, 591-600.

Ratner, B. D., Hoffman, A. S., Schoen, F. J., and Lemons, J. E. (2012) Biomaterials Science (Third Edition) - An Introduction to Materials in Medicine.

Reubinoff, B. E., Pera, M. F., Fong, C. Y., Trounson, A., and Bongso, A. (2000) Embryonic stem cell lines from human blastocysts: somatic differentiation *in vitro*. Nature Biotechnology, 18(4), 399-404.

Roda, A., Guardigli, M., Russo, C., Pasini, P., and Baraldini, M. (2000) Protein microdeposition using a conventional ink-jet printer. Biotechniques, 28, 492-496.

Rohini, A., Agrawal, N., Koyani, C. N., and Singh, R. (2010) Molecular targets and regulators of cardiac hypertrophy. Pharmacological Research, 61, 269-280.

Rojo, M. G., Bueno, G., and Slodkowska, J. (2009) Review of imaging solutions for integrated quantitative immunohistochemistry in the Pathology daily practice. Folia Histochemica et Cytobiologica, 47(3), 349-354.

Rolletschek, A., Blyszczuk, P., and Wobus, A. M. (2004) Embryonic stem cell-derived cardiac, neuronal and pancreatic cells as model systems to study toxicological effects. Toxicology Letters, 149, 361–369.

Ruiz, S. A., and Chen, C. S. (2007) Microcontact Printing: A tool to pattern. Soft Matter, 3, 1-11.

Sadoshima, J., Qiu, Z., Morgan, J. P., and Izumo, S. (1995) Angiotensin II and Other Hypertrophic Stimuli Mediated by G Protein–Coupled Receptors Activate Tyrosine Kinase, Mitogen-Activated Protein Kinase, and 90-kD S6 Kinase in Cardiac Myocytes. Circulation Research, 76(1), 1-15.

Schäfer, M., Schäfer, C., Piper, H. M., and Schlüter, K. D. (2002) Hypertrophic responsiveness of cardiomyocytes to α- or ß-adrenoceptor stimulation requires sodium-proton-exchanger-1 (NHE-1) activation but not cellular alkalization. The European Journal of Heart Failure, 4(3), 249-254.

Schneider, C. A., Rasband, W. S., and Eliceiri, K. W. (2012) NIH Image to ImageJ: 25 years of image analysis. Nature Methods, 9(7), 671-675.

Sleytr, U. B., Huber, C., Ilk, N., Pum, D., Schuster, B., & Egelseer, E. M. (2007) S-layers as a tool kit for nanobiotechnological applications. Fems Microbiology Letters, 267(2), 131-144.

Stojkovic, M., Lako, M., Stojkovic, P., Stewart, R., Przyborski, S., Armstrong, L., Evans, J., Herbert, M., Hyslop, L., Ahmad, S., Murdoch, A., and Strachan, T. (2004) Derivation of human embryonic stem cells from day-8 blastocysts recovered after three-step *in vitro* culture. Stem Cells, 22, 790-797.

Strelchenko, N., Verlinsky, O., Kukharenko, V., and Verlinsky, Y. (2004) Morula-derived human embryonic stem cells. Reprodutive Biomedicine Online. 9(6), 623-629

Streuli, C. (1999) Extracellular matrix remodelling and cellular differentiation. Cell Biology, 11, 634-640.

Strunz, C.M., Matsuda, M., Salemi, V. M., Nogueira, A., Mansur, A. P., Cestari, I. N., and Marquezini, M. V. (2011) Changes in cardiac heparan sulfate proteoglycan expression and streptozotocin-induced diastolic dysfunction in rats. Cardiovasc Diabetol 10, 35.

Taigen, T., De Windt, L. J., Lim, H. W., and Molkentin, J. D. (2000) Targeted inhibition of calcineurin prevents agonist-induced cardiomyocyte hypertrophy. PNAS, 97(3), 1196-1201.

Takahashi, K., and Yamanaka, S. (2006) Induction of pluripotent stem cells from mouse embryonic and adult fibroblast cultures by defined factors. Cell, 126(4), 663-676.

Takahashi, K., Tanabe, K., Ohnuki, M., Narita, M., Ichisaka, T., Tomoda, K., and Yamanaka, S. (2007) Induction of pluripotent stem cells from adult human fibroblasts by defined factors. Cell, 131(5), 861-872.

Takeishi, Y., Huang, Q., Abe, J. I., Glassman, M., Che, W., Lee, J. D., Kawakatsu, H., Lawrence, E. G., Hoit, B. D., Berk, B. C., and Walsh, R. A. (2001) Src and Multiple MAP Kinase Activation in Cardiac Hypertrophy and Congestive Heart Failure Under Chronic Pressure

Overload: Comparison with Acute Mechanical Stretch. Journal of Molecular and Cellular Cardiology, 33(9), 1637-1648.

Théry, M., and Piel, M. (2009) Adhesive Micropatterns for Cells: A Microcontact Printing Protocol. Cold Spring Harb Protoc, 4.

Thomson, J. A., Itskovitz-Eldor, J., Shapiro, S. S., Waknitz, M. A., Swiergiel, J. J., Marshall, V. S., and Jones, J. M. (1998) Embryonic stem cell lines derived from human blastocysts. Science 282(5391), 1145-1147.

Torres, A. J., Wu, M., Holowka, D., andBaird, B. (2008) Nanobiotechnology and cell biology: Micro- and nanofabricated surfaces to investigate receptor-mediated signaling. Annual Review of Biophysics, 37, 265-288.

Unterreiner, V., and Gabriel, D. (2011) When High Content Screening meets High-throughput. Drug Discovery World.

Valsesia, A., Colpo, P., Meziani, T., Lisboa, P., Lejeune, M., & Rossi, F. (2006) Immobilization of antibodies on biosensing devices by nanoarrayed selfassembled monolayers. Langmuir, 22(4), 1763-1767.

Von Philipsborn, A. C., Lang, S., Bernard, A., Loeschinger, J., David, C., Lehnert, D., Bastmeyer, M., and Bonhoeffer, F. (2006) Microcontact printing of axon guidance molecules for generation of graded patterns. Nature Protocols, 1(3), 1322-1328.

Wakitani, S., Takaoka, K., Hattori, T., Miyazawa, N., Iwanaga, T., Takeda, S., Watanabe, T. K., and Tanigami, A. (2003) Embryonic stem cells injected into the mouse knee joint form teratomas and subsequently destroy the joint. Rheumatology (Oxford), 42(1), 162-165.

Wang, Y., Huang, S., and Sah, V. P. (1998) Cardiac Muscle Cell Hypertrophy and Apoptosis Induced by Distinct Members of the p38 Mitogen-activated Protein Kinase Family*. The Journal of Biological Chemistry, 273(4), 2161–2168.

Whelan, D. (2012) The 10 Most Expensive Common Medical Conditions. Forbes Magazine [Online] Available from: http://www.forbes.com/sites/davidwhelan/2012/02/25/the-10-most-expensive-common-medical-conditions/ [Accessed on 6th January 2014].

Wilmut, I., Schnieke, A. E., McWhir, J., Kind, A. J., & Campbell, K. H. S. (2007) Viable offspring derived from fetal and adult mammalian cells. Cloning and stem cells, 9(1), 3-7.

Wobus, A. M., Wallukat, G., and Hescheler, J. (1991) Pluripotent mouse embryonic stem cells are able to differentiate into cardiomyocytes expressing chronotropic responses to adrenergic and cholinergic agents and Ca2+ channel blockers. Differentiation, 48(3), 173-182.

World Health Organization. (2004) The Global Burden of Disease. [Online] Available from: http://www.who.int/healthinfo/global_burden_disease/2004_report_update/en/ [Accessed on 7th August 2014].

World Health Organization. (2011) Global status report on noncommunicable diseases 2010. [Online] Available from: http://www.who.int/nmh/publications/ncd_report2010/en/ [Accessed on 7th August 2014].

Wu, X., Sun, Z., Foskett, A., Trzeciakowski, J. P., Meininger, G. A., and Muthuchamy, M. (2010) Cardiomyocyte contractile status is associated with differences in fibronectin and integrin interactions. American Journal of Physiology - Heart and Circulatory Physiology, 298(6), 2071–2081.

Xia, Y. N., and Whitesides, G. M. (1998) Soft lithography, Annual Review of Materials Science, 28, 153-184.

Xin, M., Olson, E. N., and Bassel-Duby, R. (2013) Mending broken hearts: cardiac development as a basis for adult heart regeneration and repair. Nature Reviews Molecular Cell Biology, 14, 529–541.

Yamanaka, S. (2008) Pluripotency and nuclear reprogramming. Philos Trans R Soc Lond B Biol Sci. 363, 2079-2087.

Yamazaki, T., Komuro, I., Kudoh, S., Zou, Y., Shiojima, I., Hiroi, Y., Mizuno, T., Maemura, K., Kurihara, H., Aikawa, R., Takano, H., and Yazaki, Y. (1996) Endothelin-1 Is Involved in Mechanical Stress-induced Cardiomyocyte Hypertrophy*. The Journal of Biological Chemistry, 271(6), 3221–3228.

Yan, H., Park, S. H., Finkelstein, G., Reif, J. H., and LaBean, T. H. (2003) DNA-templated self-assembly of protein arrays and highly conductive nanowires. Science, 301(5641), 1882-1884.

Yu, J., Vodyanik, M. A., Smuga-Otto, K., Antosiewicz-Bourget, J., Frane, J. L., Tian, S., Nie, J., Jonsdottir, G. A., Ruotti, V., Stewart, R., Slukvin, I. I., and Thomson, J. A. (2007) Induced pluripotent stem cell lines derived from human somatic cells. Science, 318(5858), 1917-1920.

Yurchenko, D., and Patton, L. (2009) Developmental and pathogenic mechanisms of basement membrane assembly. Curr. Pharm., 15 (12), 1277-94.

Zanella, F., Lorens, J. B., and Link, W. (2010) High content screening: seeing is believing. Trends in Biotechnology, 28(5), 237-245.

Zou, Y., Yao, A., Zhu, W., Kudoh, S., Hiroi, Y., Shimoyama, M., Uozumi, H., Kohmoto, O., Takahashi, T., Shibasaki, F., Nagai, R., Yazaki, Y., and Komuro, I. (2001) Isoproterenol Activates Extracellular Signal-Regulated Protein Kinases in Cardiomyocytes Through Calcineurin. Circulation, 104(1), 102-108.

Suplemmentary data

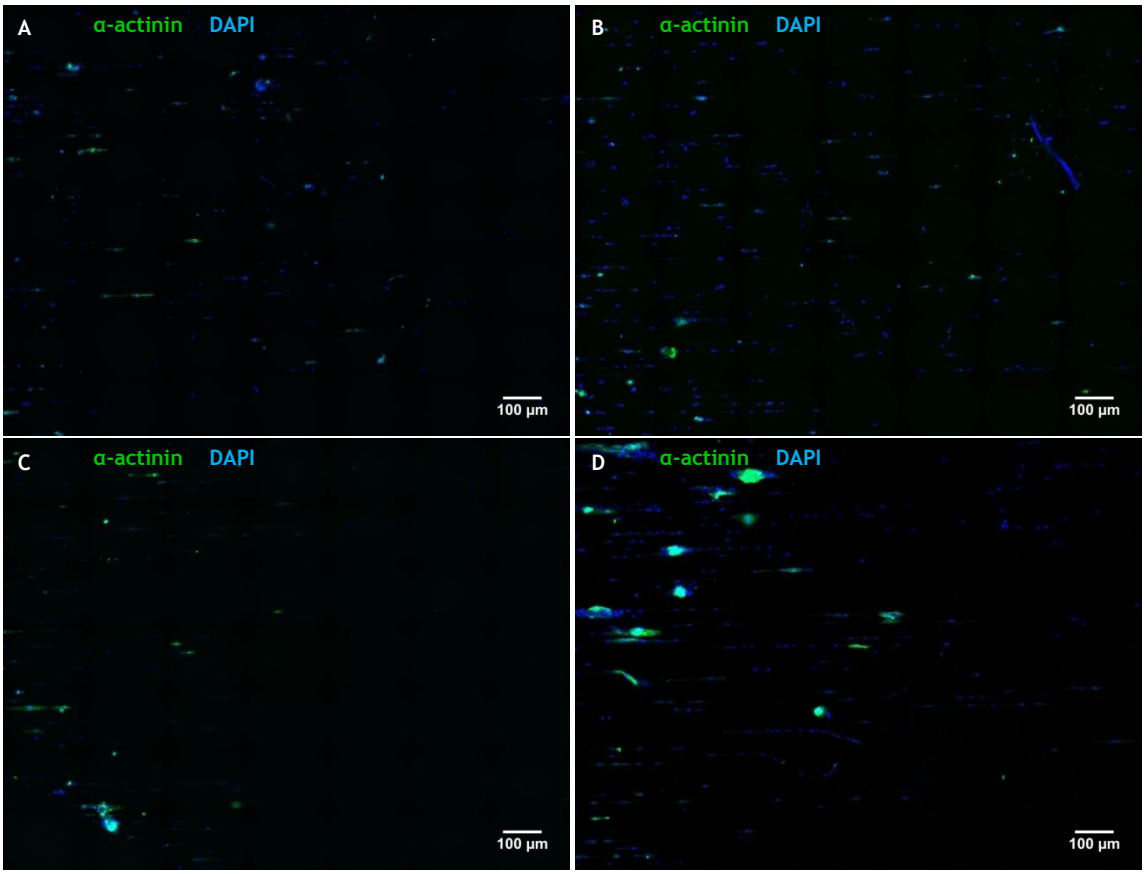

Figure 27 - Original images of cardiomyocytes cultured on fibronectin patterns (horizontal lines) in (A) control, (B) ISO, (C) PE and (D) FCS, at 10000 cells/well, and immunostained for α-actinin (green) and DAPI (blue) (magnification: 20x).

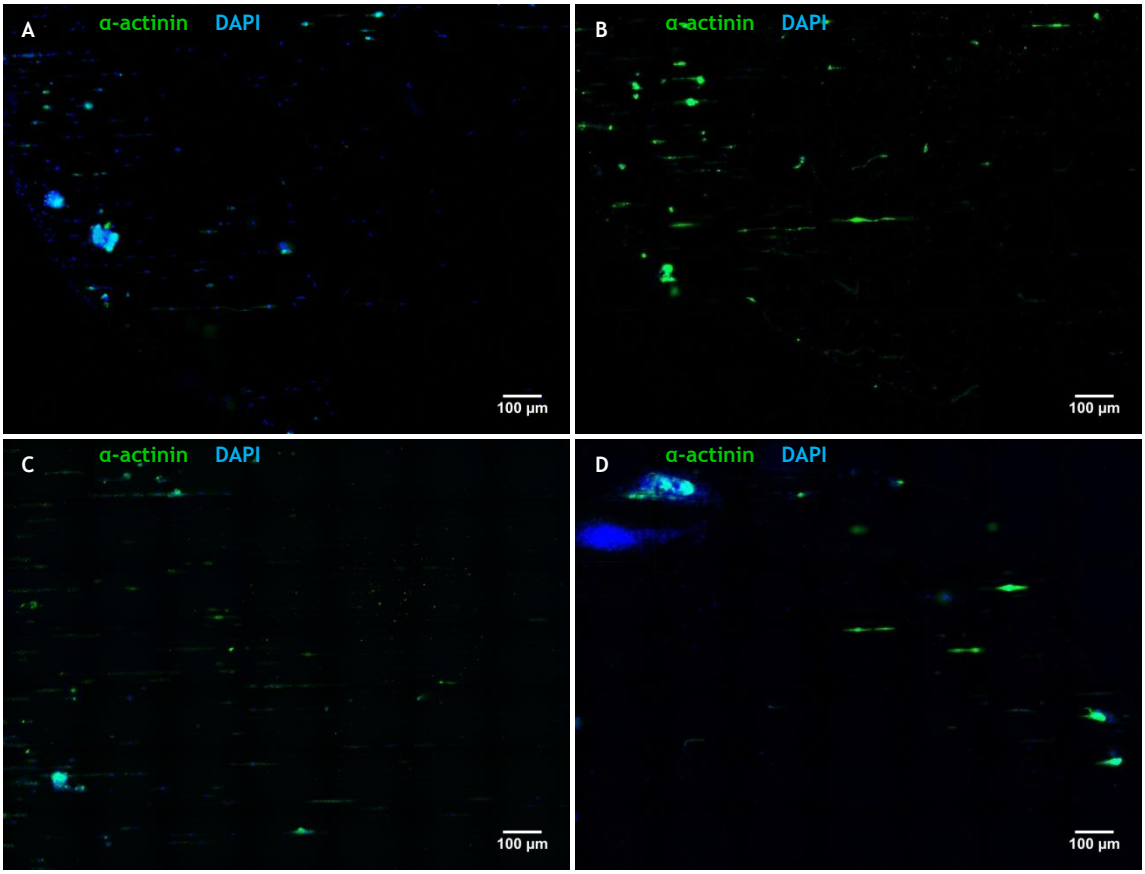

Figure 28 - Original images of cardiomyocytes cultured on fibronectin patterns (horizontal lines) in (A) control, (B) ISO, (C) PE and (D) FCS, at 15000 cells/well, and immunostained for α-actinin (green) and DAPI (blue) (magnification: 20x).